Guidelines for the Design of Segmental Tunnel Linings

ITA Working Group 2 - Research

N° ISBN: 978-2-9701242-1-4

ITA REPORT N°22 / APRIL 2019

ASSOCIATION INTERNATIONALE DES TUNNELS ET DE L'ESPACE SOUTERRAIN
AITES
ITA
INTERNATIONAL TUNNELLING AND UNDERGROUND SPACE ASSOCIATION

ITA Report n°22 - **Guidelines for the Design of Segmental Tunnel Linings**
N°ISBN : 978-2-9701242-1-4 / APRIL 2019 - Layout : Longrine – Avignon – France – www.longrine.fr

Guidelines for the Design of Segmental Tunnel Linings

ITA Working Group 2 - Research

>> TABLE OF CONTENTS

>> TABLE OF CONTENTS

MAIN AUTHORS, CONTRIBUTORS AND REVIEWERS IN ALPHABETIC ORDER

Main Authors

Mehdi Bakhshi, USA
Verya Nasri, USA

Contributors

Elena Chiriotti, France
Ron Tluczek, South Africa

WG2's Reviewers

Christoph Eberle, UK
Gernot Jediltschka, Austria
Giovanni Plizzari, Italy
Jon Hurt, USA
Markus Thewes, Germany

ITA's Reviewers

Benoît de Rivaz, France
Chungsik Yoo, South Korea
Eric Leca, France

>> List of symbols and abreviation

A = effective tension area of concrete around rebar divided by number of steel bars, mm^2

A_d = load distribution area inside segment under thrust jack forces, mm^2

A_g = gross area of concrete section, mm^2

A_j = area of contact zone between jack shoes and the segment face, mm^2

A_s = area of reinforcing bars, mm^2

a = distance from edge of vacuum lift pad to edge of segment in the load case of stripping (demolding), or dimension of final spreading surface under thrust jack forces, mm

a_l = transverse length of contact zone between jack shoes and the segment face, mm

a_t = transverse length of stress distribution zone at the centerline of segment under thrust jack forces, mm

b = average width of tunnel segment also known as the ring length, or width of tested specimen, m

C = cos(θ) in the elastic equation method

$C2$ = cos2(θ) in the elastic equation method

$C3$ = cos3(θ) in the elastic equation method

C_c = compression force in the concrete section, N

C_t = tensile force in the section due to fiber reinforcement, N

D_e = external diameters of the tunnel segmental lining, m

D_i = internal diameter of the tunnel segmental lining, m

d = thickness of tested specimen, or total width of the segment cross section, mm

d_1 = length of load transfer zone for the case of longitudinal joint bursting load, mm

d_{burst} = centroidal distance of bursting force from the face of section, mm

d_c = concrete cover over rebar, mm

d_k = contact width for the case of longitudinal joint bursting load, mm

d_s = distributed width of tension block inside the segment for the case of longitudinal joint bursting, mm

E = modulus of elasticity of concrete, MPa

E_{cm} = modulus of elasticity of concrete, MPa

E_s = oedometer stiffness of the ground also known as E_{oed}; or modulus of elasticity of rebar, MPa

EI = flexural rigidity of segmental lining considering a unit width, $N.m^2$

e = eccentricity, mm

e_l = eccentricity of normal (axial) force defined as M/N, mm

e_k = eccentricity of joint contact zone considering gasket and caulking recesses, mm

e_{anc} = eccentricity of jack pads with respect to the centroid of cross section, or maximum total eccentricity in longitudinal joints consisting of force eccentricity and eccentricity of load transfer area, mm

F = forces acting on bottom segment due to self-weight of segments positioned above, N

F_{sd} = bursting tensile forces developed close to longitudinal joints, N

$F_{sd,r}$ = spalling tensile forces developed close to longitudinal joints, N

$F_{sd,2}$ = secondary tensile forces developed close to longitudinal joints, N

f_y = yield stress of required reinforcing bars, MPa

f_1 = first peak flexural strength, MPa

f_{bot} = stress at the extreme bottom fiber of concrete section, MPa

f'_c = specified compressive strength of concrete segment, MPa

f_{cd} = concrete design compressive strength, MPa

f_{ck} = concrete characteristic compressive strength, MPa

f_{ctd} = fiber-reinforced concrete design tensile strength, MPa

$f_{ct,eff}$ = concrete tensile strength, MPa

f'_{co} = compressive strength of partially loaded concrete surface, MPa

>> List of symbols and abreviation

f^D_{150} = residual flexural strength at net deflection of L/150, MPa

f^D_{600} = residual flexural strength at net deflection of L/600, MPa

f'^D_{150} = specified residual flexural strength at net deflection of L/150, MPa

f'^D_{600} = specified residual flexural strength at net deflection of L/600, MPa

f^D_{150r} = required average residual flexural strength at net deflection of L/150, MPa

f^D_{600r} = required average residual flexural strength at net deflection of L/600, MPa

f_{Ftu} = fiber-reinforced concrete tensile strength at ultimate limit state, MPa

f_{R3} = residual flexural strength of fiber-reinforced concrete beam corresponding to crack mouth opening displacement of 2.5 mm, MPa

f_{R4} = residual flexural strength of fiber-reinforced concrete beam corresponding to crack mouth opening displacement of 3.5 mm, MPa

f_{R1} = residual flexural strength of FRC beam corresponding to crack mouth opening displacement of 0.5 mm, MPa

f_{r1k} = characteristic residual flexural strength of fiber-reinforced concrete for serviceability limit state, MPa

f_{r3k} = characteristic residual flexural strength of fiber-reinforced concrete for ultimate limit state design, MPa

f_s = stress in rebar, MPa

f_t = specified splitting tensile strength, MPa

g = self-weight of the segments per unit length, N/mm

H = overburden depth, m

H_w = groundwater depth, m

h = thickness of tunnel segment, mm

h_{anc} = length of contact zone between jack shoes and the segment face, mm

I = moment of inertia of segment for nominal lining thickness, mm^4

I_j = moment of inertia at the joint (often taken as zero in the design), mm^4

I_r = reduced moment of inertia of the lining due to the presence of segment joints, mm^4

k = required ring taper, mm; or coefficient of subgrade reaction, kg/m^3

k_r = subgrade reaction modulus in the radial direction, MN/m^3; or Janssen rotational spring stiffness of segment joints, kN.m

k_t = subgrade reaction modulus in the tangential direction, MN/m^3; or in crack width analysis, a factor depending on the duration of loading (0.6 for short and 0.4 for long term loading)

L = distance between the supports, mm

lt = height of contact area between segments in longitudinal joints, mm

M = bending moment, kN.m

M_n = nominal resistance bending moment, kN.m

n = number of segments per ring excluding the key segment ($n \geq 4$); or number of layers of tensile rebar in crack with analysis

N = axial hoop force, N

N_{Ed} = maximum normal force due to permanent ground, groundwater and surcharge loads, N

P_0 = surcharge load, N

P_{e1} = vertical earth pressure at crown of lining applied to the elastic equation method, MPa

P_{e2} = vertical earth pressure at invert of lining applied to the elastic equation method, MPa

P_g = segment dead load, MPa

P_{w1} = vertical water pressure at crown of lining applied to the elastic equation method, MPa

P_{w2} = vertical water pressure at invert of lining applied to the elastic equation method, MPa

P_{pu} = factored jacking force applied on each jack pad in circumferential joints, or maximum factored normal force from the final service loads transferred in longitudinal joints, MPa

>> List of symbols and abreviation

$qe1$ = horizontal earth pressure at crown of lining applied to the elastic equation method, MPa

$qe2$ = horizontal earth pressure at invert of lining applied to the elastic equation method, MPa

$qw1$ = horizontal water pressure at crown of lining applied to the elastic equation method, MPa

$qw2$ = horizontal water pressure at invert of lining applied to the elastic equation method, MPa

R = radius from centerline of lining, m; or minimum radius of alignment curvature, m; or reaction force in the scheme of segments stacking for storage and transportation, kN

r_o = radius of excavated tunnel, m

s = maximum rebar spacing, mm

S = distance between stack supports and free edge of segments in the load case of segment storage, m; also sin(θ) in the elastic equation method

$S2$ = $\sin^2(\theta)$ in the elastic equation method

$S3$ = $\sin^3(\theta)$ in the elastic equation method

s_s = sample standard deviations of test results

$s_{r,max}$ = maximum crack spacing, mmT_{burst} = bursting force, N

w = segment self-weight, kg/m; or maximum crack width, mm

y_c = distance from extreme compression fiber to centroid of equivalent compression force in the section, mm

y = distance from extreme tension fiber to the neutral axis, mm

β = dimension of the loaded surface under thrust jack forces according to Iyengar diagram, mm; or in crack width analysis, ratio of the distance between neutral axis and tension face to the distance between neutral axis and centroid of rebar

$\Delta P_{g,\,invert}$ = vertical gradient of radial grout pressure between the crown and invert of tunnel, MPa

δ = displacement of lining applied to the elastic equation method; or opening distance of longitudinal joint on one side due to poor ring build and tunnel deformation, mm

δ_d = diametrical distortion, mm

ε_{tu} = ultimate tensile strain

ε_{cu} = ultimate compressive strain

ε'_{csd} = compressive strain due to shrinkage and creep equal to 150×10^{-6}

ϕ = strength reduction factor; or rebar diameter, mm

ϕA = outer diameter of the segmental ring

γ = material safety factor

λ = slenderness defined as the ratio between the developed segment lengths and its thickness

θ = angle from crown in the elastic equation method; or rotation of segment joints, radian

$\rho_{concrete}$ = specific weight of concrete, kg/m^3

ρ_{eq} = equivalent specific weight of grout, kg/m^3

$\sigma_{c,i}$ = compressive stresses developed under jack pads because of axial effects of thrust jack forces, MPa

σ_{cm} = fully spread compressive stress in method of the Iyengar diagram, MPa

σ_{cx} = bursting tensile stresses using the Iyengar diagram, MPa

σ_p = specified post-crack residual tensile strength of FRC segment, MPa

τ = birdsmouthing or opening of longitudinal joint on one side due to deformation of the tunnel lining, radian or degrees

τ_{yield} = shear yield strength of grout, MPa

>> Preface

The rapid progress of mechanized tunneling to market prominence has continued and even exceeded expectations following the general worldwide trend in construction towards mechanization and automation.

Mechanized tunneling utilizing a shield Tunnel Boring Machine (TBM) is often associated with installing precast concrete segmental linings. The design and construction of these elements requires comprehensive knowledge and a good understanding of the principles specific to this type of lining.

ITA WG2 published the “Guidelines for the design of shield tunnel design” in 2000. However, continuously evolving technologies and consequent developments and clarifications of related design approaches make updates and revisions of ITA guidelines inevitable.

The ITA WG2 2019 Guideline is intended to fully update the original WG2 publication “Guidelines for the design of shield tunnel design” (2000) and it is a stand-alone document. However, in the text reference is still made to 2000 guideline for few specific aspects which general description is considered to remain valid.

The 2019 document consolidates most recent developments, international best practices, and state-of-the-art information on all aspects of design and construction of precast segmental tunnel linings. It is addressed to experienced tunnel engineers for specific needs of each project, and to entry-level engineers to provide a comprehensive general guide on major design and construction concepts related to segmental lining.

Elena Chiriotti, Incas Partners
ITA WG2 Animator

Ron Tluczek, Gibb
ITA WG2 Vice-Animator

1 >> Scope ans limitations

This document provides guidelines for the design and construction of one-pass precast reinforced concrete segmental linings for TBM tunneling in soft ground, weak and fractured hard rock. Two-pass lining systems, which are less frequently used in modern tunnels, are not specifically discussed but the basic guidelines presented in this report will still be applicable. If required, more information on the two-pass lining system can be found in the ITA WG2 (2000) guidelines. The guidelines and recommendations in this document can be applied to various tunnels including road, railway, subway and water transfer, as well as utility tunnels for potable and waste water, gas pipelines, and power cables.

The structural considerations presented in this document outline the procedures for designing concrete tunnel segments to withstand the commonly encountered temporary and permanent load cases occurring during the production, transportation, construction and final service phases.

Segmental ring geometry, design procedures, detailed design considerations for concrete, reinforcing bars and fiber reinforcement, and construction aspects (e.g., gasket systems, connection devices and segment tolerances) presented in this guideline reflect current global practice, and are based on design codes, standards, and guidelines related to precast segments in the tunneling and concrete industries.

This document does not address the actions of non-linear effects (e.g. bedding), thermal variations, or internal loads (such as internal pressure, impact loads, brake loads, etc.) within the tunnels. While some structural design portions of this guideline present the procedures adopted by specific codes, they are indicative and can be extended to other structural regional or international codes.

CODE	INSTITUTION	TITLE
ACI 544.7R (2016)	American Concrete Institute (ACI)	Report on Design and Construction of Fiber Reinforced Precast Concrete Tunnel Segments
AFTES (2005)	French Tunneling and Underground Engineering Association (AFTES)	Recommendation for the design, sizing and construction of precast concrete segments installed at the rear of a tunnel boring machine (TBM)
BSI PAS 8810 (2016)	British Standards Institute (BSI)	Tunnel design. Design of concrete segmental tunnel linings. Code of practice.
DAUB (2013)	German Tunnelling Committee (DAUB)	Lining Segment Design: Recommendations for the Design, Production, and Installation of Segmental Rings
JSCE (2007)	Japan Society of Civil Engineers (JSCE)	Standard Specifications for Tunneling-2006: Shield Tunnels
LTA (2008)	Singapore Land Transport Authority (LTA)	Civil Design Criteria for Road and Rail Transit Systems
ÖVBB (2011)	Austrian Society for Concrete and Construction Technology (ÖVBB)	Guideline for Concrete Segmental Lining Systems
STUVAtec (2005)	German Research Association for Underground Transportation Facilities	STUVA Recommendations for Testing and Application of Sealing Gaskets in Segmental Linings, Tunnel, 8 (2005)

Table 1: Relevant Codes

2.1 LIMIT STATE OR LOAD AND RESISTANCE FACTOR DESIGN

Currently, Limit State Design (LSD) also known as Load and Resistance Factor Design (LRFD) is utilized to design precast concrete tunnel segments. Limit State Design requires the structure to satisfy two principal criteria: the Ultimate Limit State (ULS) and the Serviceability Limit State (SLS). A limit state is a condition of a structure beyond which it no longer fulfils the relevant design criteria. LSD is a design philosophy that considers the variability in the prediction of loads, and properties of the structural elements and employs specified limit states to achieve its objectives for constructability, safety, and serviceability.

Concrete precast tunnel segments should be designed using load and strength reduction factors for specific load combinations as specified in concrete design codes such as ACI 318-14, EN 1992-1-1 (2004), ACI 544.7R (2016), fib Bulletin 83, (2017), AASHTO DCRT-1-2010 or the WG2 report 21373-ITA-Report-16-WG2-BD_P "Twenty years of FRC tunnel segments practice" (2016). Care should be taken to ensure that a consistent set of load or strength reduction factors are utilized and that various codes are not "mixed and matched".

2.2 GOVERNING LOAD CASES AND LOAD FACTORS

Current practice in the tunnel industry is to design the segmental tunnel lining for the following load cases, which occur during segment manufacturing, transportation, installation, and service conditions :

- Production and Transient Stages
  - (a) segment stripping (demolding)
  - (b) segment storage
  - (c) segment transportation
  - (d) segment handling including segmental ring erection
- Construction Stages
  - (e) tunnel boring machine (TBM) thrust jack forces
  - (f) tail skin back grouting pressure
  - (g) localized back grouting (secondary grouting) pressure
- Service Stages
  - (h) ground pressure, groundwater pressure, and surcharge loads
  - (i) longitudinal joint bursting load
  - (j) loads induced due to additional distortion
  - (k) other loads (for example, earthquake, fire, explosion, aerodynamic, mechanical, electrical and temperature loads as well as internal loads and the effect of adjacent tunnels)

In the design procedure, load factors are applied for specific load combinations. Typical load factors are shown in Table 2 for various governing load cases. Utilizing these load factors, the resulting axial forces, bending moments, and shear forces may be calculated to design the reinforced concrete segmental lining. For illustration, as an example the table below provides factored load combinations for segmental tunnel linings according to ACI 544.7R, 2016. If different load factors are provided by local codes, these should be used in preference.

2.3 DESIGN APPROACH

Initially an appropriate segment geometry is selected (i.e. thickness, width and length) with respect to tunnel size and anticipated loading cases. Using load factors recommended by structural codes, the design strength of the segments is compared with the required strength for specific load cases in order to determine the required concrete compressive strength (fc or fcd) and type and amount of reinforcement. The final designed geometry, compressive strength, and reinforcement are specified in order to ensure that the precast segmental lining satisfies all service conditions.

ITA WG2 (2000) provides a flowchart of shield tunnel lining design that start with inputs related to "Planning of Tunnel Project" including alignment, geology, specification/code/standard to be used and function/capacity to be given to tunnel. These inputs are connected to different design processes such as load condition, lining condition, computation of lining internal forces and check of lining safety. All these processes are connected to decision boxes such as safe and economical design and final approval and end with execution of construction works, For more details on the design approach for precast concrete tunnel segments, refer to ITA WG2 (2000).

LOAD CASE	LOAD FACTORS
Load case 1: stripping (demolding)	$1.4w$
Load case 2 : storage	$1.4\ (w + F)$
Load case 3 : transportation	$1.4\ (w + F)$
Load case 4 : handling	$1.4w$
Load case 5 : thrust jack forces	$1.2J$ (1.0 if max machine thrust available)
Load case 6 : tail skin grouting	$1.25\ (w + G)$
Load case 7 : secondary grouting	$1.25\ (w + G)$
Load case 8 : earth pressure and groundwater load	$1.25\ (w + WA_p) + 1.35\ (EH + EV) + 1.5\ ES$
Load case 9 : longitudinal joint bursting	$1.25(w + WA_p) + 1.35\ (EH + EV) + 1.5\ ES$
Load case 10 : additional distortion	$1.4M_{distortion}$

Note: w = self-weight; F = self-weight of segments positioned above; J = TBM jacking force; G = grout pressure; WA_p = groundwater pressure; EV = vertical ground pressure; EH = horizontal ground pressure; ES = surcharge load; and $M_{distortion}$ = Additional distortion effect

Table 2 : Example of load factors for various governing load cases (ACI 544.7R, 2016)

3 >> SEGMENTAL RING GEOMETRY AND SYSTEMS

Segmental tunnel linings are installed in the rear of the TBM shield and are generally in the shape of circular rings. The size of the ring is defined by the tunnel internal diameter (intrados), thickness, and length of the ring.

3.1 INTERNAL DIAMETER OF THE BORED TUNNEL

The dimension of the tunnel intrados is determined by considering the internal space requirements, which depends on the intended use of the tunnel and client requirements.

For railroad and subway tunnels, the inner dimensions of the tunnel are typically governed by the train clearance envelope (i.e. structural gauge), track structure, drainage trough, structure of the overhead catenary, when applicable, and emergency walkways (i.e. egress space). For double track tunnels, the tunnel intrados is additionally governed by the distance between the centers of tracks. Having set the tunnel intrados, the utility services (i.e. electrical, water, telecommunication, etc.) are installed in the unoccupied space. Sufficient ventilation space is generally provided if egress space and cross passageways are provided (RTRI, 2008).

For road tunnels, the geometrical configuration of the tunnel must satisfy the required horizontal and vertical traffic clearances including lane widths, shoulders, sidewalks and barriers. Additional space may be required for drainage, ventilation, lights, traffic control systems, safety systems including water supply pipes for firefighting, emergency telephones, monitoring equipment of noxious emissions and visibility (AASHTO, 2010). Beyond vehicle envelope and space required for operation equipment, other aspects such as ventilation modes and safety considerations may have considerable influence on the tunnel size.

For utility tunnels, the tunnel intrados will be governed by the size of the utilities (i.e. electrical cables, wet services, telecommunications, etc.) and by the space required for maintenance.

The tunnel intrados for water and wastewater or Combined Sewer Overflow (CSO) tunnels will be governed by the design volumes of conveyed water or design storm (e.g. 1 year, 25 years, 100 years) specified by local authorities or predicted by system modeling.

The minimum tunnel intrados is the smallest tunnel which encircles all these elements. Note that for the spaceproofing of road and railway tunnels, it is crucial to consider the impact of maximum super-elevation due to the rotation of clearance envelopes. In determining the tunnel intrados, allowance should be made for construction tolerances. For example, DAUB (2013) recommends a radius tolerance of R = ±100 mm for TBM-bored tunnels.

3.2 THICKNESS OF THE SEGMENTAL LINING RING

Initially a thickness is assumed for the segmental lining ring which is later optimized during detailed design. The following guidelines are given to assist in choosing an initial lining thickness.
A review of more than 100 projects published in ACI 544.7R (2016), AFTES (2005), Groeneweg (2007) and Blom (2002) indicates that the ratio of internal tunnel diameter (ID) to the lining thickness falls in the range of 18-25 for tunnels with an ID of more than 5.5m, and 15-25 for tunnels with an ID of 4.0m to 5.5m. JSCE (2007) recommends that the ring thickness should be less than 4% of the outer diameter of the segmental ring, which translates into an ID to thickness ratio of 23. For tunnels under 4m diameter, no correlation could be found and the lining thickness generally ranges from 150mm to 280mm. Here the lining thickness is dictated by construction and design loading requirements.

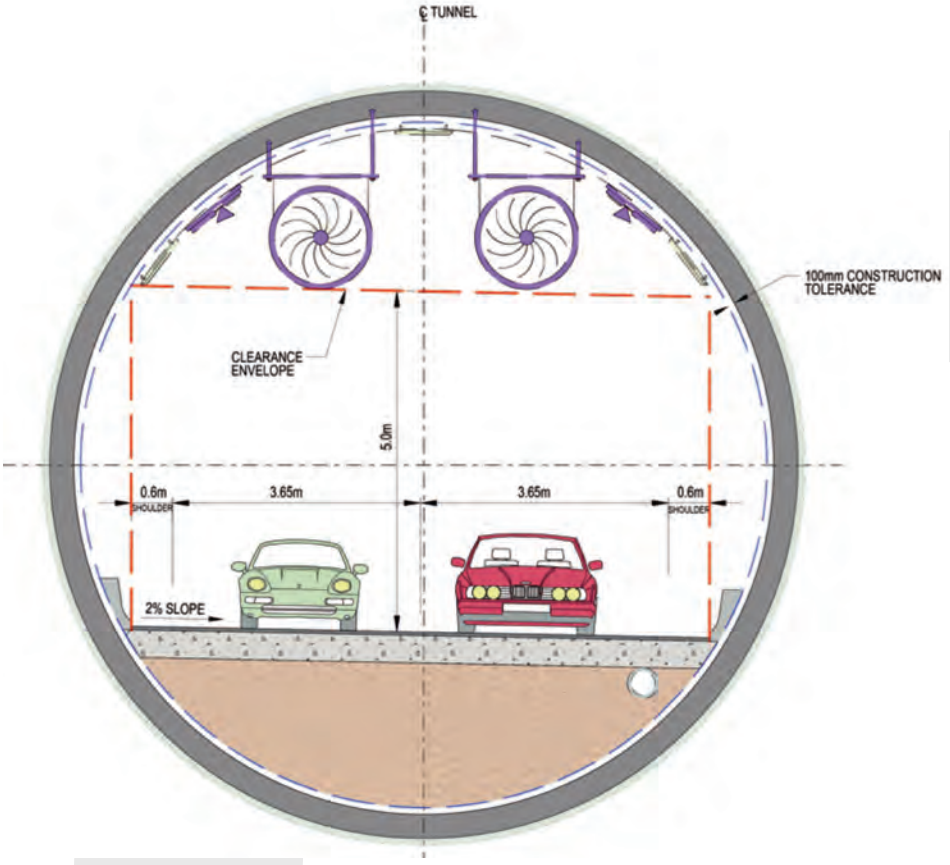

Figure 1 : Example of spaceproofing section for TBM-bored road tunnel (dimensions variable according to national standards).

The segment wall thickness should provide sufficient space and clear distance for gaskets and caulking recesses. The minimum segment wall thickness must also be compatible with the bearing surface area of the TBM longitudinal thrust cylinders (AFTES, 2005).

To achieve a robust design, the segment thickness should be capable of handling all loading cases and service conditions. The lining thickness may be increased in order to cater for unforeseen loads, particularly if sealing gaskets are installed.

In addition to structural factors, the final lining thickness should consider durability and if a sacrificial layer is considered for the design life of the tunnel, (for instance, for CSO tunnels) then the sacrificed layer thickness should be added to the required structural thickness.

The TBM shield outer diameter is determined by adding the tail clearance and shield skin plate thickness, also known as overcut, to the segmental lining outer diameter (RTRI, 2008). The shield outer diameter has an influence on the minimum radius of curvature of the alignment. A review of the more than 100 tunnel projects with different sizes (JSCE 2007) indicates that when the shield outer diameter is less than 6m, between 6-10m, or more than 12m, the minimum radius of curvature can be limited to 80m, 160m, and 300m, respectively. In practice, however, larger radii are being utilized and the above-mentioned limits may be considered to be lower bound limits for the radius of curvature. It should be noted however, that the minimum radius of curvature is a function of ring geometry (taper, ring width), overcut, shield design (articulated or not) and radial gap between segment and tailskin rather than just the shield outer diameter. All these parameters should be taken into account when determining the minimum curve radius.

3.3 LENGTH OF THE RING

The length of the lining ring needs to be optimized for the efficiency of the tunnel works. Depending on the tunnel diameter, the ring length can range between 0.75m and 2.50m (DAUB, 2013). On one hand, it is desirable to have a short ring length for ease of transportation and erection, construction of curved sections, and to reduce the length of the shield tail. On the other hand, it is desirable for the ring length to be larger to reduce production cost, the number of joints, the total perimeter of segments and gasket length, the number of bolt pockets where leakage can occur, as well as increasing the construction speed (JSCE 2007). Generally, for smaller diameters, the available space for segment supply and handling defines the limitation of the ring length, whereas for larger diameters, segment weight and production are the limiting factors. Typically, a ring length of 1.5m would be used for tunnel diameters of 6m to 7m, increasing to a ring length of 2m for tunnels larger than 9m in diameter.

3.4 SEGMENTAL RING SYSTEMS

Different systems exist for tunnel segmental rings, these include parallel rings, parallel rings with corrective rings, right/left-tapered rings, and universal ring systems (see Figure 2).

Parallel ring systems consist of rings with parallel end faces and with circumferential faces perpendicular to the tunnel axis. This system is not inherently suitable for curves and is problematic where packing between the rings is required to restore line and grade. These joints cannot always be properly sealed as the packing reduces the compression in the gasket.

The parallel rings with corrective rings system utilizes the corrective rings for directional corrections. With this system, the requirement for different sets of formwork is the main disadvantage.

The right/left ring system generally consists of tapered rings with one circumferential face perpendicular to the tunnel axis and the other one inclined to the tunnel axis. A sequence of alternating right-tapered and left-tapered rings produces a straight drive. Alternatively, a sequence of right-tapered rings or left-tapered rings results in a curve with the minimum radius of curvature. Up and down directional corrections are achieved by rotating the tapered segment ring through 90° (ÖVBB, 2011). This ring system provides good sealing performance for an impermeable tunnel but the requirement for different sets of formwork is a disadvantage.

Currently, the universal ring system is the most conventional system, where both circumferential faces of the ring are inclined to the tunnel axis. As indicated in Figure 2, the ring taper is split between the two circumferential faces and all curves and directional corrections can be negotiated through the rotation of the segmental ring. The main advantage of this system is that only one type of formwork is required (ÖVBB, 2011). The required ring taper (k) to cater for the designed alignment can be calculated with the following formula :

$$k = \frac{\emptyset_A b}{R} \qquad \text{Eq. (1)}$$

Besides the minimum radius of curvature (R), a correction curve radius should be catered for which assists in returning a TBM back to the designed tunnel alignment. The correction curve radius should be at least 20% less than the smallest designed curve radius (DAUB, 2013).

Using the universal rings, a straight alignment can be achieved by rotating each alternate ring by 180°. Horizontal and vertical curves can be negotiated by partial rotation of the rings. In recent years, by using advanced software for guiding TBM's, universal rings can produce straight drives with the key segments always above the springline by adjusting the drive error (of less than a few millimeters) in two or three consecutive rings.

a

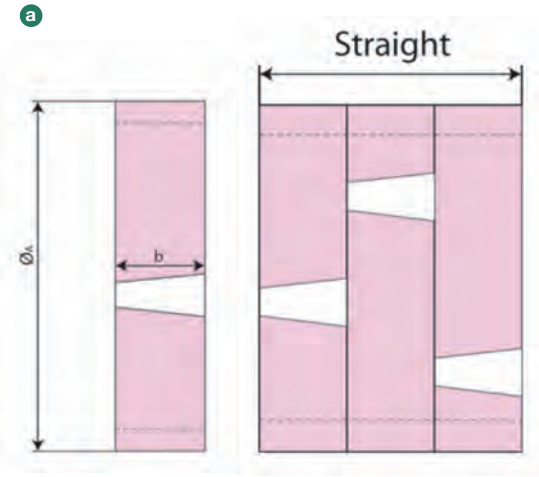

(a) Parallel rings

b

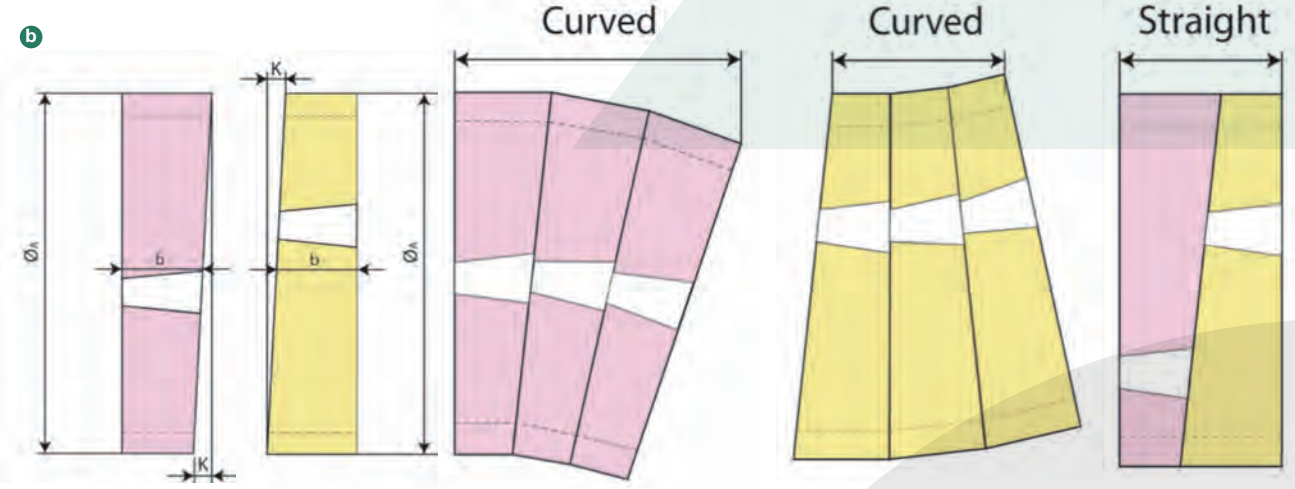

(b) Right/left tapered rings

c

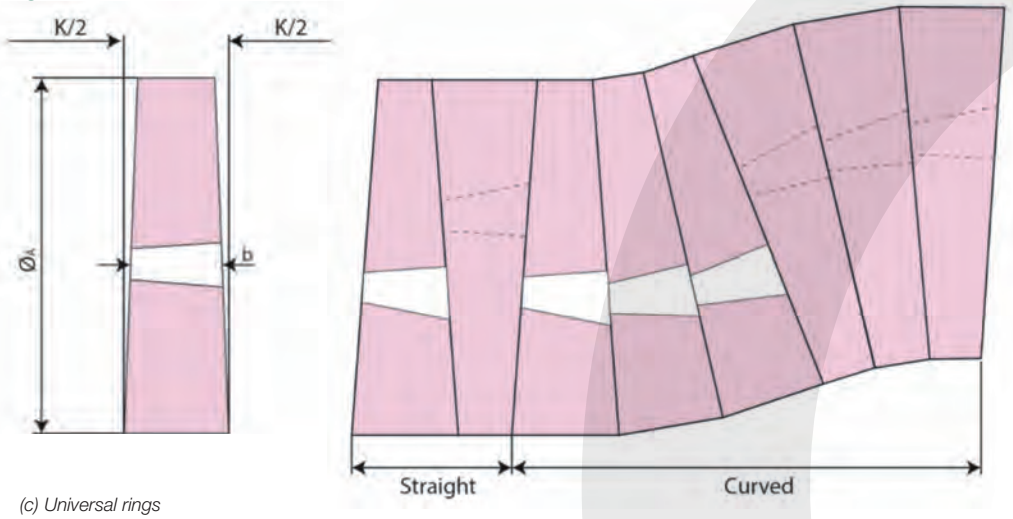

(c) Universal rings

Figure 2 : Different ring systems, tapering and curve negotiation schematics

3.5 RING CONFIGURATION

One of the main considerations in segmental lining design is the number of segments required to form a ring. Similar to the ring length, the number of ring segments needs to be optimized for the efficiency of the tunnel works. The shorter the length of each segment, the easier the transportation and erection process. However, longer segments have less joints which result in a much stiffer segmental ring, reduced production cost as well as less hardware for segment connection, i.e. less gasket length and fewer bolt pockets where leakage can occur. More importantly, with fewer segments, the construction speed can increase significantly.

The space available in the back up of the TBM to turn and erect the segments is a major factor in setting the limit for maximum length of segment. In very large diameter tunnels, however, the segment weight is a decisive factor in selection of the maximum length of segment rather than the available space for handling the segment.

The slenderness of the tunnel segment (λ), which is defined as the ratio between the curved length of the segment along its centroid and its thickness, is a key parameter in deciding segment length. A review of tunnel projects indicates that tunnel lining rings generally contain a number of segments that yields a segment slenderness ratio between 8 to 13, with FRC segments generally around the lower bound of this range. The number of segments in a ring or thickness of segments can be increased to reduce the slenderness and flexural stresses especially during production and transient stages. With latest developments in fiber technology, FRC segments with segment slenderness of more than 10 and up to 12-13 have been successfully used in recent projects. However, with recent developments in fiber technology, FRC segments with segment slenderness ratios between 12 to 13 have been successfully utilized. Since segment thickness depends on several factors which are mostly project-specific (such as related design criteria and critical load cases) the resulting slenderness values can fall outside of the mentioned ranges in some specific cases. A construction consideration is that the number of segments should be compatible with the location of the TBM thrust jacks which are used to install the segments.

A review of tunnel projects indicates that for tunnels with a diameter of 6m or less, a ring with 6 segments is common. This configuration, also known as a 5+1 configuration, generally consists of 5 ordinary segments and one smaller key segment (Figure 3). However, a 4+2 configuration with 4 ordinary segments and two key segments alternating above and below the springline is also common.

In tunnels under 4m diameter, the ring can be divided into less segments, however, a ring of 6 segments is still common.

When the tunnel diameter ranges between 6m to 8m, a 6-segment ring may result in excessively long segments while an 8-segment ring can result in too short segments. In some cases, the size of the key segment is increased to reduce the size of the ordinary segments so that a 7-segment ring can be adopted.

For tunnels between 8m to 11m in diameter, a ring commonly contains 8 segments which consists of 7 ordinary segments and one smaller key segment, i.e. a 7+1 configuration.

For tunnel diameters between 11m to 14m a 9 segment ring is not preferred. Special solutions are required, such as dividing the ring into 8 segments (each covering 45o) and dividing one of the ordinary segments into key and counter-key segments (which cover 15o and 30 o). By utilizing such a configuration, excessively large key segments can be avoided, while at the same time the configuration is compatible with the TBM thrust jacking pattern for an 8-segment ring.

For tunnels larger than 14m, a 9+1 configuration is the most common configuration.
Note that the above mentioned ring configurations are typical in practice, and there are segmental lining configurations that differ.

Figure 3 : Typical 6 segment ring configuration (5+1) used for tunnels 6m diameter or less

3.6 SEGMENT GEOMETRY

The geometry of individual segments can be divided into four main categories or systems: hexagonal, rectangular, trapezoidal, and rhomboidal.

Hexagonal systems are assembled continuously from hexagonal shaped elements, with each element acting as a key segment (Figure 4a). The geometry of this system prevents the effective use of gaskets which compromises the watertightness of the lining. Because of this, this system is rarely used. This system does however allow for very rapid advance rates. In tunnels where water tightness is not a requirement, this system may be adopted as part of a two-pass lining system in combination with double-shield TBMs.

Rectangular systems are assembled in rings which consist of rectangular or slightly tapered segments with a wedge-shaped key segment (Figure 4b). This system can provide adequate watertightness and has the advantage of simple longitudinal joint geometry. However, staggered longitudinal joints cannot always be guaranteed, and star or crucifix joints may present themselves which may cause leakage. The main disadvantage of this system is that if dowels are pre-inserted into the segments,

it is difficult to place rectangular segments without impacting or rubbing the gasket on the adjacent segment. This may limit the use of fast-connecting dowels and promote the use of time-consuming bolt systems. This system, with fastening bolts, is still in use in large-diameter tunnels where the shear capacity of the dowel system connection between the circumferential joints may not be sufficient.

a

Figure 4a : Hexagonal system

Trapezoidal systems are assembled from an even number of trapezoidal segments in a ring often with the same length at centerline. Half the segments are installed as counter key segments (wider on the side of the previously placed ring) and the other half as key segments (narrower on the side of the previously placed ring). Initially, all counter key segments are installed and then the gaps are infilled with the key segments to form the complete ring (see Figure 4c). Advantages of this system are that the staggered longitudinal joints eliminate the possibility of star or crucifix joints and the fact that every alternate segment can be used as a key segment. The main disadvantage of this system is that in order to maintain a continuous penetration rate, higher TBM thrust jack forces are applied to the counter key segments while the key segments are installed. Also the installation process makes it difficult to place several key segments between the counter key segments.

b

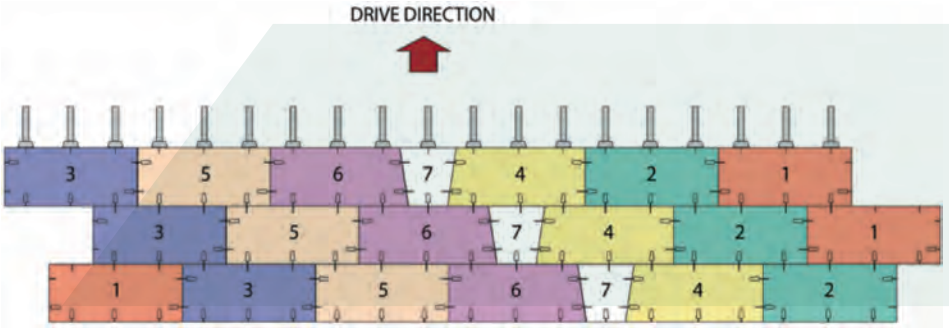

Figure 4b : Rectangular system

Rhomboidal or parallelogrammic-trapezoidal systems are assembled from ordinary segments in the shape of a parallelogram with key and counter key segments in the shape of a trapezoid (Figure 4d). The assembly procedure is carried out by initially installing the counter key trapezoidal element and then placing alternate parallelogrammic segments (left and right) around the ring. Ring assembly is completed by inserting an often smaller trapezoidal key segment. This system is currently the most common system as it eliminates crucifix joints, has improved sealing performance and allows for continuous ring erection. Other major advantages are that the angled segment joints prevent early rubbing of the gaskets during segment insertion and also facilitate the use of fast connecting dowels in circumferential joints. Bolted connections are usually required for longitudinal joints but in certain cases, longitudinal bolts may be replaced by guiding rods (see later).

c

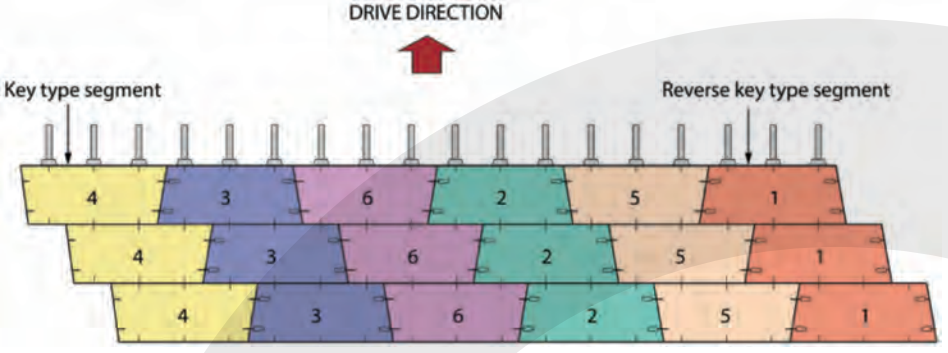

Figure 4c : Trapezoidal system

d

Figure 4d : Rhomboidal system

3.7 KEY SEGMENT GEOMETRY

ITA WG2 (2000) and JSCE (2007) present two different key segment tapering geometries according to methods historically utilized for ring assembly. ITA WG2 (2000) provides a geometry formulation which is specifically suitable for key segment insertion in the radial direction. In this method the key segment is inserted from the inside of the tunnel and the longitudinal side faces of the key segment are tapered in the direction of the tunnel radius.

The currently preferred method is to insert the key segment from the cut face side in the longitudinal direction of the tunnel, where the longitudinal side faces of the key segment are tapered in the longitudinal direction of the tunnel. The key segment tapering is defined by the angle of the side faces with respect to the longitudinal tunnel axis. Depending on the designers and contractors' previous experience, this tapering can be selected differently, but a taper angle of 8o to 12o defined with respect to the centerline of key segment is common. Tapering the joints results in reduced bearing surface available for TBM thrust jacks pushing against segments during the boring process. Therefore, design of taper angle has to be accounted for providing sufficient space between jack pads and segment corners to avoid spalling. Note that when adopting the rhomboidal or parallelogrammic-trapezoidal system, the same joint angle for key segments should be used for all other segments in the ring.

4 >> SEGMENT LINING DESIGN - PRODUCTION AND TRANSIENT STAGES

Production and transient loadings include all the loading stages from stripping (demolding) of the segment up to the time of segment erection within the TBM shield. During these phases, the internal forces and stresses developed during stripping (demolding), storage, transportation, and handling are considered for the design of the precast concrete segments. The loads developed during these stages result in significant bending moments with no axial forces.

4.1 SEGMENT STRIPPING (DEMOLDING)

Figure 5(a) shows a segment being stripped (demolded) from its formwork. The design considers the required strength when segments are stripped or demolded (i.e. 6 hours after casting) and is modeled as two cantilever beams loaded under their own self weight (w). As indicated in Figure 5(b), the self-weight (w) is the only force acting on the segment, and therefore, the applied load factor in ULS can be taken as 1.4 (see Table 2). The maximum generated bending moment and shear force are given in Table 3.

a

Figure 5(a) : Stripping (Demolding) segments from forms

b

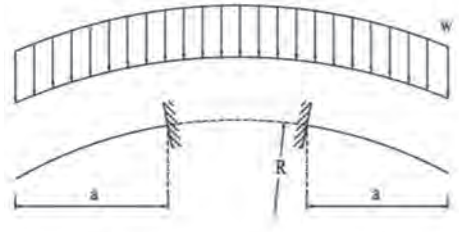

Figure 5(b) : forces acting on segments.

4.2 SEGMENT STORAGE

Segment stripping (demolding) is followed by segment storage, where segments are stacked to gain their required strength before transportation to the construction site. As shown in Figure 6(a), generally all segments comprising a full ring are piled up in one stack. Designers, in coordination with the segment manufacturer, provide the distance between the stack supports considering an eccentricity of e = 100mm between the locations of the stack support for the bottom segment and the supports of the upper segments. This load case can be modeled as a simply supported beam loaded under its self-weight (W) as well as the point loads from the upper segments (F) as shown in Figure 6(b). The applied load factor in ULS can be taken as 1.4 (see Table 2). This load factor does not consider dynamic loading during stacking. The maximum generated bending moment and shear force are given in Table 3.

a

Figure 6(a) : Segments stacking for storage and transportation

b

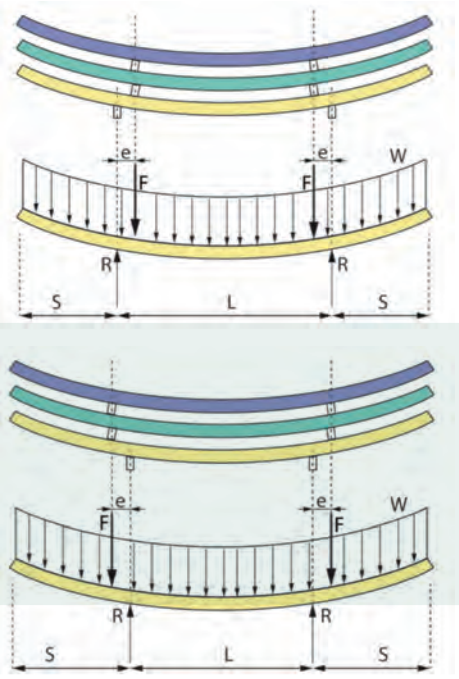

Figure 6(b) : schematics of forces acting on bottom segment with eccentricity on either side of bottom support.

4.3 SEGMENT TRANSPORTATION

During the segment transportation phase, precast segments are transported to the construction site and ultimately to the TBM trailing gear. Segments may encounter dynamic shock loads during this phase and as shown in Figure 6a, usually half of the segments of each ring are transported to the TBM on one carriage. Wooden blocks provide supports for the segments and these should be installed parallel to the segment axis. An eccentricity of 100mm is generally accepted for design. Similar to the segment storage phase, the load case can be modelled as a simply supported beam loaded under its self-weight (W) as well as the point loads from the upper segments (F) as shown in Figure 6(b). In addition to the load factor of 1.4 (see Table 2), it is recommended that a dynamic impact factor of 2.0 be applied to the forces during the transportation phase

(see Table 3). The maximum generated bending moment and shear force are given in Table 3.

4.4 SEGMENT HANDLING

Segment handling is carried out by specially designed lifting devices such as lifting lugs (Figure 7a) or vacuum lifters (Figure 7b). In such cases the design philosophy utilized for segment stripping (demolding) should be applied. However, when segments are handled by lifting lugs, the pullout capacity of the lifting inserts and concrete should be calculated (Figure 7c).

4.5 DYNAMIC LOAD FACTORS, MAXIMUM UNFACTORED BENDING MOMENTS AND SHEAR FORCES

Table 3 presents a summary of load cases with typical applied dynamic load factors and maximum unfactored bending moments for the various manufacturing, transportation, and handling stages. Designers should follow structural codes such as ACI 318-14, EN 1992-1-1 (2004) or any applicable local code to calculate the specific bending moments and shear forces in order to determine the required reinforcement to withstand these forces.

LOAD CASE NUMBER	LOADING CASE	DYNAMIC LOAD FACTOR	MAXIMUM UNFACTORED BENDING MOMENT	LOAD FACTORS
1	*stripping (demolding)*	-	$wa^2/2$	wa
2	*storage*	-	$w(L^2/8-S^2/2)+F_1e$ $w(S^2/2)+F_1e$	wS $wL/2+F_1$
3	*transportation*	2.0	$w(L^2/8-S^2/2)+F_2e$ $w(S^2/2)+F_2e$	wS $wL/2+F_2$
4	*handling*	2.0	$wa^2/2$	wa

Notes: F1 is self-weight of all segments completing a ring, excluding bottom segment; F2 is self-weight of all segments placed in one truck or rail car for transportation phase, excluding bottom segment.

Table 3: Example of dynamic load factors, maximum unfactored bending moments and shear forces for various loading cases by ACI 544.7R (2016)

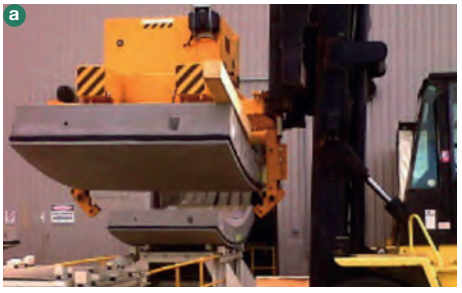

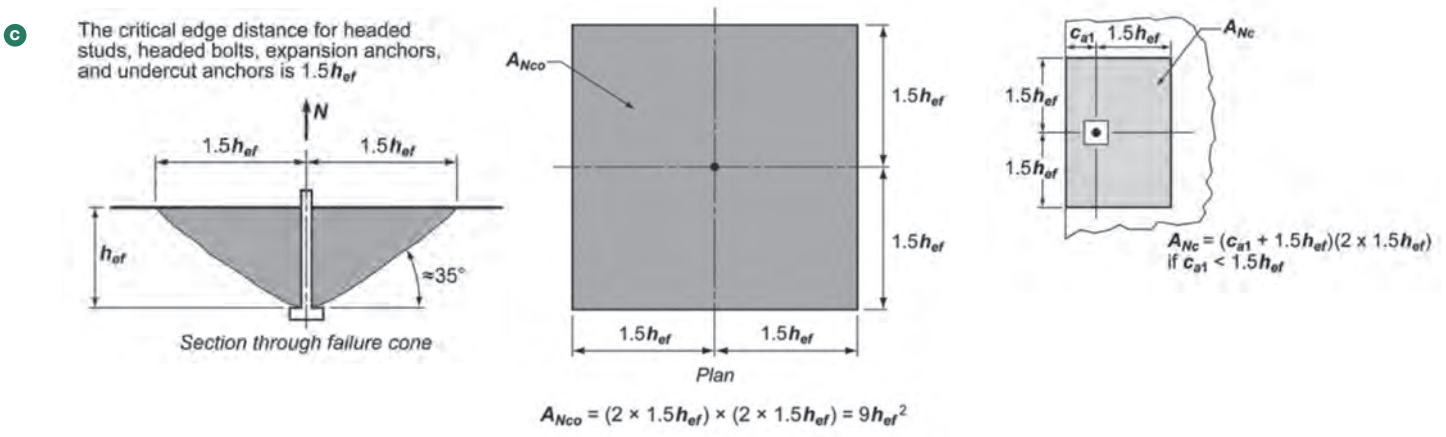

Figure 7 : Segment handling: (a) using lifting devices; (b) using vacuum lifter; and (c) diagram of pullout capacity of concrete during handling.

Construction loads on the segmental lining include the tunnel boring machine (TBM) jacking thrust loads on the circumferential ring joints and the pressures exerted against the exterior of the completed rings during grouting operations. Precast concrete segments are designed to resist significant bursting and spalling tensile stresses that develop along the circumferential joints due to advancement of the TBM. The segments must also be able to resist the axial forces and bending moments that develop when the annular space between the segment and the ground is pressure-filled with grout, initially during backfilling of the tail skin void and then during secondary grouting that may be required to ensure complete contact is achieved with the ground.

5.1 TUNNEL BORING MACHINE THRUST JACK FORCES

After assembly of a complete ring, the tunnel boring machine (TBM) advances by thrusting against the most recently assembled ring (a partially assembled ring is shown in Figure 8a). As part of this process, the TBM jacks bear against the jacking pads placed along the exposed circumferential joint. High compression stresses develop under the jacking pads which result in the formation of significant bursting tensile stresses deep within the segment (see Figure 8b). Furthermore, spalling tensile forces are generated between adjacent jack pads along the circumferential joint.

Due to the various geologic materials that can be encountered, different methods are used for estimating TBM thrust. For tunnel excavation through rock, TBM thrust can be estimated by summing the forces required to advance the machine. These forces include the forces necessary for boring through the rock, the friction between the surface of the shield and the ground, and the hauling resistance of back-up systems. Methods proposed by Fukui and Okubo (2003) or the Colorado School of Mines (CSM) (Rostami 2008) can be used to evaluate the rock thrust based on rock strength, tunnel diameter, and cutter characteristics (Bakhshi and Nasri 2013a). For soft ground tunneling applications, the method presented by JSCE (2007) can be used to calculate penetration resistance based on earth or slurry pressure that acts at the cutting face.

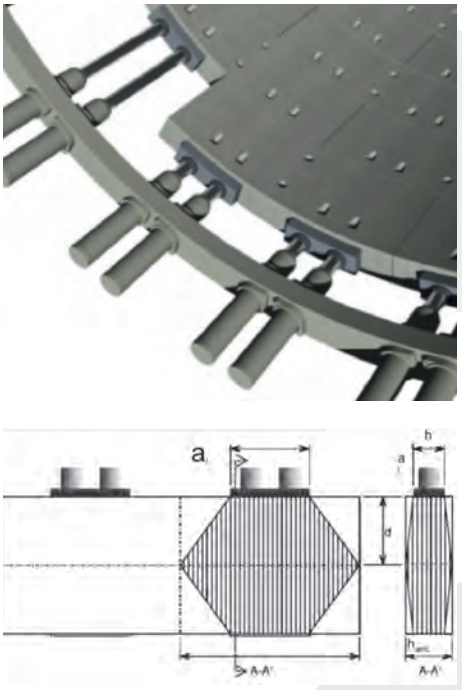

disturbance area for strut stress in transverse direction

disturbance area for strut stress in radial direction

Figure 8(a) : Thrust jacks pushing on circumferential joints; and (b) schematics of a simplified disturbance area of strut under TBM jack shoes (Groeneweg 2007).

Once the required machine thrust has been estimated for the ground conditions, the average thrust force per jack pair is determined. On sharp curves, the machine thrust is higher on the convex side of the curve than on the concave side and the different jacking loads on the segments should be considered. A simple technique used to account for the increased loading on the convex side is to double the jacking loads. Different jacking loads on individual segments should also be taken into account. When the machine characteristics are unknown, a load factor should be used. For illustration, as an example, ACI 544-7R (2016) recommends a value of 1.2 for this load factor. However, when the machine's characteristics and total thrust are known, the maximum jacking forces cannot be exceeded and a load factor of 1.0 should be used.

Different analytical and design methods are available which include simplified equations for bursting forces (ACI 318-14, DAUB, 2013), the Iyengar (1962) diagram, and two- and three-dimensional finite element simulations. These are discussed in the following sections.

5.1.1 Simplified equations

For post-tensioned anchorage zones in pre-stressed concrete sections, structural concrete codes such as ACI 318-14 permit the use of simplified equations (Eq. 2) to determine the bursting force, T_{burst}, and the centroidal distance from the face of the section, d_{burst}. These equations determine the forces and stresses that develop in the circumferential joints due to TBM advancement. DAUB (2013) recommends similar equations (Eq. 3) specifically for the design of tunnel segments.

$$ACI\ 318: \quad T_{burst} = 0.25 P_{jack}\left(1 - \frac{h_{anc}}{h}\right); \; d_{burst} = 0.5(h - 2e_{anc})$$

(Eq. 2)

$$DAUB: \quad T_{burst} = 0.25 P_{jack}\left(1 - \frac{h_{anc}}{h - 2e_{anc}}\right); \; d_{burst} = 0.4(h - 2e_{anc})$$

(Eq. 3)

The schematic representation of these equations is shown in Figure 9. If no specific value has been provided for e_{anc}, then the eccentricity of the jacking forces is generally

assumed to be 30mm. Figure 9 and Eqs. 2 and 3 represent the radial bursting stresses in the circumferential joints, but these equations are equally applicable to the tangential bursting stresses developed in the circumferential joints provided any eccentricity of the jack shoe relative to the joint is accounted for.

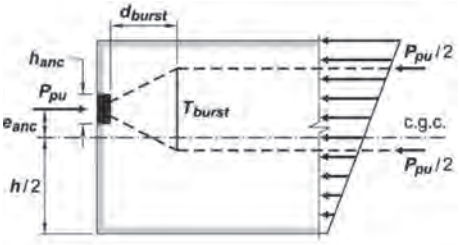

Figure 9 : Bursting tensile forces and corresponding parameters recommended by ACI 318-14; and DAUB (2013).

Reinforcing rebar or fiber reinforcement is designed to accommodate the significant bursting stresses developed by the jacking forces. Equations 4 and 5 may be utilized to determine the required area (A_s) of reinforcing bars with a yield stress of f_y for a reinforced concrete segment.

$T_{burst} = \emptyset\, f_y\, A_{s\_radial}$ for radial direction (Eq. 4)

$T_{burst} = \emptyset\, f_y\, A_{s\_tangential}$ for tangential direction (Eq. 5)

High compressive stresses can develop under the jacking pads due to the TBM thrust jacking forces. Assuming constant stress, these compressive stresses, $\sigma_{c,j,}$ can be estimated using Eq. 6.

$$\sigma_{c,j} = \frac{P_{pu}}{A_j} = \frac{P_{pu}}{a_j\, h_{anc}} \qquad \text{(Eq. 6)}$$

Because only part of the circumferential segment face is actually in contact with the pads, the allowable compressive stresses (f'_c or f_{cd}) can be factored to account for the strength of a partially pressurized surface. For illustration, as an example, ACI 318-14 recommends a formula to design the bearing strength of concrete (Eq. 7) with a partially loaded segment face. DAUB (2013) recommends a similar formula which is specifically used in the design of tunnel segment faces.

$$f'_{cb} = 0.85 f'_c \sqrt{\frac{A_d}{A_j}} = 0.85 f'_c \sqrt{\frac{a_j (h - 2e_{anc})}{a_j\, h_{anc}}} \qquad \text{(Eq. 7)}$$

5.1.2 The Iyengar diagram

The analytical method utilizing the Iyengar (1962) diagram may also be used to calculate the bursting tensile stresses in the design of tunnel segments (Groeneweg 2007). Again, the extent of load spreading and the resulting magnitude of the tensile stresses depends on the dimensions of the loaded surface (β), and the final distribution surface (a), as shown in Figure 10. Using this approach, the bursting tensile stresses (σ_{cx}), which vary significantly from the face that the TBM jacks bear against to the centerline of segment, are determined as a fraction of the fully disbursed compressive stress (σ_{cm} = F/ab). Reinforcing bars are designed to accommodate the total bursting tensile stresses which can be obtained from the integration of stresses or the area under the curve. The area of reinforcing bar required can be determined from Eqs. 4 and 5.

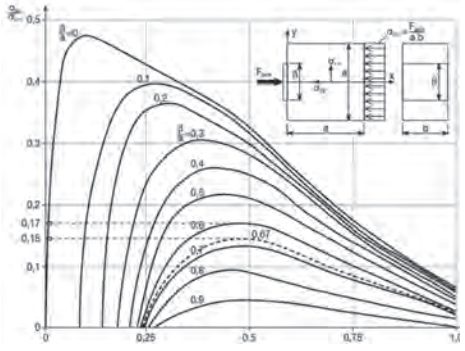

Figure 10 : Iyengar (1962) diagram for determining bursting tensile stresses (Groeneweg 2007).

5.1.3 Finite element method simulations

As shown in Figure 11, due to the concentration of the jacking forces, in addition to the bursting stresses under the jacking pads, spalling stresses develop in the areas between the jacking pads and in the areas between the jacking pads and the end faces of the segments. This problem has been analyzed with the three-dimensional finite element method (FEM), (Groeneweg 2007, Bakhshi and Nasri 2013b; 2014d).

While both linear elastic and non-linear FEM simulations can be performed for strength design, the latter is considered more suitable for service design as the non-linear analyses capture the response of the materials after failure with respect to crack opening. As shown in Figure 12, this load case is simulated by modeling segments from two adjoining rings. Factored jacking forces are applied along the contact area between the jacking pads and the segment face. Recesses for the gasket and stress relief grooves are modeled between the two segments to simulate the transfer of force through a reduced cross section. Just after installation, the compressive forces within the gasket are simulated by applying a reaction force using solid elements in the FEM program. With this approach, the translational degrees of freedom are fixed in all directions between the two installed segments. Results from the analysis are illustrated in Figure 13 which indicates the transverse and radial bursting loads under the jack pad and the spalling stresses in the areas between the jacking pads. The compressive stresses developed in this load case are illustrated in Figure 14 (Bakhshi and Nasri 2013b; 2014d).

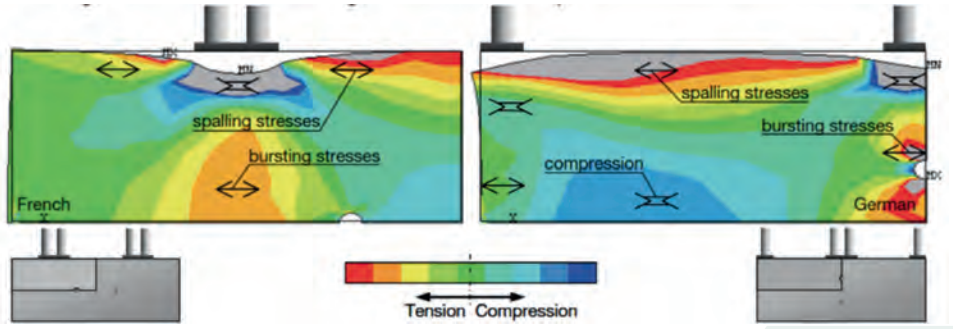

Figure 11 : Spalling and bursting stresses in segment joints due to jack thrust forces (Groeneweg 2007).

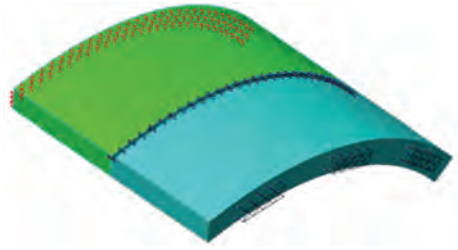

Figure 12 :Three-dimensional FEM model for load case of TBM thrust jack forces.

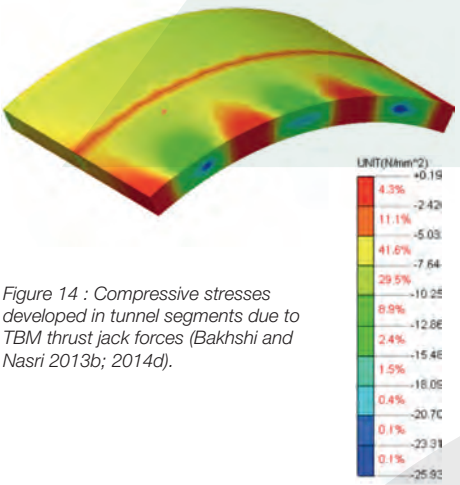

Figure 14 : Compressive stresses developed in tunnel segments due to TBM thrust jack forces (Bakhshi and Nasri 2013b; 2014d).

a

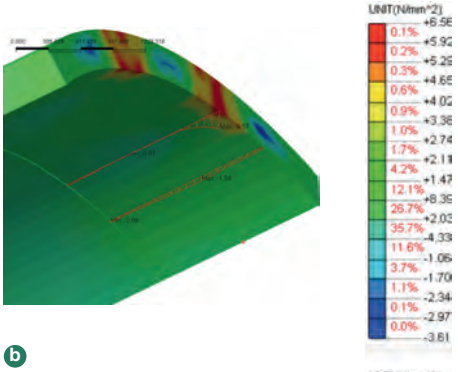

b

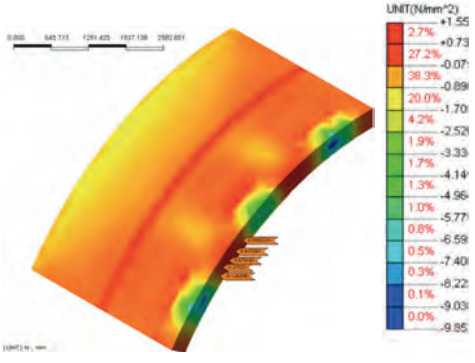

Figure 13 : Bursting and spalling tensile stresses developed in segments due to TBM thrust jack forces and gasket pressure: (a) transverse stresses; and (b) radial stresses (Bakhshi and Nasri 2013b; 2014d).

As can be seen from the above figures, the three-dimensional FEM simulation indicate that the spalling tensile stresses between the jack pads, and the jack pads and end faces can be as significant as the transverse bursting tensile stresses under the jacking pads (Bakhshi and Nasri 2013b). Precast tunnel segments should therefore be designed to withstand these high tensile stresses. Reinforcement is designed to accommodate the tensile forces which are determined by the integration of stresses through the tensile zone, similar to the Iyengar (1962) diagram method.

5.2 TAIL SKIN BACK-GROUTING PRESSURE

Tunnel rings are assembled within the shield of the tunnel boring machine (TBM). At this location, the excavated diameter of the tunnel is larger than the external diameter (extrados) of the tunnel ring. As shown in Figure 15, a void is created between the ground and the tunnel segmental lining. Loads on the lining are generated when back-grouting or filling this annular space with semi-liquid grouts under high pressure. Back-grouting is carried out to control and restrict settlement at the ground surface as well as to ensure intimate contact between the ring and the ground. Grouting material generally consists of sand, water, cement, and additives such as bentonite or plasticizers. Grout can be continuously injected into the annular space behind the TBM by means of grout pipes routed through the tail skin (Figure 15). Prior to its hardening, the grout has a very low shear strength of between 20Pa to 100Pa.

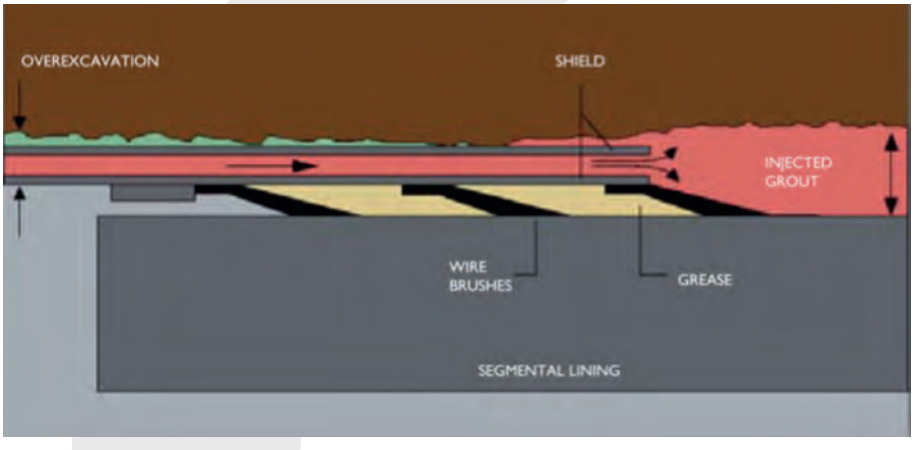

Figure 15 : Backfilling of tail-skin void (Guglielmetti et al. 2007).

To fill the annular space, the grout pressure needs to be greater than the hydrostatic head on the segmental lining. The grout pressure should also be less than the overburden pressure to prevent heave, hydrojacking, or hydrofracturing of the surrounding in-situ material. Grouting models (Zhong et al. 2011) can be developed that predict the optimal grout pressure by considering the combined effects of groundwater level, plasticity of grout, rate of advancement of the TBM, and the filling rate of the tail void.

AASHTO DCRT-1-2010 specifies that the maximum grout pressure on the lining should not be greater than 69 kPa above the groundwater pressure. However, in South East Asia, a maximum permissible grouting pressure of up to 150 kPa above the maximum groundwater pressure is often considered.

In this load case, the segmental lining ring is evaluated in cross-section perpendicular to the longitudinal direction of the tunnel and modeled as a solid ring with reduced flexural rigidity to account for the segment joints. Because the lining is initially surrounded by semi-liquid and fresh grout materials, no interaction is considered between the ring and ground. As illustrated in Figure 16, the back-grouting (cavity filling) load is modeled by applying radial pressure varying linearly from the minimum grout pressure at the crown to the maximum grout pressure at the invert of the tunnel. The self-weight of the lining and the grouting pressure are the only loads applied to the tunnel lining at this stage. For the load combination of self-weight and grout pressure, implementing load factors is suggested. For illustration, as an example, ACI 544.7R (2016) recommends a load factor of 1.25 for both loads. The analysis is performed using general structural analysis packages. As a result of these loads, significant axial forces and bending moments can be developed in the tunnel segmental lining. The precast segments should be designed to cater for the combined maximum bending moments and axial forces.

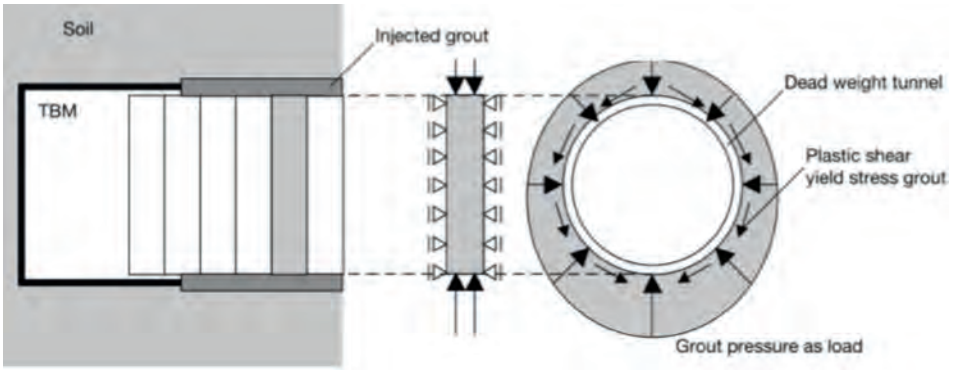

Figure 16 : Forces and definitions for load case of tail void back-grouting (Groeneweg 2007).

5.3 LOCALIZED BACK-GROUTING (SECONDARY GROUTING) PRESSURE

Localized back-grouting, also known as secondary or check grouting, is performed through holes that are pre-cast into the segments (Figure 17). The holes in the segments can be fitted with grout sockets that are screwed into position and remain closed with non-return valves and plastic covers during the ring installation process. Prior to the introduction of modern pressurized face machines, this grouting method was used to fill the annulus; however, delayed cavity grouting could result in the collapse of unstable ground into the annular space which could result in significant settlements. As such, this method is now primarily used for secondary grouting to verify whether the annular gap has been filled.

To model the effects of secondary grouting, the force is only applied to an isolated area of the lining. Following the ITA WG2 (2000) guidelines, this load case can be simulated utilizing the force distribution indicated in Figure 18. In this figure, the secondary grouting pressure is applied over one-tenth of the lining perimeter in the crown.

The lining for this load case is again modeled in cross-section perpendicular to the longitudinal direction of the tunnel using a solid ring with reduced flexural

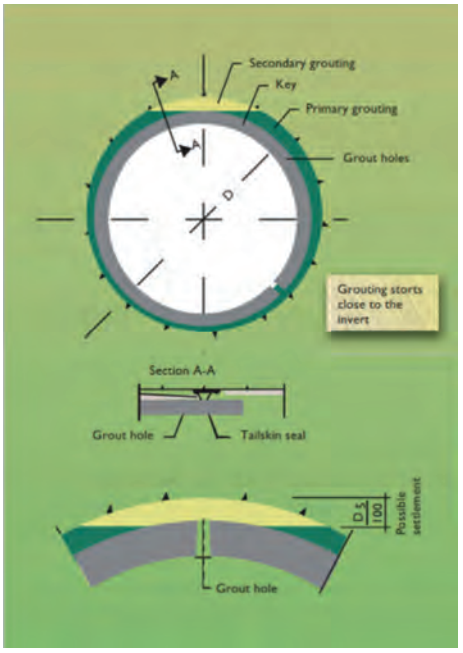

Figure 17 : Secondary grouting through segment grout hole (Guglielmetti et al. 2007).

rigidity to represent the segment joints. Because secondary grouting occurs long after the primary grouting materials have cured, it can be assumed that the tunnel lining is in full contact with the surrounding ground except in the local area where the secondary grouting is to be performed. To simulate the boundary condition for this case, the interaction between lining and surrounding ground or primary hardened grout can be modeled

using radial springs with the segments supported radially. Linear translational springs have been used to represent this type of interaction. The method described by USACE EM 1110-2-2901 (1997) is one method that can be used to determine the spring stiffness per unit of exterior tunnel surface. Using the same grout pressure in the crown as for cavity filling and with the radial spring stiffness, the bending moments and axial forces developed within the lining can be determined. This loading case results in small incremental axial forces with large bending moments. Precast segments should be designed for this load combination using axial force-bending moment interaction diagrams.

5.4 TBM BACKUP LOAD

The TBM backup load is applied on the segmental lining behind the shield. In order to control buoyancy, additional weight may be provided by the backup system inside the tunnel after ring installation and before placing ballast or installation of any precast buoyancy unit. TBM drawings as in Figure 19 indicate that this backup load is applied at specific locations on the tunnel lining intrados with two wheels on each ring. For this load case, punching shear should be considered with the assumption that the backup load is applied uniformly. The precast segments should be designed for the resulting factored bending moments, axial forces and punching shear for all critical cases (e.g. shallow cover, deep tunnel, etc) using axial force-bending moment interaction diagrams. This load case is often a governing load case in sub-sea and river crossing projects.

A consideration for the TBM backup load is the early stage strength (setting time) of the tail void grout and the TBM advance rate. The TBM advance rate may have to be limited to allow the tail void grout to achieve the strength required to support the first and second gantry.

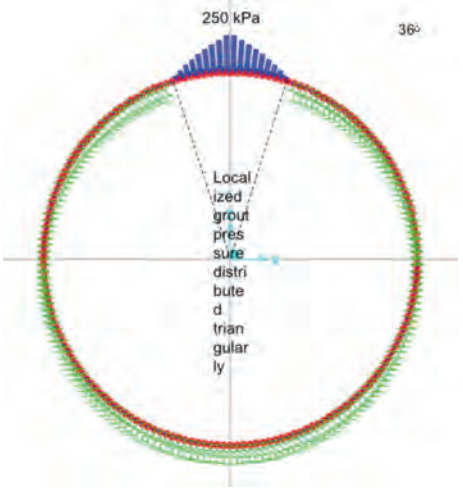

Figure 18 : Modeling localized grouting pressure applied over one-tenth of the lining (The grouting pressure of 250 kPa presented in this figure is indicative. The appropriate value will be project specific).

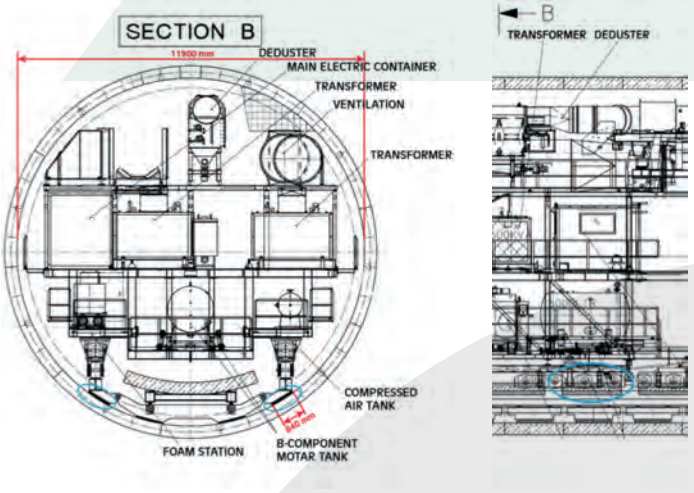

Figure 19 : Typical TBM details for a section behind the shield where backup loads are applied on segmental ring.

Forces in the lining during the final service stage are generated by the long-term loads imposed on the lining from the ground; groundwater; surcharges; internal loading and other factors such as, earthquake, fire, explosion, adjacent tunnels, and longitudinal bending moments which are generally specific to each tunnel. In addition, specific load cases such as hoop force transfer along the longitudinal joints between segments and additional distortion should be considered. For the most part, service loads generally result in axial forces and bending moments in the lining segments; however, with hoop forces in the longitudinal joints, significant bursting tensile stresses can be developed.

6.1 GROUND PRESSURE, GROUNDWATER, AND SURCHARGE LOADS

Precast concrete segments are designed to withstand various loads including vertical and horizontal ground pressure, groundwater, self-weight and surcharge. In accordance with Limit State Design (LSD), load factors as shown in Table 4 can be used to compute the ultimate limit state (ULS) and serviceability limit state (SLS) loads and forces.

The methods presented for analysis of segmental tunnel linings during the final service stage are in line with standards and guidelines from Europe, Asia, and America (Bakhshi and Nasri 2014a). The effect of ground pressure, groundwater, and surcharge loads on segments can be analyzed using elastic equations, beam-spring models, finite element methods (FEM) and discrete element methods (DEM). Other methods of analysis include Muir Wood's (1975) continuum model with discussion from Curtis et al. (1976), Duddeck and Erdmann's (1982) model, and an empirical method based on tunnel distortion ratios (Sinha 1989; Deere et al. 1969) that was originally developed by Peck (1969). The results from these analyses are used to determine the required concrete strength and level of reinforcement.

	W, WA_P		EH, EV		ES	
	Maximum	**Minimum**	**Maximum**	**Minimum**	**Maximum**	**Minimum**
ULS	1.25	0.90	1.35	0.90	1.50	0.75
SLS	1.0		1.0		1.0	

Note: w = self-weight; WA_p = groundwater pressure; EV = vertical ground pressure; EH = horizontal ground pressure; and ES = surcharge load.

Table 4: Load factors for design parameters (final service stage) (AASHTO DCRT-1-2010)

6.1.1 Elastic equation method

The elastic equation method (ITA WG2 2000; JSCE 2007) is a simple method for calculating lining internal forces for circular tunnels. As shown in Figure 20, the load distribution model consists of applying uniform vertical ground and groundwater pressures, linearly varying lateral earth and groundwater pressures, self-weight of the lining, and a triangularly distributed horizontal ground reaction.

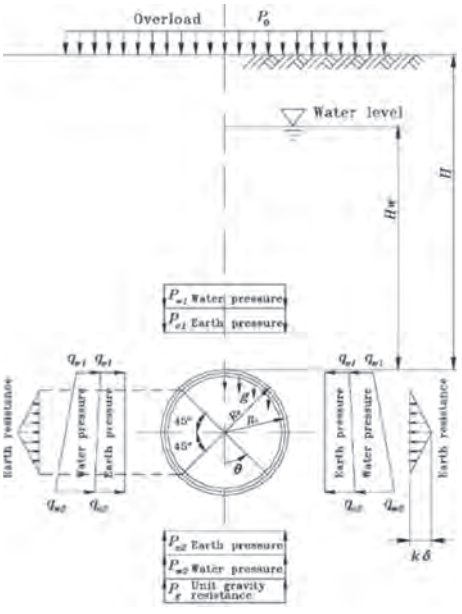

Figure 20 : Distribution of loads used in elastic equations method (JSCE 2007; ITA WG2 2000).

For this method, the segmental tunnel lining is modeled using a uniform reduced bending rigidity that considers the effect of longitudinal joints between the segments. In order to take account of the reduced flexural rigidity in the lining due to the presence of segment joints, the segmental lining moment of inertia should be reduced in accordance with Muir Wood's (1975) proposed method. The relevant formula is given in Equation 8.

$$I_r = I_j + (4/n)^2 \times I \qquad \text{(Eq. 8)}$$

Subgrade reaction modulus (spring stiffness) formulations as recommended by different guidelines are shown in Table 5. In Table 5, E_s or oedometer stiffness (E_{oed}) has the following relationship with young's modulus:

$$E_s = E_{oed} = \frac{(1-\nu)E}{(1-2\nu)(1+\nu)} \qquad \text{(Eq. 9)}$$

Assuming ν = 0.25 for the rock, E_s = 1.2 E. Lining internal forces are calculated using the elastic equations contained in Table 6 (JSCE 2007; ITA WG2 2000).

CODE	SUBGRADE REACTION MODULUS (RADIAL)	SUBGRADE REACTION MODULUS (TANGENTIAL)
USACE EM 1110-2-2901 (1997)	K_r = E/(R.(1+ν))	k_t = 0.5 kr/(1+ν)
Austrian (ÖVBB, 2011)	K_r = Es/R	k_t =0
JSCE (2007)	K_r = not reported	k_t = 1/3 Kr
AFTES (1993)	K_r = E/(R.(1+ν))	k_t = not reported
DAUB (2005)	K_r = Es/R	k_t = 0

Table 5 : Subgrade Reaction Modulus

LOAD	BENDING MOMENT	AXIAL FORCE	SHEAR FORCE
Vertical load $(P = p_{el} + p_{wl})$	$(1-2S2)\cdot P\cdot R_c^2/4$	$S2\cdot R_c\cdot P$	$-SC\cdot R_c\cdot P$
Horizontal load $(Q = q_{el} + q_{wl})$	$(1-2C2)\cdot Q\cdot R_c^2/4$	$C2\cdot R_c\cdot Q$	$-SC\cdot R_c\cdot Q$
Horizontal triangular load	$(6-3C-12C2+4C3)\cdot$	$(C+8C2-4C3)\cdot$	$(S+8SC-4SC2)\cdot$
Soil reaction $(P_k = k\cdot\delta_h)$	$0\le\theta\le\pi/4$ $(0.2346-0.3536C)\cdot R_c^2\cdot k\delta_h$ $\pi/4\le\theta\le\pi/2$ $(-0.3487+0.5S2+0.2357C3)\cdot R_c^2\cdot k\delta_h$	$0\le\theta\le\pi/4$ $0.3536C\cdot R_c\cdot k\delta_h$ $\pi/4\le\theta\le\pi/2$ $(-0.7071C+C2+0.7071S2C)\cdot R_c\cdot k\delta_h$	$0\le\theta\le\pi/4$ $0.3536C\cdot R_c\cdot k\delta_h$ $\pi/4\le\theta\le\pi/2$ $(SC-0.7071C2S)\cdot R_c\cdot k\delta_h$
Dead load $(P_g = \pi\cdot g)$	$0\le\theta\le\pi/2$ $(3/8\pi-\theta\cdot S-5/6C)\cdot R_c^2\cdot g$ $\pi/2\le\theta\le\pi$ $(-\pi/8+(\pi-\theta)S-5/6C-1/2\pi\cdot S2)\cdot R_c^2\cdot g$	$0\le\theta\le\pi/2$ $(\theta\cdot S-1/6C)\cdot R_c\cdot g$ $\pi/2\le\theta\le\pi$ $(-\pi\cdot S+\theta\cdot S+\pi\cdot S2-1/6C)\cdot R_c\cdot g$	$0\le\theta\le\pi/2$ $(\theta\cdot S-1/6S)\cdot R_c\cdot g$ $\pi/2\le\theta\le\pi$ $(-(\pi-\theta)\cdot C+\theta\cdot S+\pi\cdot SC-1/6S)\cdot R_c\cdot g$
Horizontal deformation at springline (δ_h)	$\delta_h = \frac{(2P-Q-Q'+\pi\cdot g)\cdot R_c^4}{24\cdot(EI+0.045k\cdot R_c^4)}$		

Notes: ϕ = angle from crown; S = sin ϕ; *S2* = sin² ϕ ; S3 = sin³ ϕ ; C = cos ϕ ; C2 = cos² ϕ ; C3 = cos³ ϕ ; EI = flexural rigidity in unit width.

Table 6 : Equations for calculating lining internal forces using elastic theory (JSCE 2007; ITA WG2 2000)

6.1.2 Beam-spring method

Using the beam-spring method (AASHTO (DCRT-1-2010), JSCE (2007), and ÖVBB (2011)), the lining can be modeled in cross-section as a series of beam elements that span between the longitudinal joints of the segments. The interaction between the ground and the lining is generally modeled using linear translational springs in the radial, tangential, and longitudinal directions. Because the lining and ground are represented by a series of beams and springs, this method is commonly referred to as the beam-spring method. Various two-dimensional approaches are used to evaluate the effect of the segment joints, including solid ring models with full bending rigidity, solid ring models with reduced bending rigidity (Muir Wood 1975), ring models with multiple hinged joints, and ring models with rotational springs.

Two-dimensional models cannot be used to represent circumferential joints or staggered arrangements of segments between rings. However, as shown in Figure 21, a so-called “two-and-a-half-dimensional multiple hinged segmented double ring beam-spring” has been used to model the reduction of bending rigidity and the effects from a staggered geometry. This manipulation is achieved by modeling the segments as curved beams, the flat longitudinal joints as rotational springs (Janssen (1982), Groeneweg (2007)), and the circumferential joints as shear springs. Under final service loads, the longitudinal joints may be open or closed, and the critical rotation is given by the following equations:

Closed joint: $\theta \le \frac{2N}{Ebl_t}$ (Eq. 10)

Open joint: $\theta > \frac{2N}{Ebl_t}$ (Eq. 11)

The Janssen rotational spring stiffness (k_r) is derived from the following equations.

Closed joint: $k_r = \frac{bl_t^2 E}{12}$ (Eq. 12)

Open joint: $k_r = \frac{9bl_t EM\left(\frac{2M}{Nl_t}-1\right)^2}{8N}$ (Eq. 13)

Figure 21 (c) illustrates the various parameters used in the Janssen model.

Two rings are required to evaluate the coupling effects; however, in this method, only half of the segment width is considered from each ring for the longitudinal and circumferential joint zone of influence. This approach utilizes symmetry to remove complex support conditions on both rings. Considering the self-weight of the lining, and distributing the ground, groundwater, and surcharge loads along the beam, lining internal forces can be calculated using a conventional structural analysis package.

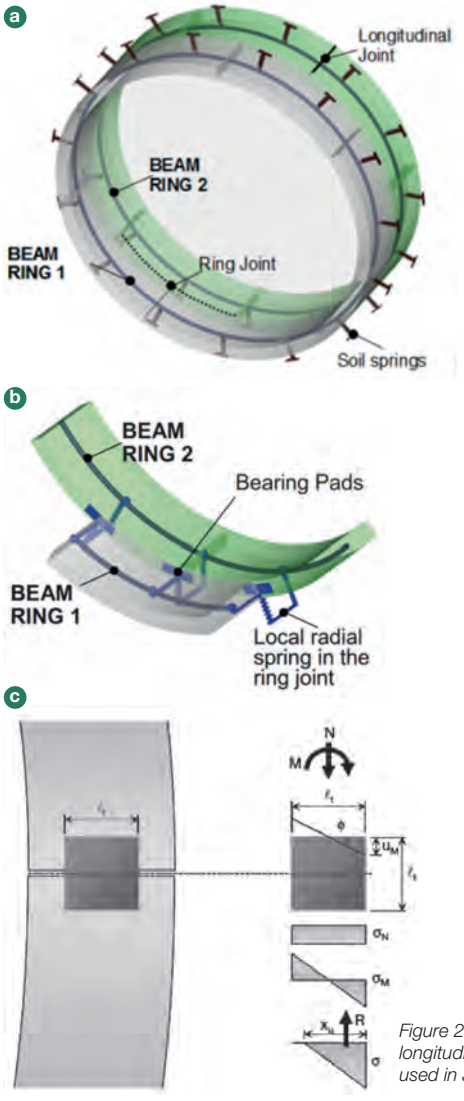

Figure 21: (a) Double ring beam-spring model with radial springs simulating ground, and joint springs simulating longitudinal and circumferential joints; and (b) scheme of ring joint (Plizzari and Tiberti 2009), (c) presentation of parameters used in Janssen model for determining rotational spring stiffness.

6.1.3 Finite element method (FEM), finite difference method (FDM,) and discrete element method (DEM) simulations

In soft ground, loose rock, and partially homogeneous solid rock, ÖVBB (2011) and AFTES (1993) recommend using the FEM and FDM methods to calculate the forces in the tunnel lining. The DEM method is generally considered more appropriate for tunnels in fractured rock. A two-dimensional approach is generally sufficient for continuous linear structures that do not contain sudden changes in cross sectional geometry or high concentrations of loadings. Three-dimensional techniques are generally used with more complex geometry and loadings such as at crosscuts that intersect the main tunnel (ÖVBB 2011), or in soft ground with 3D arching.

FEM is used to model the ground surrounding the lining (Bakhshi and Nasri 2013c). The advantage of this method is that one is able to determine the ground deformations and the post yielding behavior of the segmental lining materials, including any redistribution of stress that result from deformation of the lining and excavation of the tunnel (ÖVBB 2011). FEM analysis techniques can also be used to represent non-uniform and anisotropic stresses such as when nonsymmetrical features are present in the ground. This can be the case when several different geologic formations or external loads are present within close proximity of an existing structure (AFTES 1993). Using FEM techniques, complex underground conditions, and tunnel characteristics can be analyzed and the large axial forces and bending moments developed in the segments can be determined.

For DEM modeling, engineering properties for analysis of segmental linings in rock formations include properties of intact rock such as unit weight, modulus of elasticity, UCS, internal friction angle, tensile strength; and where relevant, properties of discontinuities such as joint spacing, joint apparent dip direction and joint apparent dip, peak and residual joint friction angle, peak and residual joint cohesion, joint normal stiffness, joint shear stiffness, Eintact/Emass, GSI and Mi (based on Hoek-Brown).

Precast segments are designed using an axial force-bending moment diagram.

6.2 LONGITUDINAL JOINT BURSTING LOAD

Normal (hoop) forces developed in the lining are transferred through a reduced cross sectional area along the longitudinal joints where gaskets and stress relief grooves are present. Bursting tensile stresses can develop along the longitudinal joints in a comparable manner to the tunnel boring machine (TBM) thrust jacking loads on the circumferential joints. The maximum normal force obtained from the ground pressure, groundwater and surcharge loads plus the gasket pressure should be applied to the longitudinal joints in order to obtain the maximum ULS design compressive force. General equations from ACI 318-14 and DAUB (2013), the Iyengar (1962) diagram, and 2D finite element method (FEM) simulations are various methods utilized for the design of longitudinal joint bursting (Bakhshi and Nasri 2014b).

6.2.1 General equations

The general equation of post-tensioned anchorage zone by structural codes such as ACI 318-14 (Eq. 2) is used to analyze this load case, where Ppu is the maximum normal force, and e_{anc} is the maximum eccentricity comprising the normal force eccentricity (M/N) and the eccentricity of the load transfer area. Alternatively, the simplified equation by DAUB (2013) (Eq. 3) is used for evaluating bursting stresses in the longitudinal joints. DAUB (2013) presents more detail on

this specific load case using an approach that transfers force by means of a tension block as shown in Figure 22. DAUB (2013) endorses placing additional reinforcement for spalling and secondary tensile stresses when there are high eccentric normal forces (e > d/6). Bursting, spalling, and secondary tensile stresses are calculated using the following equations.

$$F_{bst} = 0.25 \cdot N_{Ed} \cdot (1 - d_1 / d_s) \quad \text{(Eq. 14)}$$

$$F_{sd,r} = N_{Ed} \cdot \left(\frac{e}{d} - \frac{1}{6}\right) \quad F_{sd,2} = 0.3\, F_{sd} \quad \text{(Eq. 15)}$$

The total eccentricity, e, consists of the normal force eccentricity and the eccentricity of hinge joint considering gasket and caulking recesses *($e = e_l + e_k = M/N + e_k$), $d_1 = d_k - 2e$, and $d_s = 2e' = d - 2el$*. These parameters are shown in Figure 22. Where appropriate, the build tolerance and system deflection should be taken into account.

DAUB (2013) further endorses placing bursting tensile reinforcement at 0.4ds from the face of the segments. Reinforcement for spalling and secondary tensile stresses, if necessary, are placed at $0.1d_s$ and 2/3d from the face of the segment respectively. General equations, which include Eq. 6 and Eq. 7, can be used to determine the compressive stress and the required strength of the partially loaded surface.

6.2.2 The Iyengar diagram and FEM simulations

The Iyengar diagram method (Figure 10) and FEM simulation can be used as an alternative approach to determine the stresses within the longitudinal joints. Two-dimensional FEM models can be used to simulate the longitudinal joint and gasket using appropriately shaped ends to represent the recess for the gasket and the stress relief grooves (curvature of the elements is neglected in this analysis). Figure 23 illustrates generalized analytical results, including bursting tensile stresses and compressive stresses, in the area around longitudinal joints.

Besides considering the normal force eccentricity (M/N) and the eccentricity of the load transfer area, it may be necessary to consider the eccentricity due to ovalization of the segment and misalignment during erection of the ring. Such load cases are referred to as ring ovalization (due to the out of round ring build) or birdsmouthing (where, due to rotation, only the inner or outer surface of the longitudinal joint is in contact). The design procedure assumes that the ring is initially built in the shape of an ellipse, and that the chord length of the displaced segment, as shown in Figure 23(c) does not change. An assumption is made on the out of round build allowance over diameter, say 15mm. The joint rotation causing birdsmouthing (τ in Figure 23c) and opening distance due to poor ring build (δ in Figure 23c) are calculated. The load required to close the gap under minimum/maximum embedment loads is assessed and compared to the hoop force under the embedment loads. Depending on whether the joint remains open or close, one of the two diagrams shown in Figure 23 (d) is used for calculation of birdsmouthing eccentricity.

The above discussion only considers flat joints as they are the most conventional joint shape. For convex joints, the design approach is similar except a line load is assumed instead of a distributed load at the joint locations.

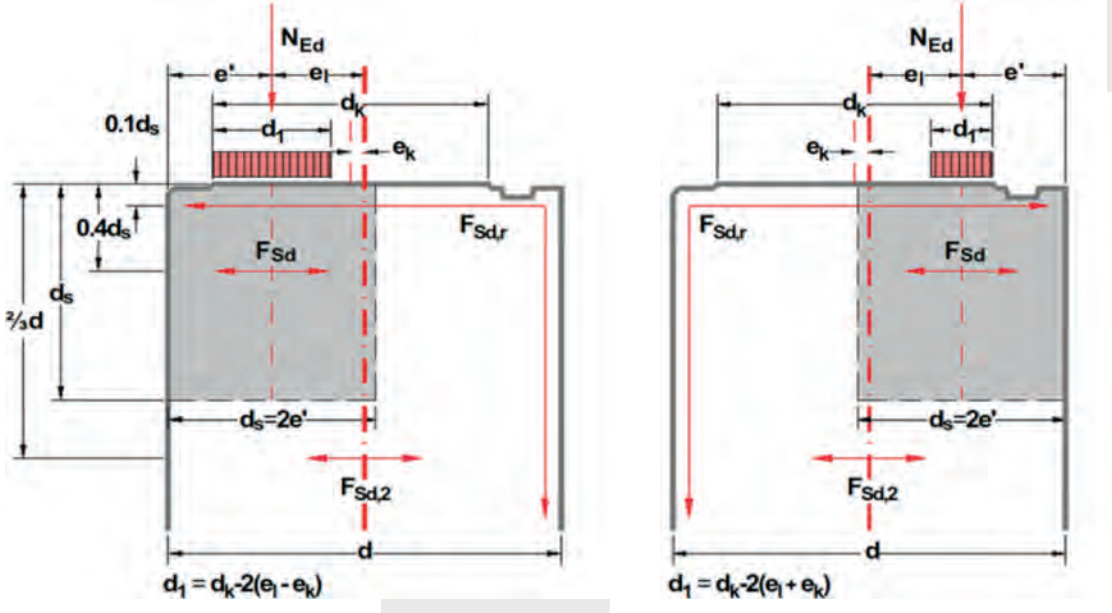

Figure 22 : Force transfer recommended by DAUB (2013) in longitudinal joints using the tension block concept.

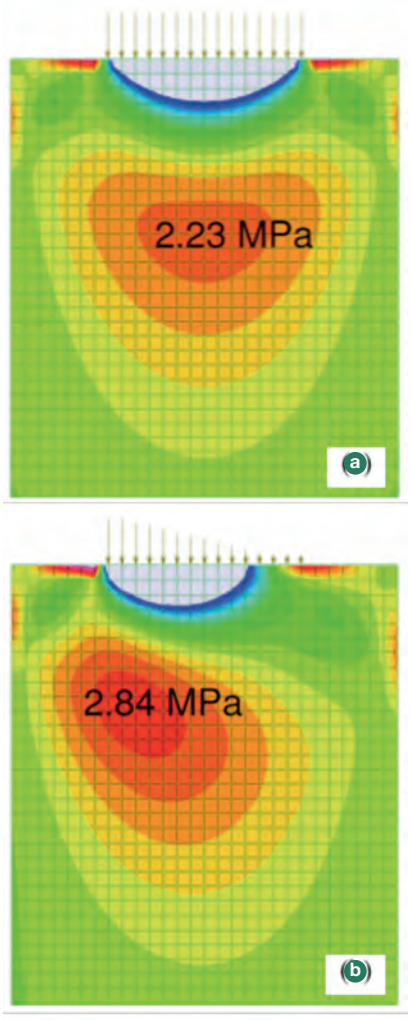

6.3 LOADS INDUCED DUE TO ADDITIONAL DISTORTION

Segmental tunnel linings are designed to take an additional diametrical distortion in addition to the deflections caused by the effects of ground, groundwater, and surcharge loads. This additional distortion may occur due to construction-related events such as joint misalignment, yielding of joint connectors, excessive grouting pressure or from ground movement caused by the construction of an adjacent tunnel. This distortion is the difference between the movement of the tunnel lining on opposite sides of the springline. Although ovalization should be considered as a matter of course, some authorities such as LACMTA (2013) and LTA (2010) stipulate the diametrical distortion to accommodate in the design. The former specifies a minimum additional diametrical distortion of 0.5 percent of diameter due to imperfect lining erection and the latter specifies an additional distortion of +/-5/8 in. (15 mm) on the diameter to allow for future development in the vicinity of the tunnel.

The following formula introduced by Morgan (1961) is commonly used to calculate the additional distortional bending moment.

$$M_{distortional} = \frac{3EI\delta_d}{2r_0^2} \qquad \text{(Eq. 16)}$$

Other approaches, such as the theory of elasticity or finite element method (FEM) may be used to calculate the maximum distortion.

6.4 OTHER LOADS

Depending on the intended use of the tunnel, other loads such as earthquake, fire, explosion, internal loads and breakouts at cross passageways, portals, and shafts should also be considered. This document does not address all of these load cases, but some of the major ones are briefly discussed below.

6.4.1 Seismic design

Seismic design of tunnels to resist the maximum design earthquake (MDE) and operating design earthquake (ODE) is often performed using a ground deformation approach that includes ovaling, axial, and curvature deformations. LACMTA (2013) contains the criteria for determining the maximum axial forces and bending moments due to seismic ovaling deformation. For the ovaling analysis, LACMTA (2013) recommend that two approaches be used based on closed-form solutions and numerical modeling. Pseudo-dynamic time-history and dynamic time-history analyses are other alternatives. The deformation analysis provided by AASHTO DCRT-1-

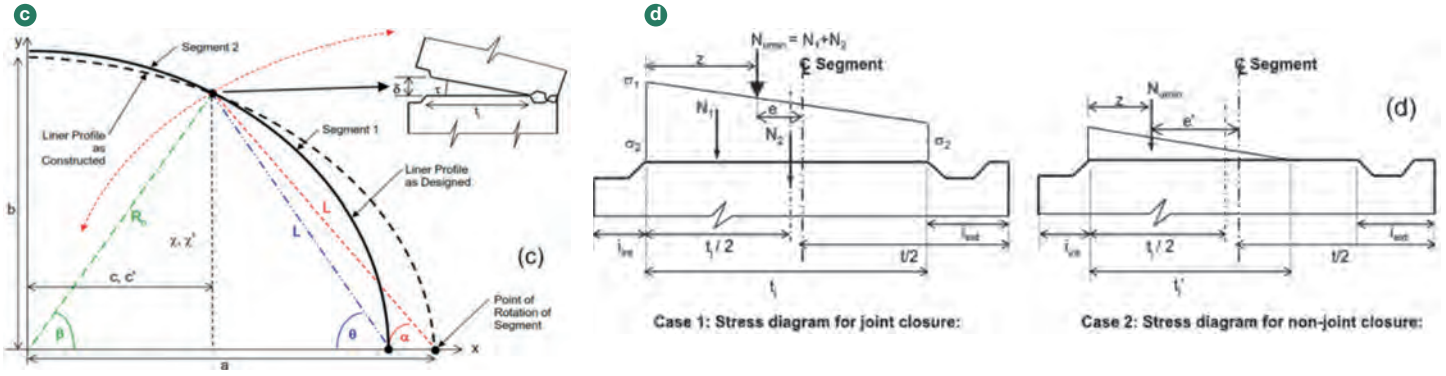

Figure 23 : Developed bursting tensile stresses around longitudinal joints under hoop (normal) forces due to service loading condition and gasket pressure: (a) no eccentricity; and (b) eccentric contact stresses (Francis and Mangione 2012), (c) ring ovalization due to out of round ring build, (d) stress diagrams for joint closure (Case 1) or non-closure (Case 2)

2010 is often used for the longitudinal seismic response (axial and curvature deformations) of tunnels located within uniform geologic deposits. This approach is based on the calculation of combined axial and bending strains from the pressure waves (P-Waves), shear waves (S-Waves), and Rayleigh waves (R-Waves).

When tunnels run through highly variable geological conditions, a numerical modeling approach is preferred.

6.4.2 Breakout Analysis and Shear Recovery Systems

Utilization of shear recovery systems minimize the problems associated with the creation of openings in the segmental lining by reducing the amount of temporary work. A system which utilizes Bicones, as shown in Figure 24, prevents any offset between the rings during ring assembly and absorbs energy when an opening is created in the tunnel lining, such as at entrances, ventilation adits and elevator adits. Although other methods such as anchors, steel connectors, and shear keys have been used, the Bicone has technical advantages which currently make it a preferred option. A Bicone with a steel insert can provide a shear strength of up to 350 kN.

Analysis is performed for the case where several segments are removed to create an opening. A three-dimensional, non-linear modeling approach, using an FEM package is adopted to evaluate the impact of excavation. Figure 24 indicates the typical geometry for a breakout and the shear stresses that develop around the penetration zone. The total shear force for a ring around the penetration area is calculated to determine the shear strength required for the shear recovery system to provide.

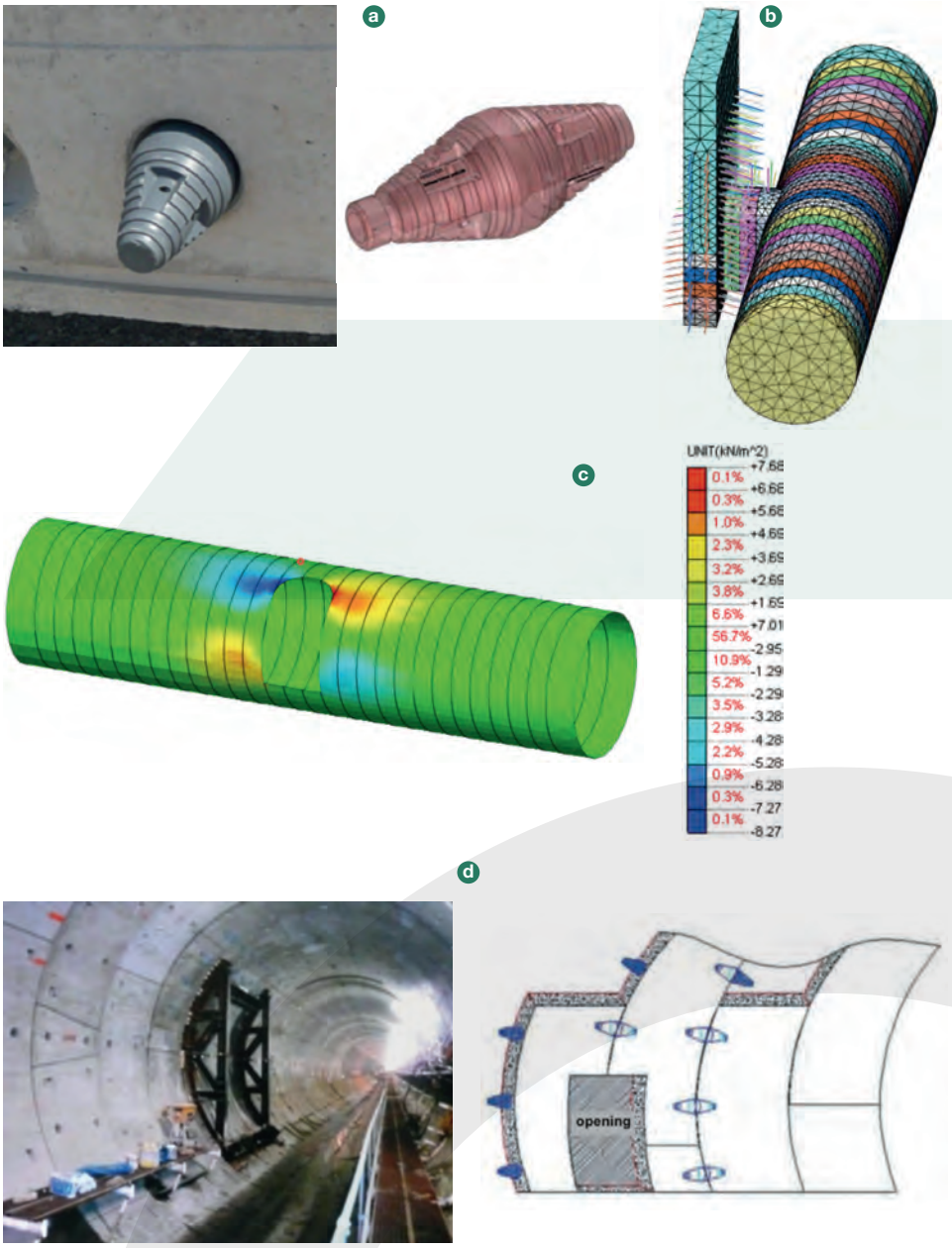

Figure 24 : (a) Bicone dowels for shear recovery, (b) 3D Model, (c) developed shear stresses, and (d) installation pattern of Bicone shear dowels for an adit penetration

6.4.3 Design for fire incident and explosion

A load case specific to road and railway tunnels is tunnel fires. One of the decisive factors for the design of tunnel structures in the load case of fire is the heat release rate. Rates from 10 MW up to 200 MW have been proposed at different projects with the majority ranging around 100 MW. Another important factor is the duration of the design fire with values ranging from 30 minutes to 3 hours, sometimes with an added cooling phase. Both heat release rate and duration will depend on intended use of tunnel and project specific conditions such as the type of traffic (train, cars, heavy goods or dangerous goods transport) and the required safety level (with stricter requirements in case of a possible impact on structures above the tunnel, or the risk of inundation) (Neun, 2012). The actual time-temperature curve resulting from such a design fire which depends on the individual cross section and wind speeds inside the tunnel can be used for simulation of a temperature gradient between the intrados and extrados of the tunnel lining. However, since adequate Computational Fluid Dynamics (CFD) modelling is very time consuming and the results are not easily transferred to a structural model, it is common to use standard deterministic time-temperature curves for the projects (Neun, 2012). Most common standard design fire curves for the structural design of tunnel structures include RABT-ZTV (Railways) also known as EBA, RABT-ZTV (Highways) also known as ZTV, ISO 834 Cellulose, HC Hydrocarbon Eurocode 1, HCM Modified Hydrocarbon (HCinc) and Rijkswaterstaat also known as RWS (ITA WG6, 2004). The ISO 834 curve is recommended up to an expected fire heat release rate of 50MW, above which the hydrocarbon curve (up to 100MW) and thereafter the RWS curve (up to the stoichiometric limit) should be applied (ITAtech Vol1, 2016). Accordingly, one of the standard design fire curves can be selected (temperature versus time) and applied on the tunnel intrados. The increase in lining temperature versus depth is calculated and the resulting reduction in concrete and reinforcement properties (modulus and strength) is determined based on available data. This will determine of the amount of the lining thickness lost during the fire. If using basic structural analysis programs, applying non-linear temperature gradients are not allowed for, an equivalent temperature load can be established that has the same impact on the equivalent section as the original temperature gradient has on the original section (Neun, 2012). This can be followed by adopting a layered section analysis where the normal force (N) and bending moment (M) can be determined by integration/summation of the stresses in the individual layers.

Explosions, on the other hand, are simulated by increasing the internal radial pressure on the tunnel lining at the service condition, by a representative value such as one atmosphere (14.5 psi or 1 bar) (Caan et al. 1998). This internal radial pressure results in reduced axial forces without significant change in the bending moments. Recently an advanced and detailed design procedure for tunnels subjected to internal explosion and possibly preceded by fire accidents was developed (Colombo et al. 2015). Simplified FE model and dynamic analyses were carried out to study the tunnel's response under internal blast loads in the form of pressure-impulse (p-i) diagrams and an ultimate limit state criteria based on eccentric flexural capacity (M-N interaction diagram) was generated. Also a limit state criterion taking into account the fire-blast interaction was introduced through the modification of the M-N diagram. This procedure is suggested for an advanced blast-fire analysis.

7.1 CONCRETE STRENGTH AND REINFORCEMENT

Several guidelines are available which recommend the compressive strength of precast concrete tunnel segments and these are summarized below.

Precast concrete segments are generally reinforced with either steel bar, welded steel wire fabric or discrete steel fibers. Specifications for various grades of the above elements can be found in local codes and standards. When segments are reinforced with steel bar or welded wire fabric, the reinforcement is often categorized to three different types:

a) transverse reinforcement - the main reinforcement placed perpendicular to the tunnel axis to resist forces and moments
b) longitudinal reinforcement – placed parallel to tunnel axis and often designed as minimum temperature and shrinkage reinforcement
c) joint reinforcement - placed in the vicinity of joints to resisting bursting and spalling stresses.

A typical plan view of transverse and longitudinal bars in a precast concrete tunnel segment is shown in Figure 25. No specifications or requirement have been found in tunnel guidelines for minimum bar size. However, a review of segmental tunnel projects reveals that transverse bar size generally ranges between ϕ10 and ϕ16 metric sizes, while bar size in the longitudinal direction ranges between ϕ6 and ϕ16 metric sizes. The choice of bar size will be influenced by local availability, design code requirements, bending radii, weldability, and improved crack control.

A general trend in recent projects is to use smaller more closely spaced bars.

AUTHORITY	COMPRESSIVE STRENGTH STRIPPING (MPA)	COMPRESSIVE STRENGTH 28 DAY (MPA)
AASHTO (DCRT-1) (2010)	Not provided	34 to 48 (5000 psi to 7000 psi)
Japan's Railway Technical Research Institute (RTRI 2008)	Not provided	42 to 60
ÖVBB (2011)	12 MPa (minimum)	40 (minimum)
DAUB (2013) (referring to local German guideline ZTV-ING (2007))	15 MPa	35 to 50
LTA (2010)	Not provided	60
USACE EM 1110-2-2901 (1997)	Not provided	42 (or higher) (6000 psi)

Table 7 : Recommendations for compressive strength of precast tunnel segments

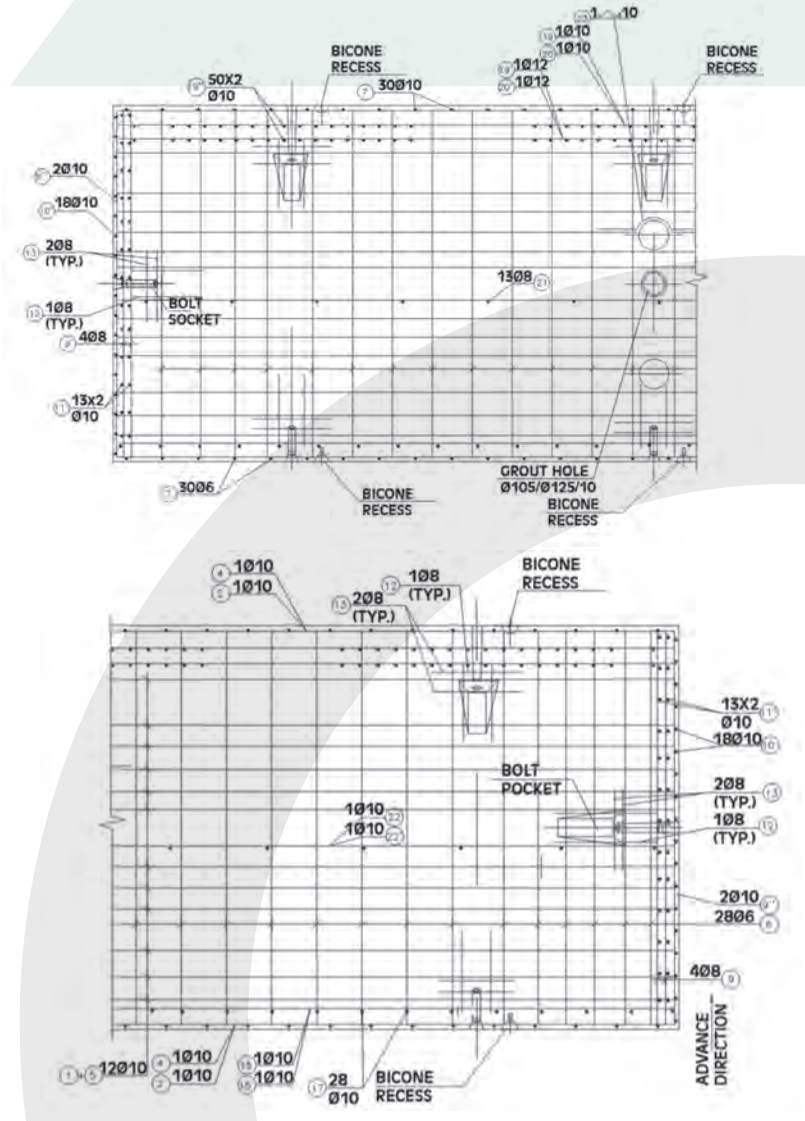

Figure 25 : A typical plan view of transverse and longitudinal bars in precast concrete tunnel segment.

Typical sectional views of joint reinforcement in circumferential and longitudinal joints in precast concrete tunnel segments are shown in Figure 26.

Circumferential joint reinforcement includes transverse and radial reinforcement. Transverse reinforcement in circumferential joints is usually the same size as the main transverse reinforcing bars, except where excessively high TBM thrust jack forces may be present. Radial bars in circumferential joints range between ϕ10 or ϕ13 metric sizes and consist of ties or U bars with more closely spaced bars around the TBM jack shoe locations.

Longitudinal joint reinforcement in the radial direction is sometimes designed as ladder bars (instead of ties or U bars) due to the simplicity of welding ladder bars along a flat surface compared to the curved face for the circumferential joint. Radial bars in longitudinal joints range between ϕ10 or ϕ13 metric sizes. Longitudinal reinforcing bars in longitudinal joints are generally the same size as the longitudinal reinforcement inside the segment.

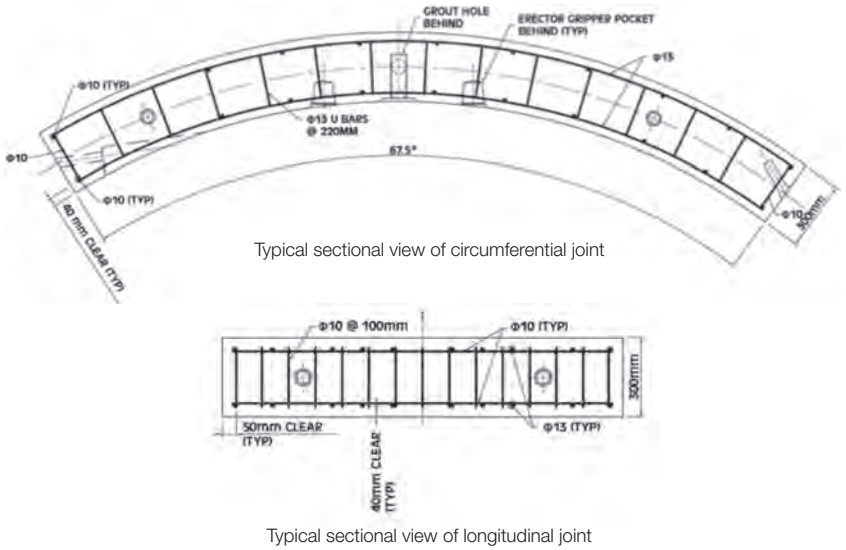

Figure 26 : Typical sectional views of joint reinforcement in precast tunnel segments.

7.2 CONCRETE COVER

Several guidelines are available for minimum concrete cover and these are summarized below. Note should be taken however of durability requirements as defined in codes, which take priority.

AUTHORITY	MINIMUM COVER (mm)	COMMENT
DAUB (2013)	40 20	Surface of segment End faces and bolt sockets
ACI 318-14	1-1/2 in (38 mm)	Exposed to earth
JSCE (2007)	25 35	Over reinforcement Corrosive environment
ÖVBB (2011) refers to Austrian standard ÖNORM EN 1992-1-1	25 to 45	Depending on exposure conditions
AFTES (2005)	30mm 20mm	Intrados and extrados Other zones
NEN 6720 (1995)	35	-

Table 8 : Recommended minimum concrete cover for RC precast segments

7.3 REINFORCEMENT SPACING

General guidelines for spacing of reinforcement are given in the table below. Note should be taken however of specific design code requirements such as for crack control.

AUTHORITY	REBAR SPACING	COMMENT
ACI 318 (2014) (not specific to precast tunnel segments)	25 mm (1 in) 457 mm (18 in)	Minimum spacing Maximum spacing
DAUB (2013)	100 mm to 150 mm 90 mm	Typical range Minimum clear spacing
AASHTO DCRT-1 (2010), ÖVBB (2011), and JSCE (2007)	1.25 x max aggregate size plus bar diameter	Minimum bar spacing
AFTES (2005) referring to Section 4.4.5 of BAEL 91 (2007)	Smaller of : 200 1.5 x segment thickness	Maximum bar spacing
NEN 6720 (1995)	Largest of : 25 mm 4/3 x max aggregate size Largest bar diameter	-

Table 9 : Recommended rebar spacing for RC precast segments

7.4 FIBER REINFORCEMENT

Fiber reinforcement has emerged as an alternative to traditional reinforcing bars and welded wire mesh reinforcement for precast concrete tunnel segments. Due to significantly improved post-cracking behavior and crack control characteristics,

fiber-reinforced concrete (FRC) segments offer advantages over traditionally reinforced concrete segments such as cost saving and reduction in production time while providing a robust product with improved handling and long-term durability.

FRC technology has developed in recent years with the introduction of high-strength concrete, allowing the use of fibers as the sole reinforcement system. In some cases, fiber and reinforcing bars have been used in conjunction to reinforce the tunnel segments. Ladder bars at the longitudinal joint as well as bursting ties at the circumferential joint may be significantly reduced by adding fibers. Tunnels with internal diameters ranging from 2.2 m to 13.9 m have been built using fiber reinforcement. Minimum and maximum thickness of the FRC precast segments range from 0.15 m to 0.46 m, respectively.

Recently, new guidelines have been produced for the design and construction of these segments (ACI 544.7R, (2016); fib Bulletin 83, (2017), PAS 8810 (2016), ITAtech Vol1 (2016), ITA WG2 (2016)). These guidelines provide design procedures for FRC tunnel segments to withstand all the appropriate temporary and permanent load cases occurring during the production, construction and design life of segmental tunnels. To classify the post-cracking strength of FRC, a linear elastic behavior can be assumed by considering the characteristic residual flexural strength. The guidelines utilize the post-cracking characteristic residual tensile strengths of fr1k and fr3k which are the most important parameters for the design of FRC segments for the serviceability limit state and the ultimate limit state, respectively.

It should be noted that applying raw parameters from standard ASTM C1609 or EN 14651 beam tests, such as f^D_{150} or $f_{R,3}$, requires caution to prevent over-estimating the residual tensile strength when using elastic analysis (Bakhshi et al. 2014). A back-calculation procedure can be adopted to obtain the specified residual tensile strength parameter σ_p (Soranakom and Mobasher 2007). Alternatively, the

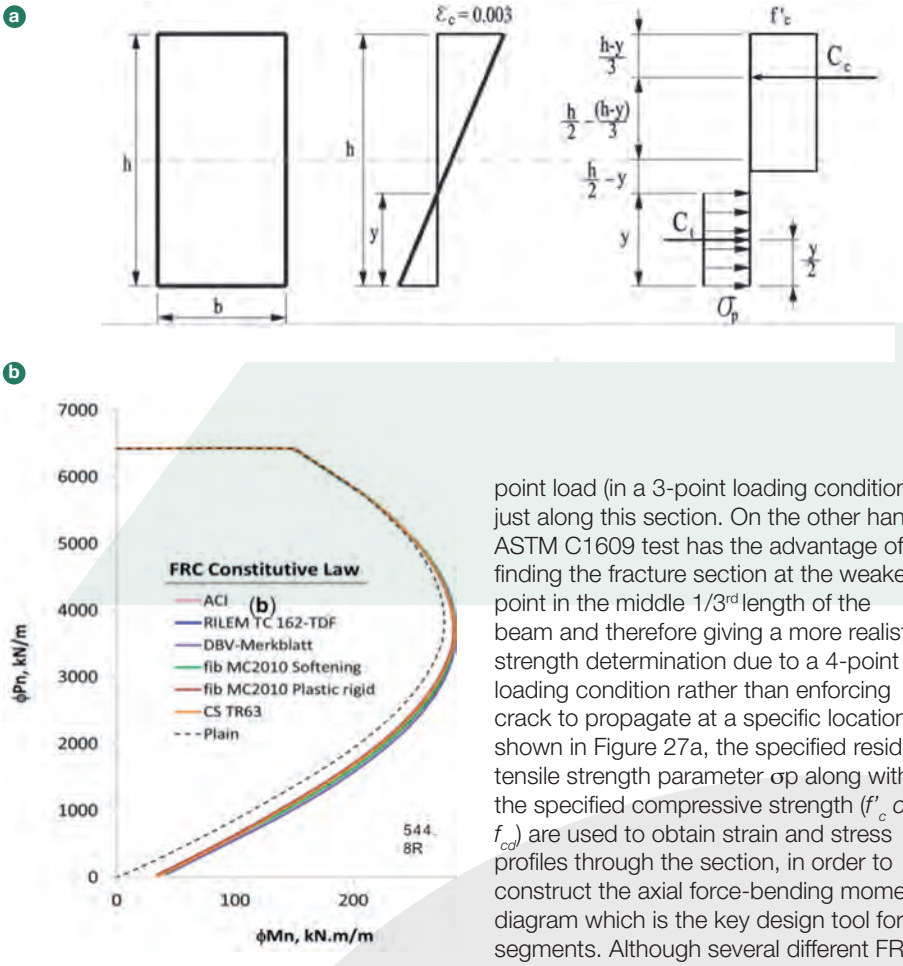

Figure 27(a) Strain and stress distributions through the section as part of it undergoes tension, (b) effect of choice of constitutive law on the axial force-bending moment interaction diagrams as a key design tool (Bakhshi and Nasri 2014c)

post-crack flexural strength parameters determined in accordance with standards (ASTM C1609/C1609M; EN 14651) can be scaled by an adjustment factor ranging from 0.33 to 0.37 (Bakhshi et al. 2014; Mobasher et al. 2014; Vandewalle, 2000; Barros et al. 2005; fib Model Code 2010, 2013). Note that EN 14651 standard test has the advantage of a better testing control compared to ASTM C1609. This is because test controlling parameter of EN 14651 which is crack mouth opening dimension (CMOD) is measured at a known location which is the middle of the beam due to cutting a notch and applying a point load (in a 3-point loading condition) just along this section. On the other hand, ASTM C1609 test has the advantage of finding the fracture section at the weakest point in the middle 1/3rd length of the beam and therefore giving a more realistic strength determination due to a 4-point loading condition rather than enforcing crack to propagate at a specific location. As shown in Figure 27a, the specified residual tensile strength parameter σp along with the specified compressive strength (f'_c *or* f_{cd}) are used to obtain strain and stress profiles through the section, in order to construct the axial force-bending moment diagram which is the key design tool for segments. Although several different FRC constitutive laws (fib Model Code 2010, DBV 2001, RILEM TC 162-TDF 2003, CNR-DT 204/2006, EHE-08) have been used for the design of these elements, results from studies by Bakhshi and Nasri (2014c) shown in Figure 27b, reveal that the choice of constitutive law does not have a significant effect on the axial force-bending moment interaction diagrams and therefore on the design outcome.

For Fiber Reinforced Concrete (FRC) elements, ACI 544-7R (2016) and fib Bulletin No. 83 (2017) suggest appropriate strength reduction factors or material safety factors for flexure, compression, shear, and bearing actions of concrete segments. Such factors account for the uncertainty of post-crack tensile strength when calculating the design strength of FRC elements.

Performance testing or proof testing as a means to validate design assumptions or models is endorsed by most structural codes. This is especially true for repetitive units, where large numbers are required to meet performance criteria such as with the manufacture of precast concrete segments. Full-scale tests are often conducted to evaluate the design and performance of FRC segments with slenderness ratios between 10 to 13.

Nonstructural tests on precast concrete tunnel segments include ASTM E119, which helps to ensure the 4-hour fire resistance using standard time-temperature curves (Alder et al. 2010).

Full scale bending and point load tests are conducted to loads much higher than the TBM nominal service load, and the strength results are compared with the results predicted from design.

Bending tests, as shown in Figure 28, are performed to verify the design and performance of segments during the production stages of stripping (demolding), storage, transportation, and handling, as well as for asymmetrical earth pressure during the service stage.

Full-scale point load tests, as shown in Figure 29, simulate the TBM thrust jack forces on the segment during the excavation process (Caratelli et al. 2012), as well as the force transfer through the reduced cross section in longitudinal joints.

The cantilever load test, as shown in Figure 30, is another full-scale test that is used to investigate the circumferential joint strength under misaligned jacking loads (Poh et al. 2009). Concrete tunnel lining strength has also been evaluated by full-scale tests, such as those shown in Figure 31 to simulate dominant effects of axial forces, bending moments, and the combined action of axial loads and bending moments (Mashimo et al. 2002).

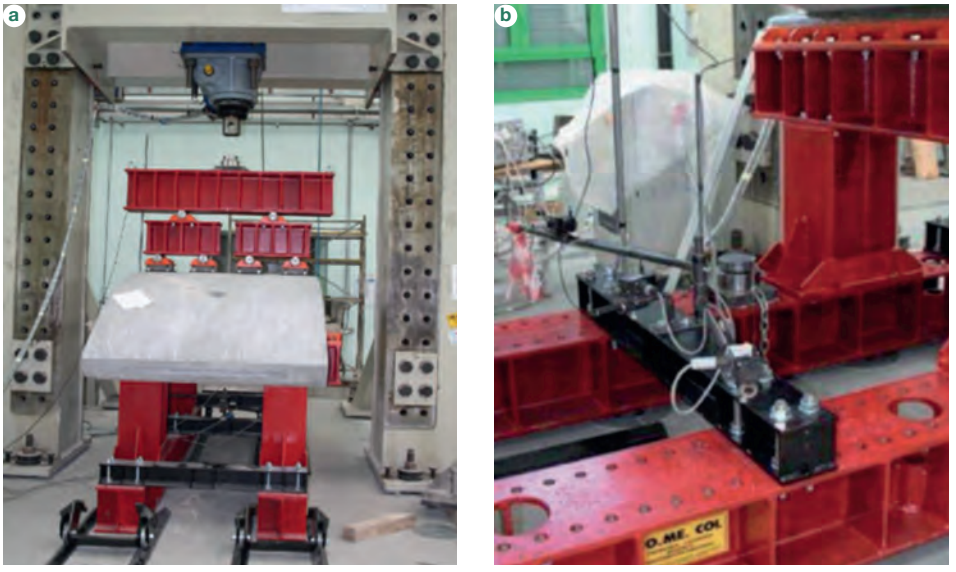

Figure 28 : Bending test: (a) test setup; and (b) measurement instrumentation (Moccichino et al. 2010).

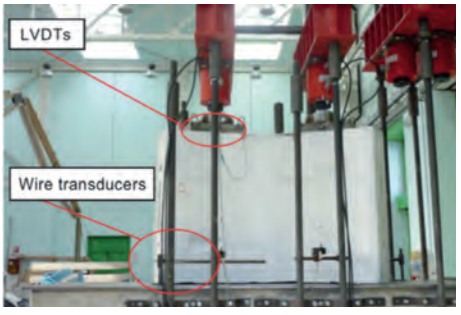

Figure 29 : Point load test setup and measurement instrumentation simulating TBM thrust jack force (Caratelli et al. 2012).

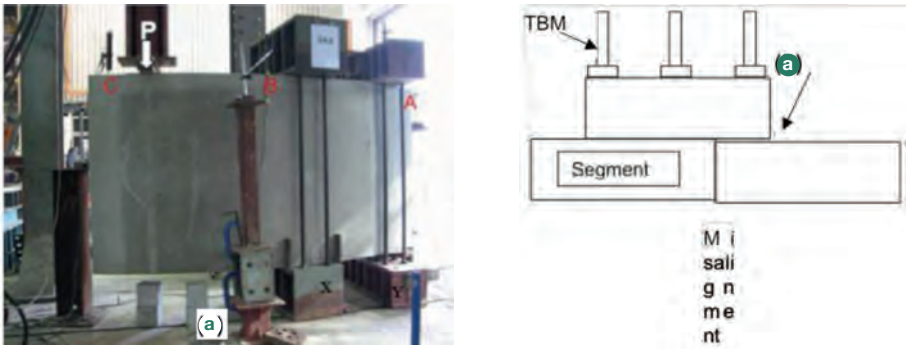

Figure 30 : Cantilever load test set-up and instrumentation (Poh et al. 2009).

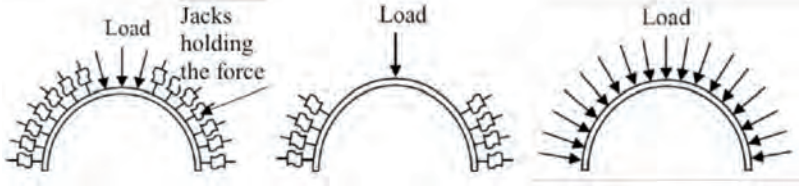

Figure 31 : Full scale loading cases simulating dominant effects of axial forces, bending moments, and combined action of axial loads and bending moments (Mashimo et al. 2002).

9 >> SERVICEABILITY LIMIT STATE DESIGN

Considering the requirements of the LSD or LRFD method, the design engineer needs to design precast concrete tunnel segments for the ultimate limit and serviceability limit state (JSCE, 2007). A limit state (ULS or SLS) is a state beyond which the specified service requirements for the precast tunnel lining are no longer met. The SLS in segmental tunnel lining systems correspond to excessive stresses, deflections and cracking of concrete segments and segment joints. These limit states may not only cause excessive deformations, but may result in durability and watertightness issues due to rebar corrosion, water leakage from segment cracks, or enlarged gaps between segment joints (JSCE, 2007; Mendez Lorenzo, 1998; Çimentepe, 2010). Figure 32 and Table 10 illustrate a flowchart and the required design checks for verifying the serviceability limit states of tunnel segments. These various states and particularly SLS of cracking are discussed below.

9.1 VERIFICATION FOR SLS IN TUNNEL SEGMENT

The SLS design for the tunnel segments considers different load combinations which act on the tunnel lining from the time of production through to the final service stage. Different SLS conditions are discussed and corresponding calculation methods and limiting values are presented according to international standards and guidelines.

As previously discussed, critical load cases for segment design include production and transient load cases for segment demolding, storage, transportation and handling, while construction loads include TBM thrust jack forces, tail skin and localized back grouting pressure. Final service loads include earth pressure, groundwater and surcharge loads, longitudinal joint bursting load, and special loads such as earthquake, fire, explosion and loads induced due to additional distortion. The design engineer can refer to Table 2 and use all possible SLS load combinations considering a load factor of 1.

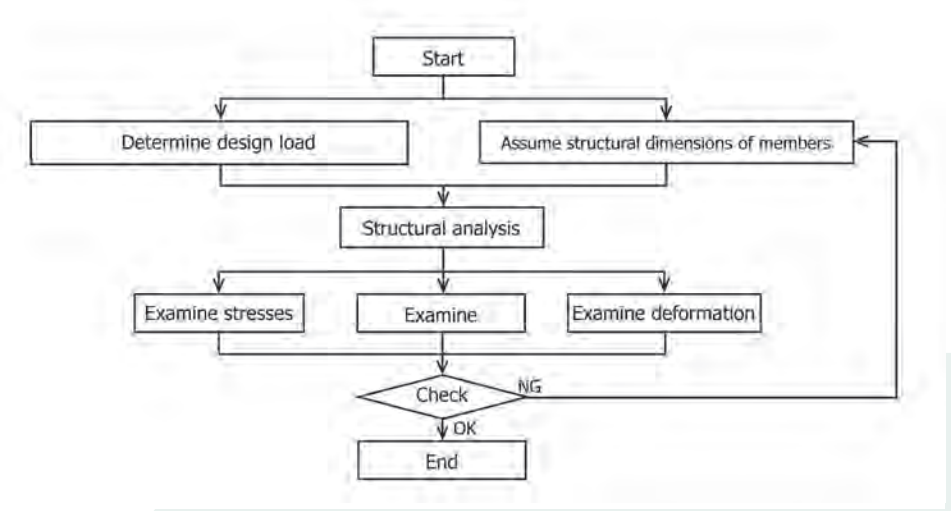

Figure 32 : Design flowchart for Serviceability Limit State-SLS (JSCE 2007)

SLS States	Location	Items to Check	Critical Design Parameter
Stress	Segment section	Stress in concrete	Allowable compressive stress of concrete
		Stress in reinforcement	Allowable tensile stress of steel bars
	Segment joints	Stress in concrete	Allowable compressive stress of concrete
		Stress in connectors	Allowable stress of connecting bolts
Deformation	Segmental ring	Ring deformation	Allowable deformation
	Segment joints	Joint opening	Allowable gap between segments joints
		Joint offset	Allowable offset between segments joints
Cracking	Segment section	Flexural crack width	Allowable concrete crack width
			Shear crack capacity

Table 10: Design checks and critical design parameters for SLS of tunnel segments

9.2 STRESS VERIFICATION

Critical stresses in the segments at SLS are calculated for a combination of maximum bending moments and corresponding axial forces. Compressive stresses are limited in the structural codes in order to avoid microcracking which may lead to a reduction in durability. Maximum compressive stresses in both rebar reinforced and fiber-reinforced concrete at SLS are limited to values of $0.4f'_c$ according to JSCE (2007), and to $0.6f'_c$ according to EN 1992-1-1 (2004), AFTES (1993) and fib Model Code 2010 (2013). On the other hand, tensile stresses in the rebar are limited to f_y according to JSCE (2007) and to $0.8\,f_y$ according to EN 1992-1-1 (2004) and fib Model Code 2010 (2013). AFTES (1993) limits reinforcement tensile stresses to 240 MPa (34.8 ksi) for detrimental cracking and 200 MPa (29 ksi) for highly detrimental cracking.

Flexural stresses in the joints are evaluated using the maximum bending moments and corresponding axial forces obtained from analysis such as beam-spring modelling, considering the joints as reinforced concrete sections with bolts acting as tension rebar (where the bolts comply with the durability and design life requirements). Developed stresses in the concrete at segment joints are limited to the allowable compressive stress of concrete. Developed stresses and forces in the bolts are limited to the allowable stress of the connecting bolts as published by the manufacturer.

9.3 DEFORMATION VERIFICATION

Segment deformations are obtained from the different analytical models presented above. However, joint gap and joint offset are only obtained from models that simulate joints between segments and rings. For SLS verification, these deformations are limited to allowable values recommended by standards, guidelines and often project specifications. As an example, the Austrian Society for Concrete and Construction Technology (ÖVBB, 2011) recommends allowable deformations, shown in Figure 33, for both segments and joints for tunnels with diameters up to 8 m (26 ft).

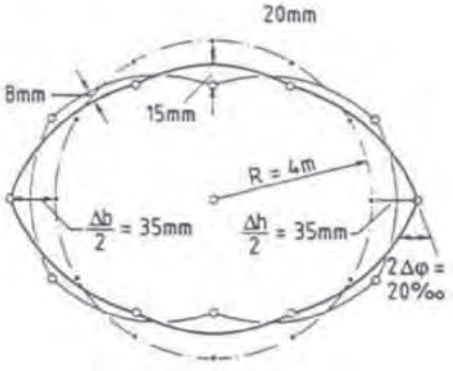

Figure 33 : Ring deformation criteria (ÖVBB, 2011).

9.4 CRACKING VERIFICATION

Cracking in segments is a major contributor to reduction in serviceability due to reduction of watertightness and reinforcement corrosion. In particular, cracking has a significant effect on the durability of the tunnel in an environment with frequent freeze-thaw cycles. Analyses using appropriate methods should be carried out to ensure that cracking in segments does not impair the serviceability, durability or intended purposes of the tunnel lining. Cracks induced in segments under service loads are mainly caused by bending moments and axial forces and the designer should ensure that the flexural crack width is not greater than the allowable crack width (see Table 11 below). The flexural crack width calculation for reinforced concrete (RC) and fiber reinforced concrete (FRC) segments is presented below. Note that in the SLS, the maximum shear force developed at segment joints as a result of modeling with joint simulation should be limited to the shear crack capacity.

9.4.1 Flexural crack width in segments

The flexural crack width in reinforced concrete tunnel segments due to bending moment and axial force is calculated using ACI 224.1R (2007), JSCE (2007) and EN 1992-1-1 (2004) formulas as shown in Eqs. 17, 18 and 19, respectively.

$$w = 0.011\beta f_s \sqrt[3]{d_c A} \times 10^{-3} \quad \text{and} \quad w = 2\frac{f_s}{E_s}\beta\sqrt{d_c^2 + \left(\frac{s}{2}\right)^2}$$

(Eq. 17)

$$w = s\left(\frac{f_s}{E_s} + \varepsilon'_{csh}\right); \; s > 0.55\left(\frac{15}{f'_c + 20} + 0.7\right)\cdot\frac{5(n+2)}{7n+8}\cdot\left(4\cdot d_c + 0.7\cdot(s-\phi)\right)$$

$$w = s_{r,max}\left(\frac{f_s - k_t\frac{f_{ct,eff}}{\left(\frac{A_s}{A}\right)}\left(1 + \frac{E_s}{E_{cm}}\cdot\frac{A_s}{A}\right)}{E_s}\right) \geq s_{r,max}\left(0.6\frac{f_s}{E_s}\right)$$

(Eq. 18-19)

9.4.2 Maximum allowable crack width

Cracking in tunnel segments is controlled by limiting the crack width to prevent durability issues as a result of increased permeability, excessive water leaks, and reinforcement corrosion. Allowable crack widths are recommended by standards and guidelines which consider the function, importance, service, life span, purpose, surrounding environment, and surrounding soil conditions of the tunnel (JSCE, 2007). General guidelines for allowable crack widths are given in the Table 11.

As a most comprehensive guideline, the Austrian Society for Concrete and Construction Technology (ÖVBB, 2011) specifies the allowable crack width in segments based on the tunnel function, and corresponding watertightness requirements, as illustrated in Table 12.

Fib Model Code 2010 (2013), Italian standard CNR-DT 204 (2006), RILEM TC 162-TDF (2003) recommendation, and German DAfStb guideline (2012) can be used to calculate the crack width in concrete sections reinforced by fibers with and without conventional reinforcement. The flexural crack width of FRC segments is well documented in fib Bulletin N°. 83 (2017) which considers analytical sectional approaches as well as finite element methods.

AUTHORITY	ALLOWABLE CRACK WIDTH	COMMENT
ACI 224 (2007)	0.30 mm	Structures exposed to soil
EN 1992-1-1 (2004)	0.30 mm	RC members
fib Model Code 2010 (2013)	0.20 mm	Leakage to be limited with some surface staining
Singapore Land Transport Authority design criteria (2010)	0.30 mm	-
(DAUB, 2013)	0.20 mm	0.15 mm when below groundwater table
JSCE standard (2007)	$0.004d_c$	d_c is the concrete cover over the rebar
RILEM TC 162-TDF (2003)	0.30 mm	Fiber-reinforced concrete

Table 11 : Allowable Crack Widths

REQUIREMENT CLASS	DESIGNATION	APPLICATION	REQUIREMENT	ALLOWABLE CRACK WIDTH
AT1	Largely dry	One-pass lining with very tight waterproofing requirements	Impermeable	0.20 mm (0.008 in)
AT2	Slightly moist	One-pass lining for road and railway tunnels with normal waterproofing requirements (excluding portals)	Moist, no running water in tunnel	0.25 mm (0.010 in)
AT3	Moist	One-pass lining without waterproofing requirements	Water dripping from individual	0.30 mm (0.012 in)
AT4	Wet	One-pass lining without waterproofing requirements	Water running in some places	0.30 mm (0.012 in)

Table 12 : Allowable crack width for tunnel segments (ÖVBB, 2011)

10 >> Design of segment gasket

Watertightness of service tunnels (i.e. utility, rail and road) must be ensured during design and construction in order to prevent water infiltration, minimize maintenance and repair costs, maintain operational safety, and protect mechanical and electrical equipment inside the tunnels. In the one-pass segmental lining system, the watertightness of the tunnel is guaranteed by the individual components of the support system, namely the precast concrete segments and the segment gaskets which are placed between segments in the longitudinal and circumferential joints. As shown in Figure 34, gaskets are positioned around the individual segment like a frame and primarily near the lining extrados to provide the joint watertightness.

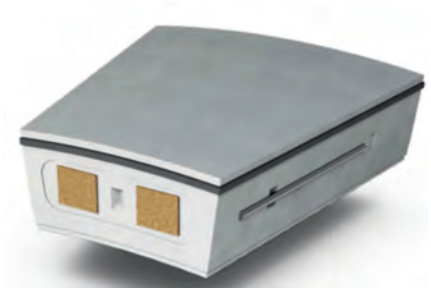

Figure 34 : Segment gaskets positioned near the lining extrados for joint watertightness.

10.1 GASKET MATERIALS

The gasket material must be suitable for the encountered ground and groundwater conditions. EPDM (Ethylene Propylene Diene Monomer) has been established as the preferred material, however, it is not resistant to hydrocarbons. Alternative materials such as Chloroprene Rubber/ Styrene Butadiene Rubber (CR/SBR) are available for such situations, but they do not perform well in acidic environments.

For the gasket to perform as intended, several material-specific requirements must be met. One of these properties is the hardness of the rubber compound. BSI PAS 8810 (2016) requires a maximum shore hardness of 75 (as determined by ASTM D2240), whereas STUVAtec (2005) and AFTES (2005) call for a maximum hardness of 85. Other important properties include tensile strength and elongation (as determined by ASTM D412) which are recommended to be greater than 12 MPa (1700 psi) and 300 percent, respectively. Regardless of the design parameters, the ultimate performance of the gasket will be tested when the lining is installed. The technical solutions that engineers need to implement to achieve the required watertightness depend on specific project circumstances. The important factors for sealing gaskets are the water pressure, safety factor, size of tunnel and segments, gap and offset between segments, and tolerances.

10.2 WATER PRESSURE AND GASKET DESIGN

An important consideration in the design of gaskets is the maximum ground water pressure. Depending on the expected ground water pressure, different gasket profiles may be selected. The first generation of gaskets could only withstand a maximum water pressure of 3 bar. Today, with the advance of technology and limited offset between adjacent segments due to more accurate segment erection inside the TBM, water tightness of up to 10 bar is often achievable with a standard mono-extrusion EPDM gasket profile. As shown in Figure 35, water tightness between segments is created through compression of the gaskets during the assembly process of the segments.

To resist higher ground water pressures, two main solutions are available. The first solution consists of a composite seal which combines the two different sealing technologies of an EPDM compression gasket and a hydrophilic seal. As shown in Figure 36, this may consist of co-extruded gaskets with a hydrophilic layer, composite profiles with hydrophilic cord, or designing a composite solution with a separate hydrophilic seal next to the standard EPDM gasket.

Figure 37 indicates how the hydrophilic insertion improves the sealing performance of a composite EPDM gasket in terms of resisting higher water pressure after several days of immersion in water. The hydrophilic insertion swells under water pressure and acts as an extra backup to the EPDM profile. About 50% of the swelling occurs within 7 days with nearly 100% of the swelling occurring within 30 days.

A second solution is to install two sealing gaskets, one near the extrados and one near the intrados of the segment, thus providing double security for the waterproofing performance. When used in combination with sealing bars installed between the extrados and intrados gaskets, isolation chambers can be created that confine any localizing leakages thus permitting precise repairs by grout injection methods. The connecting gasket bars are generally glued in place at the segment precast plant. Note should be taken that the watertightness of a double gasket system is defined by the higher capacity of the two gaskets, not by the sum of both gaskets' capacity (BSI PAS 8810, 2016).

10.3 GASKET RELAXATION AND FACTOR OF SAFETY

In addition to the expected ground water pressure, the design has to define the watertightness performance of a sealing gasket and include a safety factor that takes rubber relaxation effects into account. It is crucial that the gasket profile and rubber compound uphold the designed reaction force to withstand the applied ground water pressure years after its installation. The majority of the relaxation occurs within months after installation. The relaxation can be tested with so-called aging tests using an accelerated procedure with elevated temperatures in order to get results within a reasonable timeframe (Figure 38). As the relaxation behavior of a sealing gasket is mainly influenced by the geometry of the gasket profile, such aging tests should be carried out for each profile type.

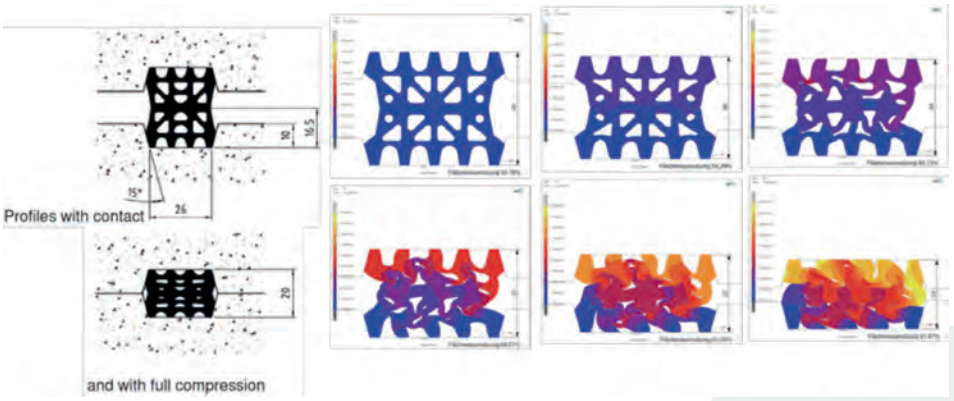

Figure 35 : Water tightness between segments created through gasket compression

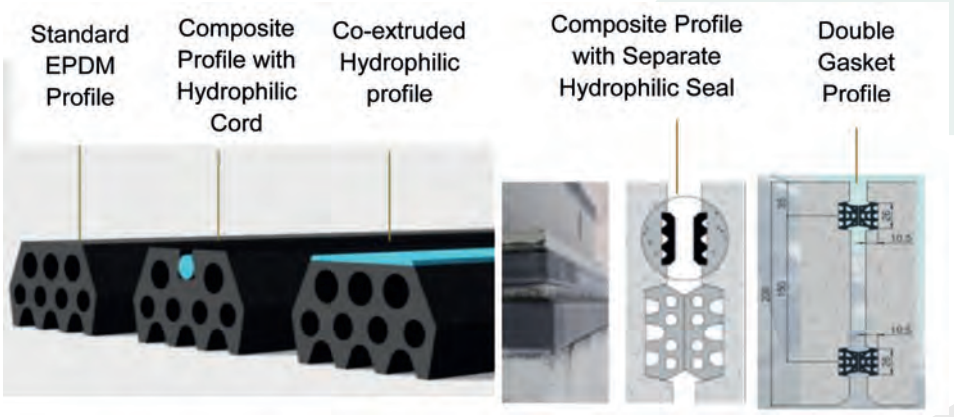

Figure 36 : Standard, composite and double gasket solutions for projects with different watertightness requirements

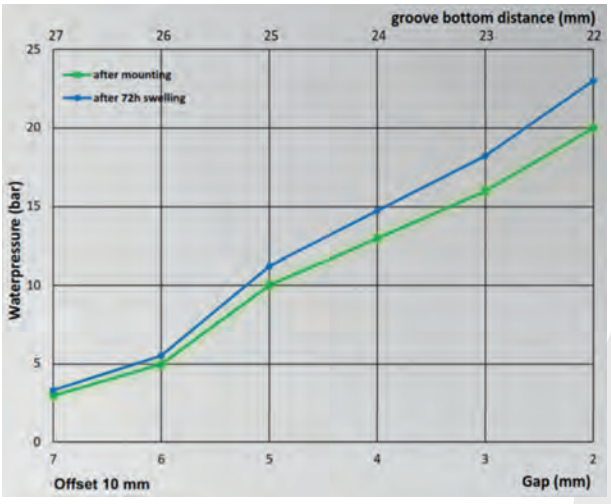

Figure 37 : Effect of hydrophilic swelling cord on improving sealing performance of a composite EPDM gasket in terms of resisting higher water pressure after several days of immersion in water

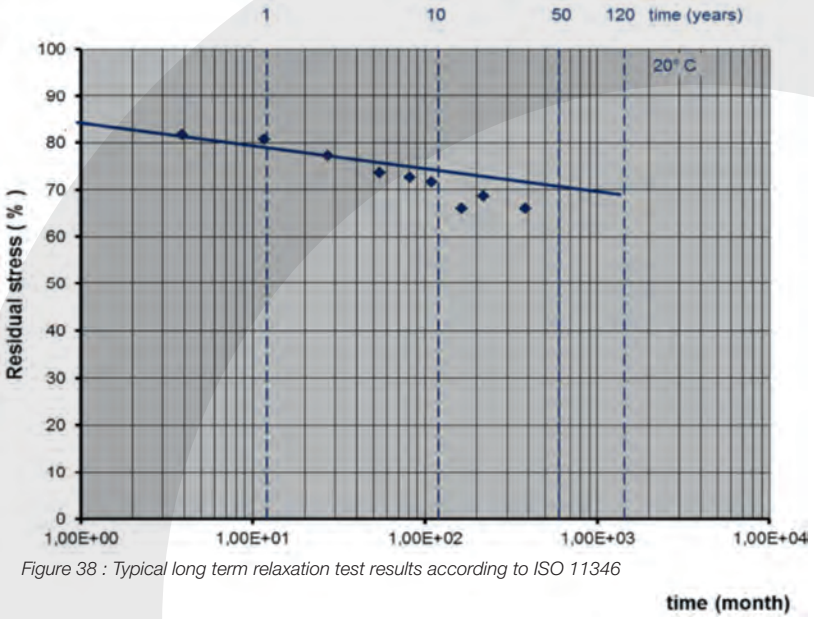

Figure 38 : Typical long term relaxation test results according to ISO 11346

Most of the specifications ask for a minimum residual compressive stress of 60% after 100 years which equates to a safety factor of 1.67 (1/0.60=1.67) for gasket profiles. Considering the relaxation effects of rubber and the design life of most tunnels is 100 to 120 years, a safety factor of two is advisable to ensure that the gasket is able to withstand the design pressure in the long term.

10.4 TOLERANCES AND DESIGN FOR REQUIRED GAP/OFFSET

The width of the gasket profile is a function of the segment thickness which is a function of tunnel diameter. The following gasket profile widths are commonly used with regard to the tunnel diameter:

- Tunnel Diameter < 4m, Gasket Width = 20mm
- 4m < Tunnel Diameter < 7m, Gasket Width = 26mm
- 7m < Tunnel Diameter < 11m, Gasket Width = 33 or 36mm
- 12m < Tunnel Diameter, Gasket Width = 36 or 44mm

Gasket size, however, is also governed by erection tolerances which in turn depend on the diameter of the tunnel (segment size) and the connection system. Bolts and dowels are two typical connection systems that allow for different gap and offset tolerances during the segment erection process. Gap openings and offsets are illustrated in Figure 39. A connection system with bolts usually allows offsets up to 15mm, which can be reduced to 5mm with high precision workmanship. Dowels, however, work to much lower tolerances.

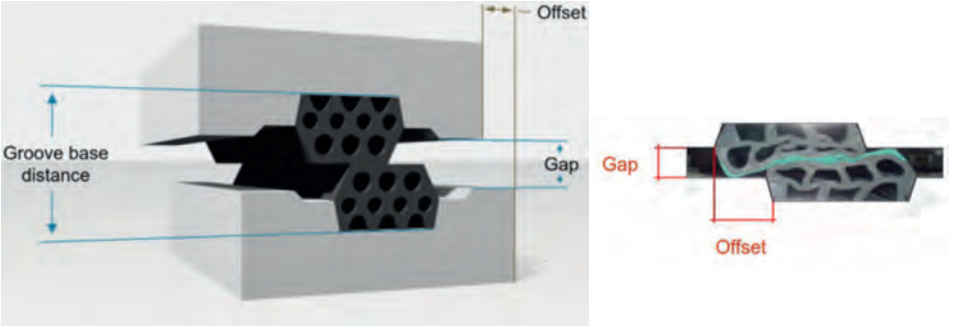

Figure 39 : Illustration of gap opening and offset before and after compression

Reducing the offset tolerance has the following advantages: firstly, the gasket needs to cover a smaller offset range and therefore a narrower gasket profile can be selected, and secondly, the required gasket resistance pressure is reduced. In addition to being able to utilize a smaller gasket with a lower cost, other advantages of a sealing system with reduced offset tolerances include:

- reduction of TBM erector forces (up to ~50%)
- reduction of induced forces in connectors (up to ~50%) and in turn reduction in size of connection system
- reduction of designed space for connection and gasket systems

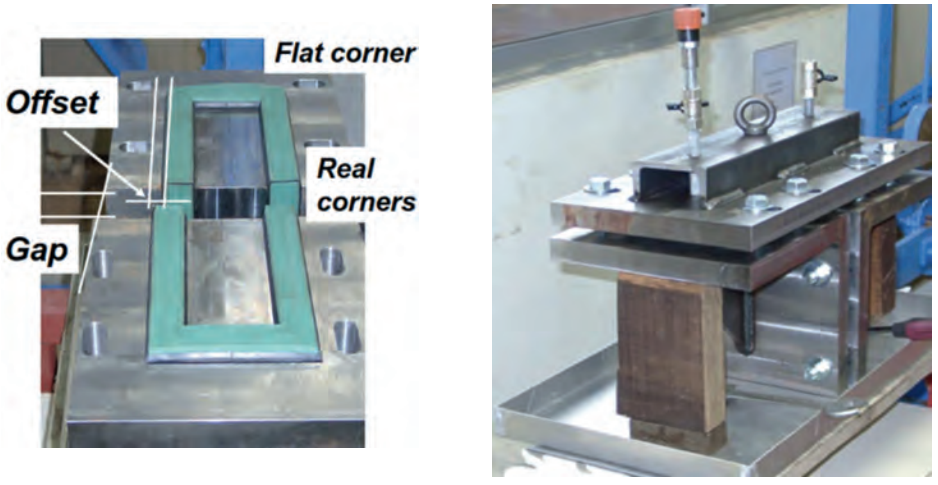

Figure 40 : T joint watertightness test setup for segment gaskets as recommended by STUVAtec (2005)

Some tunnel project specifications specify a 5 mm gap and 10 mm offset for segment gaskets. Dowels can easily provide this requirement, and the segment installation process is easier than when using bolts. Bolts are generally the preferred connection system in longitudinal joints, and in order to avoid additional time and labor costs to achieve the above tolerances, contractors tend to change to higher gap and especially higher offset values. While engineers design gaskets for a specified gap and offset, they are encouraged to consider possible larger gap and offset tolerances. Although this will result in a larger, more expensive gasket, it will result in potential cost saving due to faster erection and construction time.

Watertightness tests using gaskets can be performed on steel or concrete specimens. Working with concrete specimens is time consuming and prone to failure so practically all tests are currently carried out on steel specimens. Test approaches vary, but following STUVAtec's (2005) recommendations and as shown in Figure 40, the geometric situation is simulated on a T-joint in the laboratory, whereby, as on the circumferential joint, a straight piece of sealing profile is pressed against the end of a longitudinal joint. Gaskets must guarantee the water tightness under all possible gaps and offsets. Therefore, it is necessary to run the watertightness test with different gaps and off-sets. For every offset setting (0 – 20 mm), the test has to run through a range of different gaps. For every gap, the water pressure is built up in steps of 1 bar and is held there for 5 minutes. In this manner, every combination is tested until leakage occurs. Plotting all "failure points" results in a watertightness-gap diagram as shown in Figure 41. From the watertightness diagram, the gasket resisting pressure corresponding to designed gap and offset should be higher than the maximum factored working pressure for the project.

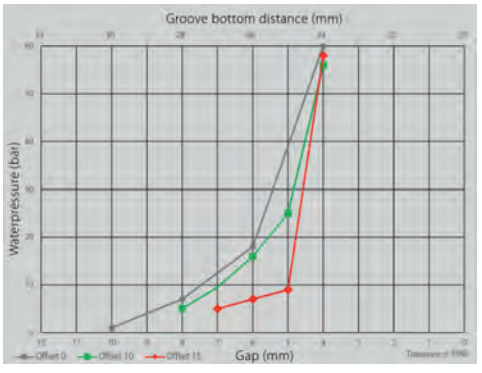

Figure 41 : Typical watertightness-gap diagram

10.5 GASKET LOAD DEFLECTION

If during segment installation the reaction force from the gasket is too high, a strong erection force has to be provided to properly compress the segments and there is a risk of cracking in the concrete groove near the segment edge. This could result in water penetration beneath the gaskets and result in durability and serviceability issues in the lining.

Connection systems are designed based on the initial reaction force of gaskets during segment installation. Therefore gasket short-term behavior should be determined and a load-deflection curve obtained which will depend on the shape of gasket profile and required gap and offset (see Figure 42a where deflection is represented by the gap). Connection systems are designed for maximum gasket load, which in Figure 42a corresponds to a zero gap. However, connection systems can be designed less stringently by designing for the maximum reaction force from the gasket after short-term relaxation (within 5 minutes) as indicated in Figure 42b. Note that 5 minutes would be the minimum time before the connectors are required to start acting against the compressive force from the gaskets, and the minimum time required prior to TBM thrust jack force release.

10.6 GASKET GROOVE DESIGN

The watertightness of a segmental joint is dependent on the groove geometry which has to be in line with the chosen gasket. In addition, cracking in the concrete can occur when the gasket and its groove are placed too close to the edge of the segment. To avoid spalling of concrete, it is crucial that the net volume of the rubber can be housed within the groove when the tunnel segments are fully closed or the gap is zero. To achieve this, the net profile volume of the gasket (seen in cross section) should be slightly smaller than the groove cross section (smaller than approximately 90% of the groove cross section). This will ensure that, even in case very high forces are applied to the segment joints (e.g. TBM jacks) there is enough space for the gasket to 'fit' in the groove.

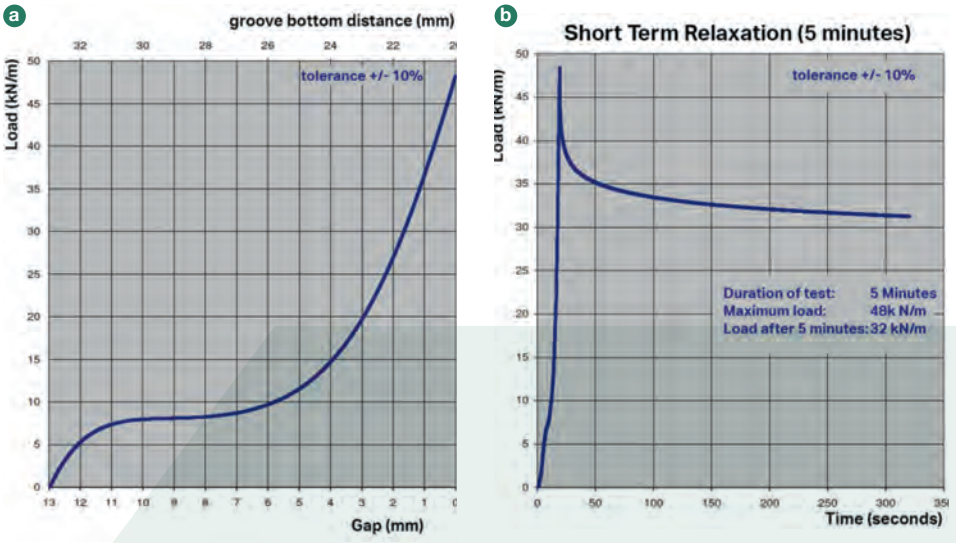

Figure 42a) : typical gasket load-deflection or reaction force test results, b) typical short-term relaxation

However, segments with narrow deep grooves and high TBM jack forces have displayed failure of the concrete segment corners even when the above criterion of volume ratio is fulfilled. A simplistic explanation may be that when the gasket reaches its full compression (no voids), the applied force (R) will be redistributed along the groove flanks and the groove bottom (p) as indicated in Figure 43. Therefore, the spalling force (P_1 or P_2 in Figure 43) on the flanks is directly dependent on the groove depth. The larger spalling force (P2) is only partially compensated for by the slightly longer shear area (a≈b). This leads to the conclusion that the danger of spalling increases with a deeper gasket groove and that a flat profile design is more favorable. In the end, a successful installation without spalling depends on the experience of the involved parties, especially on the skills of the worker guiding the TBM-erector.

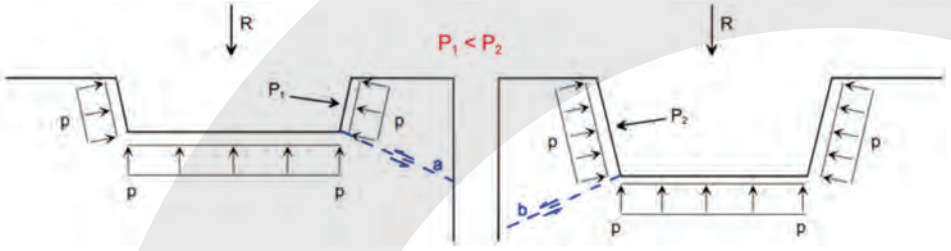

Figure 43 : Re-distribution of impact force R in (a) a shallow and (b) deep gasket groove

10.7 NEW DEVELOPMENTS IN GASKET SYSTEMS

Conventional gasket systems incorporate the gasket groove in the segment molds, so that after casting, the gasket can be glued into the groove. In this gasket system, also referred to as glued gasket, gluing of the gaskets is carried out to ensure that they remain in their grooves. A drawback with this system is the low bond strength of glued gaskets to the segments to prevent the gasket coming loose, especially during key segment installation.

A recent development incorporates anchored gaskets which provide higher bonding forces between the gasket and the segment. As shown in Figure 44, the gasket has anchoring legs which are embedded in concrete in the process of segment production. This results in an extended seepage path beneath the gasket and the gasket is held safely in place during installation (ÖVBB, 2011).

Another development is the design and production of gasket corners. Most of the manufactures now provide prefabricated corners with reduced stiffness. This technology provides soft corners and reduces the risk of spalling of concrete at the segment corners.

A recent development in gasket design is the use of fiber anchored technology. This essentially replaces the anchored feet with plastic fibers as the anchoring element (Figure 45). This offers additional pull-out resistance compared to the conventional glued gasket system.

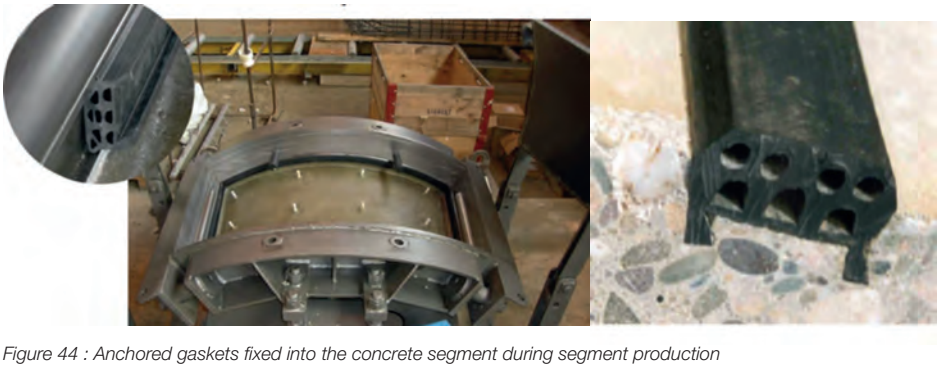

Figure 44 : Anchored gaskets fixed into the concrete segment during segment production

Figure 45 : Anchored segment gasket using fiber anchorage system

10.8 NEW DEVELOPMENT IN GASKET REPAIR SYSTEMS

A new repair methodology for post sealing segment joints has been developed. Leaking joints in segmentally lined tunnels is a well-known phenomenon which is caused by displacement of the gasket during segment installation, lack or loss of compression force on gaskets (due to an unprecedented increased gap between the segments faces), or damaged concrete segments and cracked concrete edges due to eccentric forces during TBM jacking. This repair method is based on drilling and injection through the joint sealing gasket (Kirschke et al. 2013). The four steps for this repair method (shown on Figure 46) are:

Step 1: Pre-drilling Ø 14 mm to the joint sealing profile
Step 2: Drill and push injection needle through the entire joint gasket
Step 3: Injection using accelerated injection material
Step 4: Removal of extension tube. The injection needle remains in the joint gasket

The advantages of this repair system are an efficient injection procedure with less time, material and labor cost; less drilling work with no significant damage to the concrete or steel reinforcement; and injection works are restricted to the leaking areas.

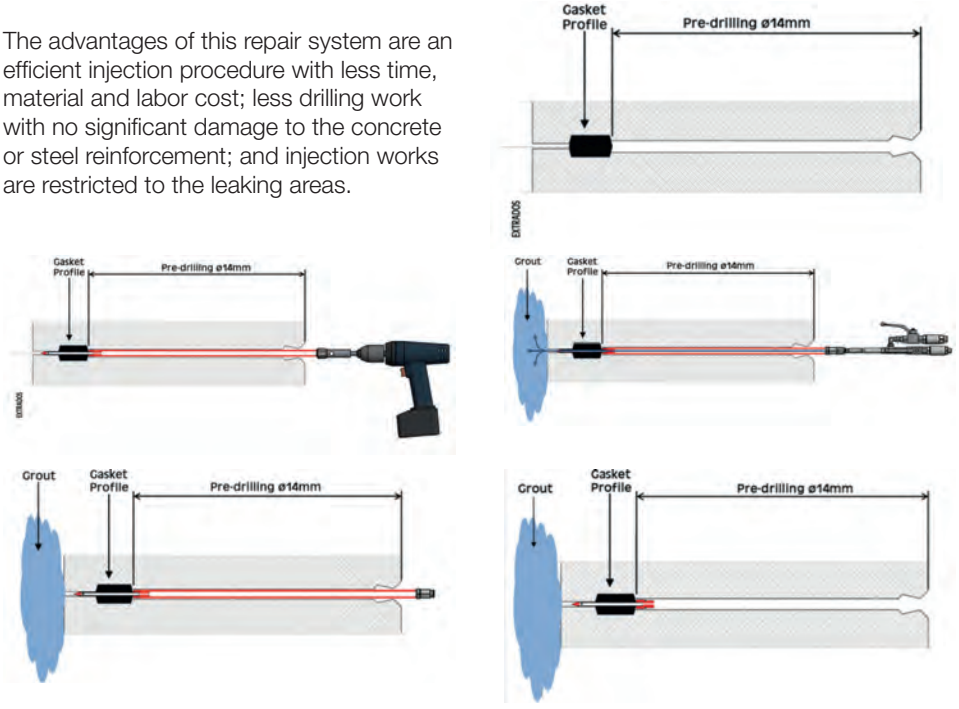

Figure 46 : A step-by-step schematics of a recently developed repair method to control groundwater inflow using injection through gaskets in leaking segmental tunnels (Kirschke et al. 2013)

11.1 BOLTS, DOWELS AND GUIDING RODS

The connections between segments within a ring and between rings can be divided into three categories; joint connections with bolts, dowels and guiding rods.

In the bolt type connection, the segment is first placed in position and then the bolts are inserted and tightened. Bolt connections require more effort in the construction of the mold as it is necessary to create pockets and grooves into which the bolts are inserted. It is also necessary to have more personnel in the tunnel to insert the bolts. This type of connection is traditionally associated with rectangular segments and is generally used between rings and between segments within a ring.

The bolts are metallic while the embedded threads are generally plastic. Figure 47 shows a typical arrangement for a straight bolt. Note should be taken of the following geometrical details:

- The pockets should be large enough for head of the bolt and pneumatic wrench to be easily inserted
- The slot side of the pocket should have a conicity of at least 1°.
- The bolt slot in the segment that houses the plastic bolt socket should have a compatible conicity.
- The bolt axis should pass through the center of the segment.
- The distance between the end of the nut and the extrados of the segment should be sufficient.

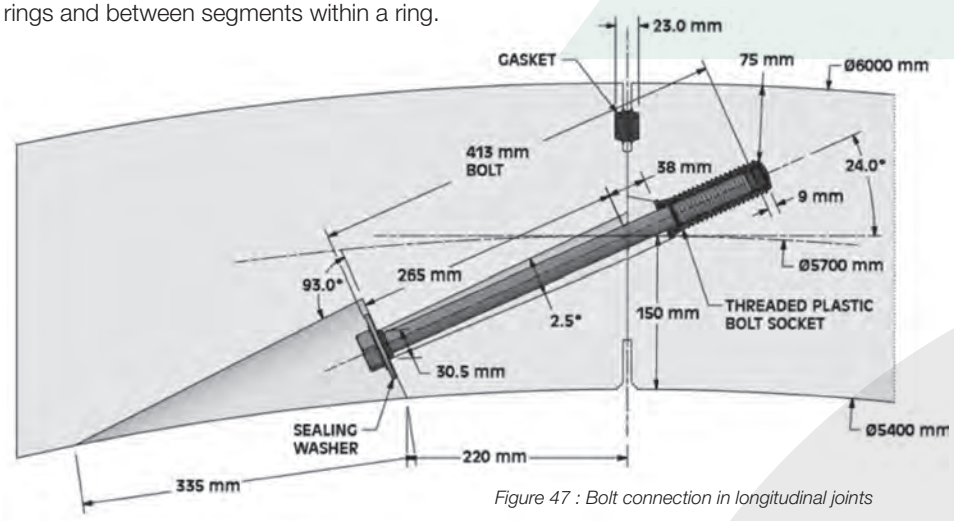

Figure 47 : Bolt connection in longitudinal joints

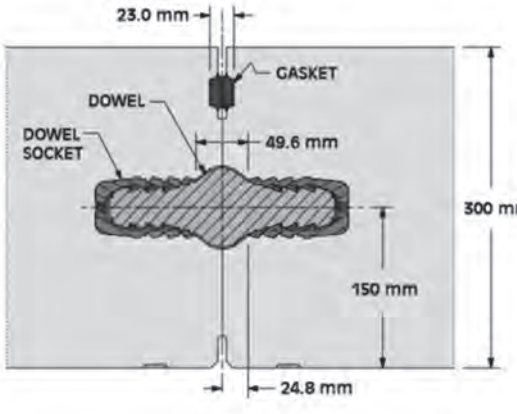

Figure 48 : Dowel connection in circumferential joints

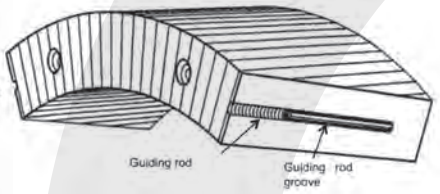

Figure 49 : Location and geometry of guiding rod and guiding rod groove (ÖVBB, 2011)

In the dowel type connection, the dowels are inserted into the segment during ring assembly and are either mortise inserted or dove-tailed into the segment of the last assembled ring. Dowel connections require less work for the construction of the mold and less manpower in the tunnel. The dowels and sockets are made of plastic and sometimes have a core of steel. Figure 48 shows a typical arrangement of a dowel, which is placed on the neutral axis at the middle point of the segment. Because of the kinematics of the assembling process, this type of connection is only used between the rings in circumferential joints. In most cases, the dowel connections are used with rhomboidal and trapezoidal segments to avoid early crawling or creeping of the gaskets when the segments are being inserted.

Besides bolts and dowels, guiding rods (Figure 49) can be used as a movable centering device that provides guidance and centering during segment installation with locking functionality. In addition, guiding rods absorb shear forces in the longitudinal joints (OVBB 2011). An advantage of using guiding rods in the longitudinal joints is that the inserted rods can prevent the segments slipping away from each other during ring building (DAUB, 2013). Guiding rods are usually utilized in conjunction with dowel connection systems.

11.2 DESIGN OF CONNECTION DEVICE FOR GASKET PRESSURE

Dowels are designed to withstand the reaction force of the gasket profile after short term relaxation has taken place. Depending on the size of the tunnel lining, as well as the total number of dowels in the ring, the gasket force per dowel can be calculated. A safety factor of 1.25 should be considered for the dowel connection system, and the required pullout force will determine the selection of dowel types.

Bolts are designed in a similar way, taking into account their designed angle with the centerline of the longitudinal joints (e.g.

24o in Figure 47). The length of gasket in a longitudinal joint is approximately equal to the ring length. Taking account of the number of bolts in each longitudinal joint (generally two) , the gasket force per bolt is calculated. Again, a factor of safety of 1.25 is advisable and the bolt connection system should be selected based on the required pullout force and tensile yield strength.

11.3 LATEST DEVELOPMENTS IN JOINT CONNECTION SYSTEMS

Dowels have become the preferred connection system in circumferential joints replacing conventional bolts. Their advantages are faster installation and reduction of offset between the rings. However, in large-diameter tunnels they may provide insufficient shear capacity. To overcome this issue, new dowel systems have been introduced utilizing new plastic materials which have a higher resistance (i.e. less displacement) and are less susceptible to variations in humidity.

Another modification includes integration of a screw-able socket on one side of the dowel in order to reduce the installation tolerance, and provide the workers with a smoother assembly process (see Figure 50). Pull-out resistance and shear capacity of up to 250 kN is achievable with this system.

Currently bolts are used in longitudinal joints as the pre-dominant connection system. Although bolts provide high pull-out and yield tensile strength, bolting is a time-consuming process and recesses are required to be provided for fastening the bolts.

11.4 FASTENING SYSTEMS TO SEGMENTS

Fastening systems to segments are important elements for service tunnels (i.e. utility, rail and road).

They are used when fitting out a tunnel, i.e. when fixing system components of the railway overhead catenary systems, and fixing mechanical and electrical equipment. Other applications of fastening systems include fixing and supporting intermediate slabs, cross-passageway connecting doors, and platform screen doors. Fixing failures in tunnels are rare but when they happen, the consequences can be very costly and tragic. In general, these fasteners can be divided into two main categories, post-installed and cast-in place systems.

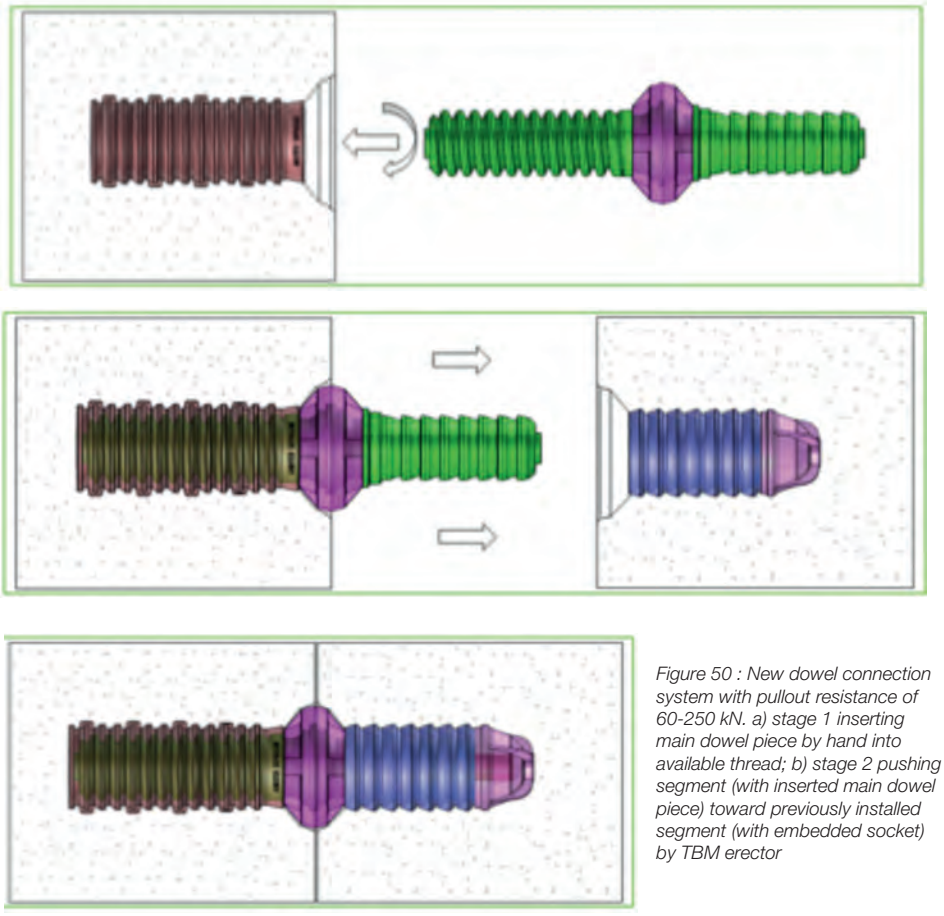

Figure 50 : New dowel connection system with pullout resistance of 60-250 kN. a) stage 1 inserting main dowel piece by hand into available thread; b) stage 2 pushing segment (with inserted main dowel piece) toward previously installed segment (with embedded socket) by TBM erector

11.4.1 Post-Installed Fastening Systems

Post-installed anchors as a traditional fastening system have some disadvantages, mainly the issues of drilling and installation quality, which have made this system less favorable. Drilling procedures generate dust and noise during installation, and power tools are needed when installing anchors in high-strength concrete. Drilling may damage concrete, reinforcement or segment gaskets with negative impacts on structural behavior, sealing performance, corrosion protection and long-term durability.
Fixing failures generally occur as a result of poor installation quality where incorrect adhesives or installation procedures have been adopted.
Some of the issues with traditional post-installed anchor systems are illustrated in Figure 51.

Post-installed straight or curved framing channels, as an alternative to direct anchor fastening systems, can provide some advantages regarding fixing flexibility. With framing channels, subsequent installation or fixing of further components is always possible. This is important for repair and rehabilitation projects where expansion or upgrade of utility equipment and production facilities are required. However, the main issue of drilling and installation quality still remains.

Figure 51 : Issues with post-installed anchors: a) drilling, b) installation quality, c) fixing failure

11.4.2 Cast-in-Place Fastening systems

In order to overcome these problems, a solution has been developed by fixing framing channels to segments via the connection bolts without drilling as illustrated in Figure 52.The figure illustrates the installation of curved framing channels with mounting plates at the back which are held in position with the bolt connection system in the circumferential joints. This fastening system is suitable for fixing utilities, mechanical and electrical equipment in the tunnel and can provide over 30 kN service point load capacity every 300 mm.

Latest segmental lining systems are utilizing dowel connections in circumferential joints and therefore, circumferential pockets for fastening bolts are often not available. To overcome this, fastening technology is shifting towards the use of cast-in channels with a mechanical interlock system, as illustrated in Figure 53. This cast-in system consists of framing channels with welded anchors which are placed in segment forms prior to casting the concrete segment.

Cast-in place systems have lower maintenance cost and result in better quality control both in the precast plant and in the tunnel.

One application of cast-in channels is in railway tunnel and especially high-speed rail tunnels because of the requirement to

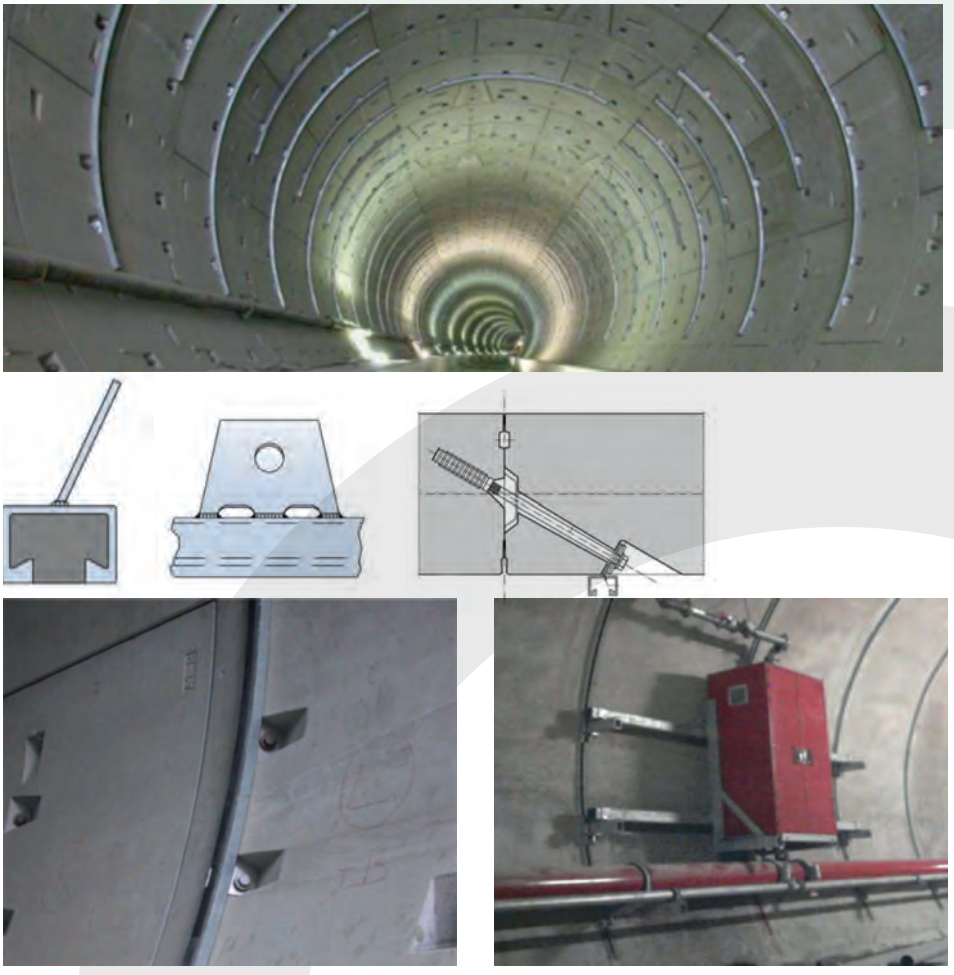

Figure 52 : Post-installed framing channels fixed to segments using connection bolts and mounting plates at the back

fix many electrification components to the tunnel lining, as illustrated in Figure 54. In addition, in these tunnels, resistance to fatigue from dynamic loading is a key requirement that is not easily met by post-installed anchors.

To provide protection against fresh concrete penetrating the anchor channels, a filling strip is provided which can be removed once the segment is installed. This integrated fastening system can be employed for the temporary assembly of walkways or working platforms while the tunnel is being driven.

Cast-in fastening systems also provide similar opportunities for road tunnels for fixing lighting, signal facilities, ventilation, and exhaust air ducts. Figure 55 illustrates another major opportunity for modern fastening systems in road and rail tunnels for supporting intermediate slabs. Tension rod systems are quick and reliable mounting fasteners and favorable solutions when there is a high demand for load capacity and corrosion and fire protection.

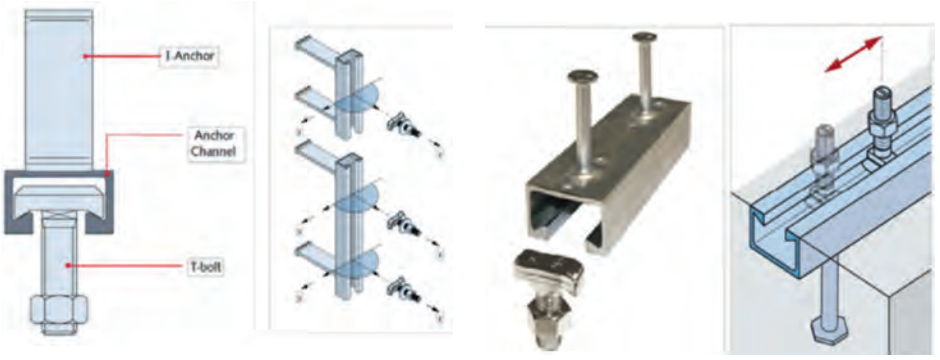

Figure 53 : Cast-in fastening system for segments including channels with welded anchors and bolts

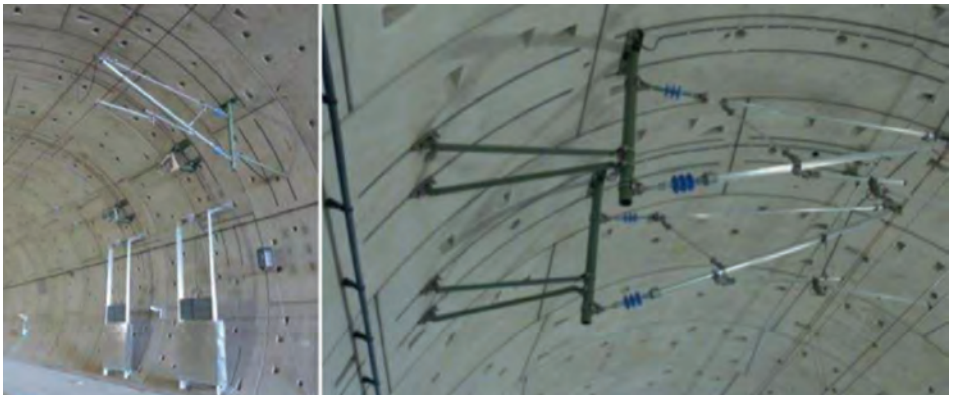

Figure 54 : Curved cast-in channels used as fastening system in railway and high-speed rail tunnels

Figure 55 : Modern fastening systems with tension rods for supporting intermediate slab

Tolerances are allowable deviations from the actual dimensions of the segmental lining (either as individual components or as a system) compared to their design dimensions. Deviations from the designed geometry are acceptable as long as they don't result in damage to the segmental lining and don't negatively impact on the intended function of the tunnel. Although it is important to achieve the highest possible level of accuracy during the production and installation of segments, tolerances should not be unjustifiably tight which would drive costs up through extravagant demands in terms of accuracy. Accordingly, the design engineer should specify tolerances on a project-specific basis and consider them in all the relevant stages of segment design.
Segmental lining tolerances are often broken down into two main categories, i.e. production tolerances and construction tolerances. Production tolerances are the allowable deviations of individual segment dimensions from the design dimension after manufacture. Construction tolerances which include installation tolerances of the segmental ring, and subsequent deformations of the ring during and after TBM advances need to be considered separately from production tolerances.

12.1 Production tolerances

When considering production tolerances, a distinction should be made between formwork tolerances and segment tolerances. Tolerances for formwork should be stringent enough to guarantee the required production tolerances. High-precision formwork is therefore required for the production of precast tunnel segments. ÖVBB (2011) generally specifies ±0.1 to ± 0.3 mm as the range of tolerances for high-precision steel forms for the reference dimensions indicated in Figure 56.

Tolerances of manufactured segments before storage, transportation and installation should take into account the effects of temperature, shrinkage, creep, and segment self-weight. The effect of creep is generally negligible and guidelines such as ÖVBB (2011) define segment tolerances as a summation of formwork tolerances and allowable segment deformations due to temperature and shrinkage. Table 13 compares formwork and segment tolerances for the reference dimensions shown in Figure 56.

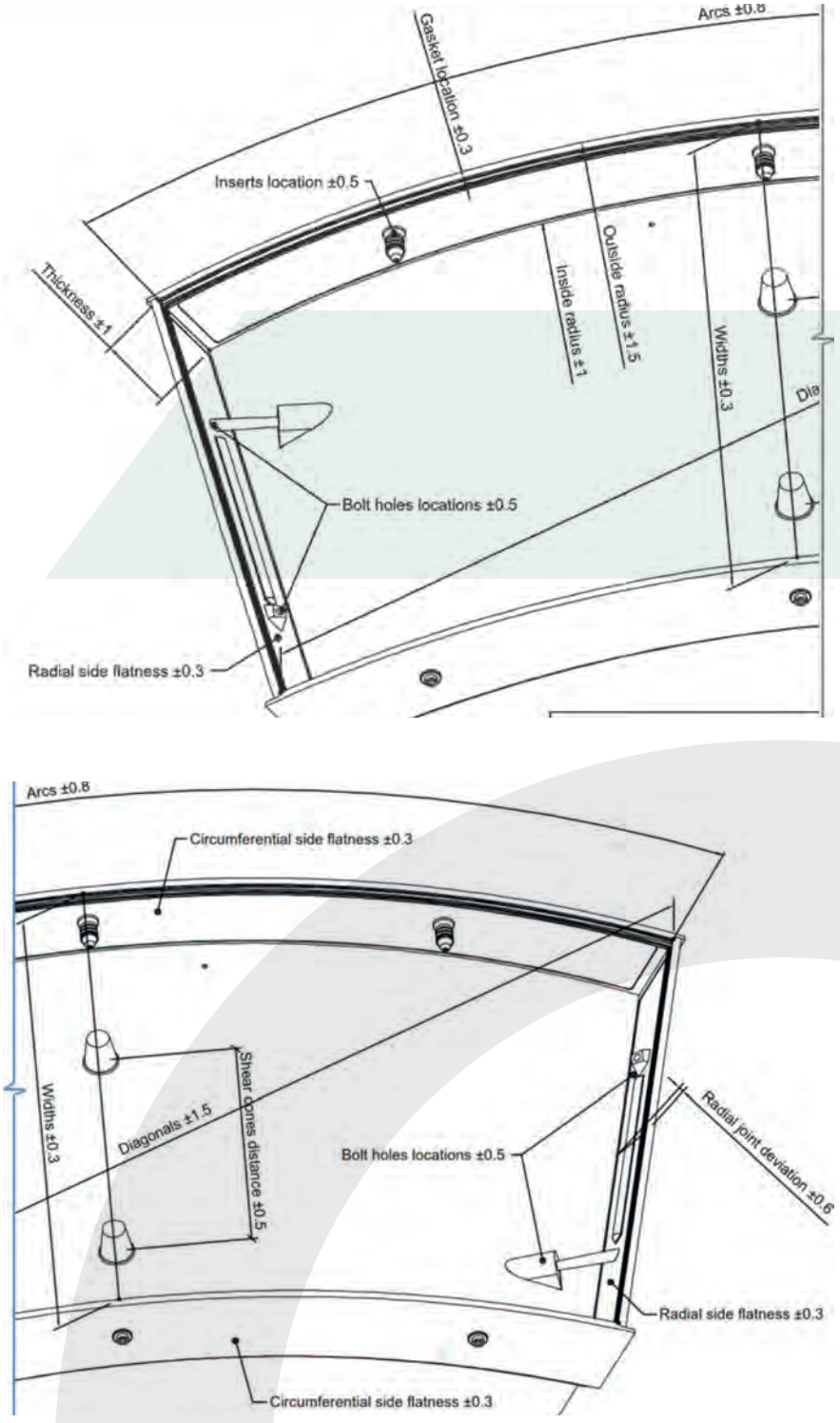

Figure 56 : Typical segment formwork tolerances for mid-size tunnel projects (values are in mm)

Current practice is to specify segment dimension tolerances in contract drawings and specifications, and to control these during manufacture of the segments. The allowable dimensional tolerances for segments depends mainly on serviceability requirements of the tunnel, as well as the size of the tunnel segmental ring. Different guidelines provide different ranges of segment tolerances. Besides the recommendations given in Table 13, Table 14 illustrates the segment tolerances specified by various guidelines and standards, i.e. JSCE (2007), Ril 853 (2011), ZTV-ING (2007), and DAUB (2013). Production tolerances specified by DAUB (2013) in Table 14 are for segmental rings with an internal diameter either less than 8m or larger than 11m. DAUB (2013) recommends a linear interpolation of tolerances between these two size categories. The specified tolerances for each reference dimension presented in Table 14 are in general agreement, with DAUB (2013) specifying the most stringent and complete set of tolerances.

The reference dimensions in Table 14 are divided to four major categories, namely:
a) linear segment dimensions;
b) angular deviations and flatness of joints (or sides);
c) dimensions of gasket, connectors and accessories; and
d) closed-ring dimensions.

Note that the closed-ring dimension tolerances relate to the tolerances of the segmental test-ring mock-up which is erected horizontally in the precast plant. This is a production tolerance and not a construction tolerance.

Among the tolerances described in Table 14, four major categories emerge as the most critical and which need special attention. These four categories include:
a) Segment width
b) Longitudinal joint taper/conicity deviation
c) Segment circumferential (arch) length, and
d) Gasket groove (Handke, 2012).

Segmental width inaccuracies may cause severe damage as a result of wide longitudinal cracks. Excessive deviations in longitudinal joint conicity may result in excessive forces being transferred between segments in the longitudinal joints which may result in the concrete crushing or

REFERENCE DIMENSIONS	FORMWORK TOLERANCES	SEGMENT TOLERANCES
Width	±0.3mm (1/84")	±1.6mm (1/16")
Thickness	±1mm (1/25")	±3.2mm (1/8")
Circumferential length (arc)	±0.8mm (1/32")	±1.6mm (1/16")
Inside radius	±1mm (1/25")	±1.6mm (1/16")
Outside radius	±1.5mm (1/17")	±6.3mm (1/4")
Diagonals	±1.5mm (1/17")	±1.6mm (1/16")
Warping	±1.5mm (1/17")	±2mm (1/12")
Longitudinal/Radial joint deviation	±0.2mm (1/42")	±0.8mm (1/32")
Sides flatness	±0.3mm (1/84")	±0.8mm (1/32")
Location of gasket groove axis	±0.3mm (1/84")	±0.8mm (1/32")
Dowel insert location	±0.5mm (1/50")	±0.8mm (1/32")
Bolt hole location	±0.5mm (1/50")	±0.8mm (1/32")
Shear cones/erector pocket location	±0.5mm (1/50")	±1.6mm (1/16")

Table 13 : Comparison between formwork tolerances and segment tolerances for mid-size tunnel projects

TYPE OF TOLERANCE	REFERENCE DIMENSIONS	JSCE (2007)	RIL 853 (2011)	ZTV-ING (2007)	DAUB (2013) ID <8M	DAUB (2013) ID >11M
Linear segment dimensions	Width	±1mm	±0.5mm	±0.6mm	±0.5mm	±0.7mm
	Thickness	+5mm -1mm	±3mm	±3mm	±3mm	±4mm
	Circumferential length (arc)	±1mm	±0.6mm	-	±0.6mm	±0.7mm
	Inside radius	-	±1.5mm	±1.5mm	±1.5mm	±2.5mm
	Outside radius	-	-	±2mm	-	-
	Diagonals	-	-	-	±1mm	±2mm
	Warping (Vertical spacing of fourth segment corner from plane formed by other three corners)	-	-	-	±5mm	±8mm
Joints angular deviations and flatness	Longitudinal joint deviation	-	±0.3mm (±0.04o *)	±0.3mm	±0.3mm	±0.5mm
	Longitudinal joint taper/ conicity deviation	-	±0.5mm	±0.5mm	±0.5mm	±0.7mm
	Longitudinal/ circumferential joint flatness	-	±1mm	±0.5mm	±0.3mm	±0.5mm
Gasket, connectors, and accessories dimensions	Location of gasket groove axis	-	+0.2mm	±1.5mm	±1mm	±1mm
	Sealing groove width/ depth	-	-0mm	±0.2mm	±0.2mm	±0.2mm
	Bolt hole/ Dowel insert location	±1mm	±1mm*	-	±1mm	±1mm
	Shear cones/erector pocket location	-	±2mm*	-	±2mm	±2mm
Closed-ring dimensions	Outer diameter	±7mm (2m<ID<4m) ±10mm (4m<ID<6m) ±15mm (6m<ID<8m) ±20mm (8m<ID<12m)	±10mm	-	±10mm	±15mm
	Inner diameter	-	±10mm	-	±10mm	±15mm
	Outer circumference (to be measured in three planes)	-	±30mm	-	±30mm	±45mm
	Assembly misalignment	±7mm (2m<ID<4m) ±10mm (4m<ID<6m) ±10mm (6m<ID<8m) ±15mm (8m<ID<12m)	±10mm	-	-	-

Table 14 : Production segment tolerances specified by guidelines and standards

* Only available in Ril (DS) 853 1993 version

spalling. Circumferential length (arc) and gasket groove tolerances may have a major impact on the sealing performance of gaskets as a result of excessive gap or offset.

Some project specifications do not allow for the use of segments that have been produced outside the tolerance requirements. DAUB (2013), however, permits these segments to be used in areas with low projected tunnelling forces, providing gasket performance is not compromised and calculations demonstrate adequate capacity of reinforcement in the joints in the event of exceeding joint distortion and segment width tolerances.

12.2 Measurement and Dimensional Control

A proper quality control system is essential to ensure the production of high-precision segments with tolerances which fall within the limits imposed by contract documentation. Segments, like any other concrete element, are subject to temperature, shrinkage and creep deformations after casting. However, due to the fact that the temperature, relative humidity and other ambient conditions are maintained relatively constant in the production plant, any dimensional deviation due to temperature and shrinkage can be neglected. Therefore, it is not necessary to wait until the concrete segments have gained full maturity (i.e. at 28 days) to carry out the dimensional control measurements. However, it is highly recommended to conduct these measurements at one specific phase of the production cycle, for instance after segment stripping (demolding).

The dimensional control program should be implemented on individual segments as well as segmental systems in the form of test rings. The most traditional measurement methods are manual measurement by means of steel templates, micron rods, caliper squares, precision measuring tapes and measurement arms (ÖVBB, 2011). However, conventional instruments like micron rods or templates lack global geometrical certification. Measurement systems using theodolite and photogrammetry are alternative methods which lack the necessary speed and accuracy (to within few tenths of a millimeter) needed for regular quality control. 3D industrial measurement prevails as the only accurate measuring system that can meet such high demands at a rate required for a high speed quality control/ quality assurance program. As shown in Figure 57, 3D measurements using a laser interferometer system facilitates the accurate digitization of surfaces by direct polar coordinate measurement. A skilled operator can comprehensively measure the full profile of over 20 segments per shift (Clarke-Hackston et al. 2006). In addition to measurements taken from a single standpoint, a laser tracker system can be employed where a second instrument is utilized (see Figure 57b) in order to perform a complete measurement of form. Figure 58 indicates typical output from the spatial analyzer 3D graphical software platform with tolerances, best-fit of external surfaces and deviations from referenced dimensions.

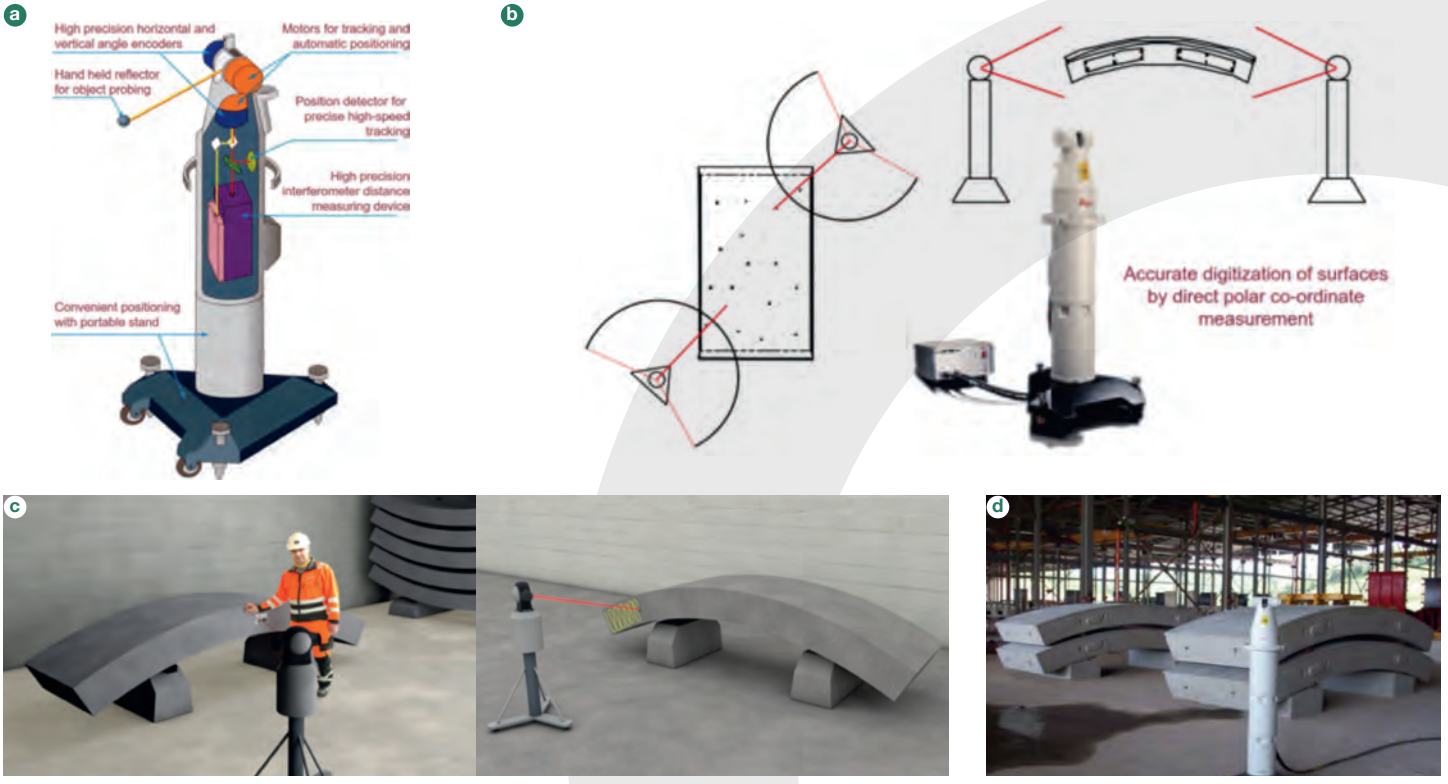

Figure 57 : 3D measurement: (a) laser Interferometer schematic, (b) laser tracker system, (c) instrument location for mold, (d) stacked segments for rapid measurement

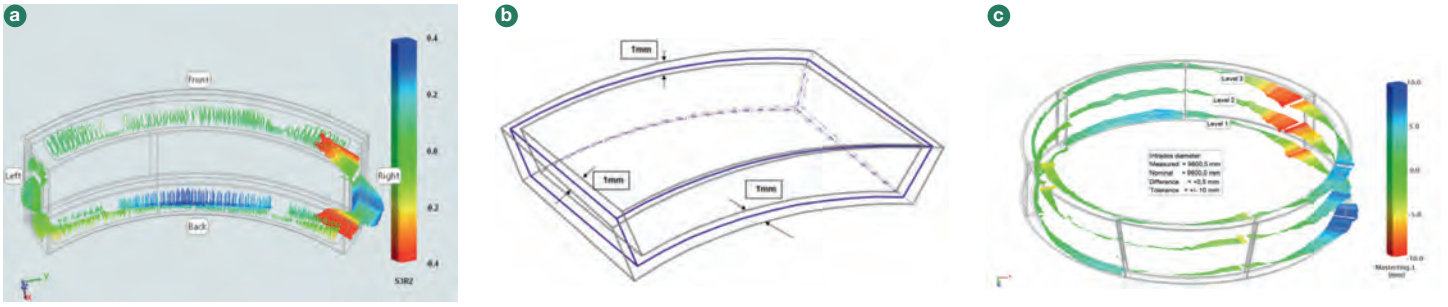

Figure 58 : Spatial analyzer 3D graphical software platform output: (a) typical segment tolerances, (b) best-fit of external surfaces and typical deviations from referenced dimensions, (c) tolerances on virtual (test) ring build.

12.3 TEST RING AND DIMENSIONAL CONTROL FREQUENCY

Dimensional control is carried out on formwork or segments to measure tolerances on reference dimensions, and on the test rings for controlling system tolerances.

a) Test Ring Assembly and Tolerances

One of the original goals of early test ring assembly was to check for alignment of bolting systems and general ring assembly including segment to segment and ring to ring connections. However, with current 3-D computational modelling, the risk of bolting or assembly location errors within the forms is minimal.

In a test ring system, the recommendation is to build a single ring or a double ring where the bottom test ring is measured completely. Generally, the test rings are assembled without the elastomer gasket in place, in order to avoid recovery forces. As indicated in Table 14, reference dimensions to be verified on the assembled test ring include outer and inner diameters (on at least two axes), outer circumference (to be measured in three planes) and joint assembly misalignment. (ÖVBB, 2011), in addition, recommends joint opening and joint misalignment as other system tolerances to be verified on the test ring.

A 10-measurement system as illustrated in Figure 59 has recently been presented as an alternative formwork tolerance measurement method as opposed to the individual reference dimensions given in Figure 56 and Table 14. Both systems are acceptable as they both assure segment dimension accuracies compatible with the reference dimensions given in Table 14. With this alternative method, if there are any issues with the 10 measurements, then the segment direct measurements are to be followed as per Table 14.

b) Dimensional Control Frequency

Two major factors are considered to ensure dimensional control during the production phase, i.e. the testing objects and testing frequency. Forms, individual segments and test rings are the three main testing objects that can be measured. Standard practice is to measure the tolerances of every segment for the first 10 castings, and then measure every 50th segment after that. Some projects, however, call for a more frequent controlling program. A dimensional controlling program based on monthly measurements is not recommended. Some tender design documents require assembling an extra ring on the test ring after a specific number of castings. This is not recommended considering the degree of difficulty, the high cost and little value of such a practice. For segment dimension control, testing should be resumed at the initial frequency soon after detection of any inadmissible deviations.

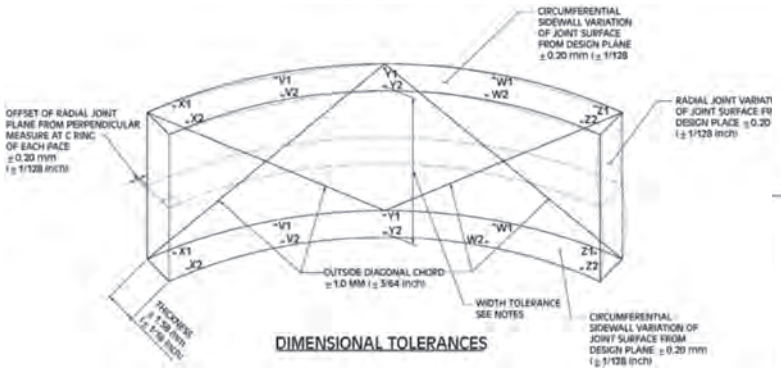

Figure 59 : Alternative tolerance measurement method for formwork dimension control

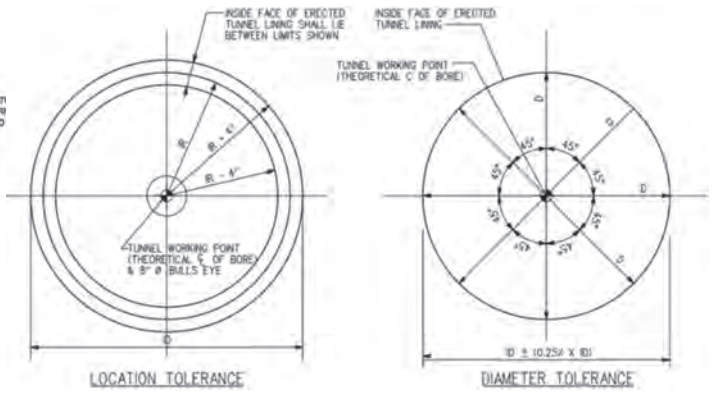

Figure 60 : Typical construction tolerances in contract documents

12.4 CONSTRUCTION TOLERANCES

Accurate segment geometry is a pre-requisite for the smooth installation of segments without any significant constraints. However, deviations from the design geometry of the segments occur during the installation phase that are independent of production accuracies and are related to construction activities. Construction deviations include installation tolerances of the segmental ring, and subsequent deformations of the ring during and after TBM advances. These deviations are referred to as construction tolerance. Ovalization of the ring with corresponding angular deviations and joint misalignment are among the unavoidable construction tolerances. Excessive construction deviations have significant implications including reduction in quality of the finished tunnel, reduction in advance rate, and decreased sealing performance at segment and ring joints.

Newly-assembled segmental rings may undergo ovalization due to segment self-weight or yielding of bolts or dowels. Ovalization can also occur due to loading exerted by the back-up system, uneven bedding of the segmental ring in the backfill grout or tunnel uplift after passing of the TBM. While ovalization cannot be completely avoided, it can be limited to significantly low values through controlled ring assembly systems and self-guiding connectors such as dowels and guiding rods. Ovalization tolerance depends on diameter and the number of segment joints in a ring and is generally specified as an allowable deviation from the nominal diameter. Generally it is recommended to limit the deviation to between 0.25-0.5% of the internal diameter, but BTS specifies an upper bound of 1%. Figure 60 illustrates typical allowable ring diameter and ring location tolerances which are specified in contract documents.

Joint misalignment and deviations from the designed full contact area are also unavoidable and need to be limited to acceptable values. Ring installation inaccuracies can impact joint misalignment and joint opening. In addition, uneven segmental ring bedding, ovalization and uncontrolled torsion in longitudinal joints, can cause joint misalignment in circumferential joints. ÖVBB (2011) recommends ± 5mm as the joint misalignment tolerance for tunnel diameters in the range of 3-8 m, while DAUB (2013) specifies ± 10mm. Nonetheless, allowable joint misalignment can be modified taking into account the required sealing performance and the maximum allowable offset for the type of gaskets selected for the project.

Typical allowable construction tolerances for ring erection are summarized in Table 15. The maximum relative ring roll, which is defined as the roll of every single ring relative to adjacent rings relates to circumferential joint misalignment, while ring step or slips are related to longitudinal joint misalignment. The maximum allowed gap between joint contact faces ensures the best gasket performance, while tolerances on absolute vertical position of lining invert are important where the tunnel lining is under excessive uplift pressure, or in transportation tunnels where accurate location of top of rail or profile grade is required. Planarity of the leading face of the ring is also a critical tolerance and if not achieved leads to segment damage.

Maximum ring roll	±100mm (4")
Ring shape (ovalization) on diameter	±0.25% x ID to ±0.5% x ID
Maximum relative ring roll	±10mm (0.4")
Step, slip or lip due to joint misalignment	±5mm (0.2")
Maximum gap between joint contact faces	±5mm (0.2")
Tolerances on absolute vertical position of lining invert	*±75mm (3")*
Planarity of the faces of the ring	±0.75mm from theoretical plane

Table 15 : Construction tolerances for ring erection

13 >> Concluding remarks

This document has been prepared by Working Group 2 of the ITA after numerous rounds of internal and external reviews, and is intended to update the original WG2 publication “Guidelines for the design of shield tunnel design” (2000). The document consolidates most recent developments, international best practices, and state-of-the-art information on all aspects of design and construction of precast segments, and can be used as a general guide for segmental tunnel linings. In addition to structural design rules and procedures for ultimate limit state and serviceability design for loading conditions particular to segments, this guideline addresses details of segmental ring geometry, shapes, configuration and systems, and detailed concrete design considerations such as concrete strength, curing, and reinforcement detailing. Gasket design procedure and most recent innovations in gasket systems are presented, and special attention was devoted to other design and construction aspects such as segment connection devices, anchorage systems, tolerances, measurement and dimensional control of segments. This document has been written in a fashion that in addition to being useful to experienced tunnel engineers for addressing specific needs of each project, it is focused on helping students and entry-level engineers to understand major design and construction concepts. Prepared guidelines are the state of the practice at the current time on a continuously evolving technology field which makes future updates and revisions to the document inevitable.

14 >> References

American Association of State Highway and Transportation Officials (AASHTO)

DCRT-1-2010—Technical Manual for Design and Construction of Road Tunnels - Civil Elements

American Concrete Institute (ACI)

ACI 224.1R-07 (2007)—Causes, Evaluation, and Repair of Cracks in Concrete Structures

ACI 318 (2014)—Building Code Requirements for Structural Concrete and Commentary

ACI 544.7R (2016)—Report on Design and Construction of Fiber Reinforced Precast Concrete Tunnel Segments

ACI 544.8R (2016)—Report on Indirect Method to Obtain a Stress-Strain Diagram for Strain Softening Fiber-Reinforced Concretes (FRCs)

ASTM International

ASTM C1609/C1609M (2012)—Standard Test Method for Flexural Performance of Fiber-Reinforced Concrete (Using beam with Third-Point Loading)

ASTM D412 (2016)—Standard Test Methods for Vulcanized Rubber and Thermoplastic Elastomers—Tension

ASTM D2240 (2015)—Standard Test Method for Rubber Property—Durometer Hardness

ASTM E119-14—Standard Test Methods for Fire Tests of Building Construction and Materials

Austrian Society for Concrete and Construction Technology (ÖVBB)

ÖVBB 2011—Guideline for Concrete Segmental Lining Systems

British Standards Institute (BSI)

PAS 8810:2016—Tunnel design. Design of concrete segmental tunnel linings. Code of practice.

British Tunneling Society (BTS)

Specification for Tunneling, 3rd Edition

Comité Européen de Normalisation (CEN)

EN 1992-1-1 :2004: E—Eurocode 2: Design of concrete structures - Part 1-1 : General rules and rules for buildings

EN 14651:2005+A1-2007—Test Method for Metallic Fiber Concrete. Measuring the Flexural Tensile Strength (Limit of Proportionality (LOP), residual)

Concrete Society (CS)

TR63 2007—Guidance for the design of steel-fibre-reinforced concrete

French Tunneling and Underground Engineering Association (AFTES)

AFTES–WG7 (1993)—Considerations on the Usual Methods of Tunnel Lining Design. Working Group No.7-Temporary Supports and Permanent Lining

AFTES (2005) —Recommendation for the design, sizing and construction of precast concrete segments installed at the rear of a tunnel boring machine (TBM)

German Committee for Structural Concrete within German Institute for Standardization (DafStb)

DAfStb Stahlfaserbeton:2012-11. Richtlinie Stahlfaserbeton/Technical Guidelines for Steel Fiber Reinforced Concrete, part 1-3.

German Concrete Association (DBV)

DBV 1992—Design Principles of Steel Fibre-Reinforced Concrete for Tunneling Works

German Federal Ministry of Transport (BMV)

ZTV-ING (2007) —Zusätzliche Technische Vertragsbedingungen und Richtlinien für den Bau von Straßentunneln (ZTV-ING) - Teil 5, Tunnelbau, Abschnitt 3 Maschinelle Schildvortriebsverfahren, 2007

14 >> References

German Railway Company (Deutsche Bahn AG)

Ril 853 (2011)—Richtlinie Eisenbahntunnel planen, bauen und in Stand halten

German Research Association for Underground Transportation Facilities (STUVA)

STUVAtec (2005)—STUVA Recommendations for Testing and Application of Sealing Gaskets in Segmental Linings, Tunnel, 8 (2005)

German Tunnelling Committee (DAUB)

DAUB 2013—Lining Segment Design: Recommendations for the Design, Production, and Installation of Segmental Rings

DAUB 2005— Recommendations for static Analysis of Shield Tunnelling Machines. Tunnel 7/2005.

International Federation for Structural Concrete (fib)

fib Model Code 2010 (2013)—Model Code for Concrete Structures

fib Bulletin n.83 (2017)—fib Working Party 1.4.1 (Fédération Internationale du Béton, Lausanne, Switzerland): «Tunnels in fiber reinforced concrete», fib Bulletin n.83, «Precast tunnel segments in fibre-reinforced concrete», ISSN 1562-3610, ISBN 978-2-88394-123-6, October 2017.

International Organization for Standardization (ISO)

ISO 11346:2004—Rubber, vulcanized or thermoplastic—Estimation of life-time and maximum temperature of use

International Tunneling Association (ITA)

ITA WG2 2000—Guidelines for the Design of Shield Tunnel Lining

ITA WG2 2016—Twenty years of FRC tunnel segments practice: lessons learnt and proposed design principles. Report n.16, April 2016, pp. 71, ISBN 978-2-970-1013-5-2.

ITA WG6 2004— Guidelines for structural fire resistance for road tunnels.

ITAtech Guidance for Precast Fibre Reinforced Concrete Segments – Vol 1 Design Aspects, 2016. Report 21374-ITATECH-REPORT-7-PFRCS-BD_P.

ITAtech Guideline for Good Practice of Fiber Reinforced Precast Segment – Vol 2: Production Aspects 2018. Report 21786-ITATECH-REPORT-9-PFRCS-V2-WEB-PAP.

Italian National Research Council (CNR)

CNR DT 204/2006 2007—Guidelines for the Design, Construction and Production Control of Fibre Reinforced Concrete Structures

Japan Society of Civil Engineers (JSCE)

JSCE 2007—Standard Specifications for Tunneling-2006: Shield Tunnels

Japanese Railway Technical Research Institute (RTRI)

RTRI 2008—Design standards for railway structures and commentary (shield tunnels)

Los Angeles County Metropolitan Transportation Authority (LACMTA)

LACMTA 2013—Metro Rail Design Criteria–Section 5 Structural/Geotechnical

Dutch Standardization Institute (NEN)

NEN 6720 (1995)—Regulations for concrete - structural requirements and calculation methods. Dutch Code NEN 6720

International Union of Laboratories and Experts in Construction Materials, Systems and Structures (RILEM)

RILEM TC 162-TDF 2003—Test and Design Methods for Steel Fibre Reinforced Concrete. σ–ε Design Method: Final Recommendation

Singapore Land Transport Authority (LTA)

LTA 2010—Civil Design Criteria for Road and Rail Transit Systems

14 >> References

Spanish Ministry of Public Works and Transport

EHE-08 2010—Code on Structural Concrete, ANNEX 14 – Recommendations for Using Concrete with Fibres

U.S. Army Corps of Engineers (USACE) EM 1110-2-2901 1997—Tunnels and Shafts in Rock

AUTHORED DOCUMENTS

Alder, A.; Dhanda, D.; Hillyar, W.; and Runacres, A., 2010, "Extending London's Docklands Light Railway to Woolwich", Proceedings of the ICE-Civil Engineering, V. 163, No. 2, pp. 81-90.

Bakhshi, M.; and Nasri, V., 2014a, "Review of International Practice on Critical Aspects of Segmental Tunnel Lining Design", Proceedings of the 2014 North American Tunneling (NAT) Conference, Los Angeles, CA, pp. 274-282.

Bakhshi, M.; Nasri, V., 2014b, "Guidelines and Methods on Segmental Tunnel Lining Analysis and Design – Review and Best Practice Recommendation", Proceedings of the World Tunnel Congress 2014. Iguassu Falls, Brazil.

Bakhshi, M.; and Nasri, V., 2014c, "Developments in Design for Fiber Reinforced Concrete Segmental Tunnel Lining", 2nd FRC International Workshop (1st ACI–fib Joint Workshop) on Fibre Reinforced Concrete, Montreal, Canada, pp. 441-452.

Bakhshi, M.; and Nasri, V., 2014d, "Design Considerations for Precast Tunnel Segments According to International Recommendations, Guidelines and Standards", TAC 2014, Vancouver, Canada.

Bakhshi, M.; Nasri, V., 2013a., "Latest Developments in Design of Segmental Tunnel Linings", Proceedings of the Canadian Society for Civil Engineering General Conference (CSCE 2013), Montréal, Québec, Canada.

Bakhshi, M.; and Nasri, V., 2013b, "Practical Aspects of Segmental Tunnel Lining Design", Underground—The way to the future: Proceedings of the World Tunnel Congress 2013., G. Anagnostou, and H. Ehrbar, eds., Geneva, Switzerland.

Bakhshi, M.; and Nasri, V., 2013c, "Structural Design of Segmental Tunnel Linings", Proceedings of 3rd International Conference on Computational Methods in Tunnelling and Subsurface Engineering: EURO: TUN 2013. Ruhr University, Bochum, Germany, pp. 131-138.

Bakhshi, M.; Barsby, C.; and Mobasher, B., 2014, "Comparative Evaluation of Early Age Toughness Parameters in Fiber Reinforced Concrete," Materials and Structures, V. 47, No. 5, pp. 853-872.

Barros, J. A. O.; Cunha, V. M. C. F.; Ribeiro, A. F.; and Antunes, J. A. B., 2005, "Postcracking Behaviour of Steel Fibre Reinforced Concrete," Materials and Structures, V. 38, No. 1, pp. 47-56.

Blom, C.B.M., 2002, "Design philosophy of concrete linings for tunnels in soft soil," PhD dissertation. Delft University Press, December 2002.

Caan, C.P.; Jansen, J. A. G.; Heijmans, R. W. M. G.; and van der Put, J. L., 1998, "High Speed Line – South: The Groene Hart Tunnel-Lining Design", Reference Design. Report No. 9G4 0001 981028, 52p.

Caratelli, A.; Meda, A.; Rinaldi, Z., 2012, "Design According to MC2010 of a Fibre-Reinforced Concrete Tunnel in Monte Lirio, Panama", Structural Concrete, V. 13, No. 3, pp. 166-173.

Cavalaro, S. H. P., Blom, C. B. M., Aguado, A., & Walraven, J. C., 2011, "New design method for the production tolerances of concrete tunnel segments". Journal of Performance of Constructed Facilities, 26(6), 824-834.

Çimentepe, A.G. 2010, "Evaluation of Structural Analysis methods used for the Design of TBM Segmental Linings", MSc Thesis, Middle East Technical University, Ankara, Turkey.

Clarke-Hackston, N., Messing, M., Loh, D., & Lott, R., 2006, "Modern high precision high speed measurement of segments and moulds", Tunnelling and Underground Space Technology, 21(3), 258-258.

Colombo, M.; Martinelli, P.; di Prisco, M., 2015, "A design approach for tunnels exposed to blast and fire", Structural Concrete, V. 16, No. 2, pp. 262-272.

Curtis, D.J.; Hay, M.; and Croydon, A., 1976, "Discussion on 'The Circular Tunnel in Elastic Ground'" Géotechnique, V. 26, No. 1, pp. 231-237.

Deere, D. U.; Peck, R. B.; Monsees, J. E.; and Schmidt, B., 1969, "Design of Tunnel Liners and Support Systems", Highway Research

14 >> References

Record 889, Final Report to Urban Mass Transit Administration, U.S. Department of Transportation, Washington, D.C.

Duddeck, H.; and Erdmann, J., 1982, "Structural Design Models for Tunnels", Tunneling '82-Proceedings of the Third International Symposium. Inst. of Mining and Metallurgy S, London, UK, pp. 83-91.

Francis, O.; and Mangione, M., 2012, "Developments in Joint Design for Steel Fibre Reinforced Concrete Segmental Tunnel Linings", Proceedings of the World Tunnelling Congress 2012. Bangkok, Thailand.

Fukui, K.; and Okubo, S., 2003, "TBM Cutting Forces with Particular Reference to Cutter and Tunnel Diameters", ISRM 2003–Technology Roadmap for Rock Mechanics, South African Institute of Mining and Metallurgy.

Groeneweg, T., 2007, "Shield Driven Tunnels in Ultra High Strength Concrete: Reduction of the Tunnel Lining Thickness", MSc Thesis, Delft University of Technology, The Netherlands.

Guglielmetti, V.; Grasso, P.; Mahtab, A.; and Xu, S., 2007, Mechanized Tunnelling in Urban Areas: Design Methodology and Construction Control, CRC Press, 528p.

Handke, D., 2012, "High-Precision Segments: Prerequisite for a high-quality monocoque tunnel", Tunnel, 8: 42.

Iyengar, K. T., 1962, "Two-Dimensional Theories of Anchorage Zone Stresses in Post-Tensioned Beams", Journal of the American Concrete Institute (ACI), V. 59, No. 10, pp. 1443–1466.

Kirschke, D.; Schälicke, H.; and Fraas, D., 2013, "Finne Tunnel: Innovative targeted resealing of segment bore joints – Part 2", Tunnel, 4/2013. pp. 30-40.

Mashimo, H.; Isago, N.; Yoshinaga, S.; Shiroma, H.; and Baba, K., 2002, "Experimental Investigation on Load-Carrying Capacity of Concrete Tunnel Lining", Proceedings of AITES-ITA 2002 - 28th General Assembly & World Tunnelling Congress 2002, Sydney, Australia, pp. 1-10.

Mendez Lorenzo, M.G., 1998, "Reliability analysis of a steel fibre reinforced concrete tunnel lining", Master Thesis. Delft University of Technology, Delft, the Netherlands.

Mobasher, B.; Bakhshi, M.; and Barsby, C., 2014, "Backcalculation of Residual Tensile Strength of Regular and High Performance Fiber Reinforced," Construction & Building Materials, V. 70, pp. 243-253.

Moccichino, M.; Romualdi, P.; Perruzza, P.; Meda, A.; and Rinaldi, Z., 2010, "Experimental Tests on Tunnel Precast Segmental Lining with Fiber Reinforced Concrete", ITA 2010 World Tunnel Congress, Vancouver, Canada.

Morgan, H.D., 1961, "A Contribution to the Analysis of Stress in A Circular Tunnel", Geotechnique, V. 11, pp. 37-46.

Muir Wood, A. M., 1975, "The Circular Tunnel in Elastic Ground", Géotechnique, V. 25, No. 1, pp. 115–127.

Neun, E., 2012, "Structural Fire Safety Engineering. Eurocode Approach and Practical Application", Proceedings of the World Tunnelling Congress 2012. Bangkok, Thailand.

Peck, R. B., 1969, "Deep Excavation and Tunnelling in Soft Ground, State of the Art Report", 7th International Conference on Soil Mechanics and Foundation Engineering, Mexico City, Mexico, pp. 225-290.

Plizzari, G.; Tiberti, G., 2009, "Tunnel Linings Made by Precast Concrete Segments", Construction Methodologies and Structural Performance of Tunnel Linings, G.A. Plizzari, ed., Brescia, Italy, pp. 136-131.

Poh, J; Tan, K. H.; Peterson, G. L.; and Wen, D., 2009, Structural Testing of Steel Fibre Reinforced Concrete (SFRC) Tunnel Lining Segments in Singapore", Proceedings of the World Tunnelling Congress (WTC) 2009, Budapest, Hungary.

Rostami, J., 2008, "Hard Rock TBM Cutterhead Modeling for Design and Performance Prediction", Geomechanics and Tunneling, V. 1, No. 1, pp. 18-28.

Sinha, R. S., 1989, Underground Structures: Design and Instrumentation, Elsevier Science, New York, NY, 500p.

Soranakom, C., and Mobasher, B., 2007, "Closed Form Solutions for Flexural Response of Fiber Reinforced Concrete Beams," Journal of Engineering Mechanics, V. 133, No. 8, pp. 933-941.

Vandewalle, L., 2000, "Cracking Behaviour of Concrete Beams Reinforced with a Combination of Ordinary Reinforcement and Steel Fibers," Materials and Structures, V. 33, No. 3, pp. 164-170.

Zhong, X.-C.; Liu, Q.-W.; and Zhao, H., 2011, "Study on the Grouting Pressure of Shield Tunnel", ASCE Geotechnical Special Publication, V. 215, pp. 183-190.

15 >> Glossary

Annular gap – space between the surrounding ground and the outer surface of the segments.

CIP – Cast-in-Place.

Circumferential joint – joint between two adjacent segmental rings.

Connections – devices for temporary or permanent connection of two segments or segment rings in the longitudinal and circumferential joints.

Cover – vertical distance to nearest ground surface from the tunnel crown.

Crosscut – connecting structure between two tunnel tubes or between a tunnel tube and the ground surface or a shaft

Crown – the highest part of a tunnel in cross section.

CSO – Combined Sewer Overflow.

DEM – Distinct Element Method.

Demolding – process of removing a precast concrete segment from the form in which it was cast.

Extrados – the exterior curve of an arch, i.e. the outer surface of the segment or the segment ring

FEM – Finite Element Method, the model representation of a structure as a combination of a finite number of two-dimensional or three-dimensional components.

Gasket – sealing strips placed in one or more layers around individual segments to ensure permanent sealing of the tunnel tube against the ingress of water from the surrounding rock mass.

Grout – cement mortar which is injected into the annular gap behind segments to fill the void between segments and excavated ground profile.

Intrados – the inner curve of an arch, i.e. the inner surface of the segment or segment ring

Invert – the lowest part of a tunnel in cross section.

Longitudinal joint – joint between adjacent segments in a ring.

One-pass lining – segmental lining is considered a one-pass lining when all static and structural requirements of the tunnel lining are catered for and no further internal lining is required.

Ovalization – deformation of an initially circular segmental ring to an oval shape due to earth pressure, grout pressure, segment self-weight or uplift.

Ring width – dimension of the segment ring in the longitudinal direction of the tunnel.

Segment – curved prefabricated element that forms part of a ring of support or tunnel lining; commonly precast concrete.

Segment thickness – distance between the inner and outer surfaces of the lining segment, i.e. the distance between the lining intrados and extrados.

Segmental lining – a set of precast segments assembled in a ring to form the tunnel lining

Springline – opposite sides of the tunnel at center line level.

Stripping – see demolding.

Tail void – annular space between the outside diameter (extrados) of the shield and the extrados of the segmental lining.

TBM – Tunnel boring machine which consists of a cutterhead in front of a shield which excavates tunnels with a circular cross section through different rock and soil strata.

Test ring – complete segment ring, usually assembled in horizontal position at segment precast plant, for test purposes.

Thrust jacks – hydraulic jacks serving to transmit the thrust forces of the tunnel boring machine to the segment ring, facilitating installation, or both.

Two-pass lining – tunnel lining consisting of two shells with different structural and constructional requirements which are produced in independent operations and with different construction methods (e.g. outer shell as a segmental lining, inner shell as a CIP).

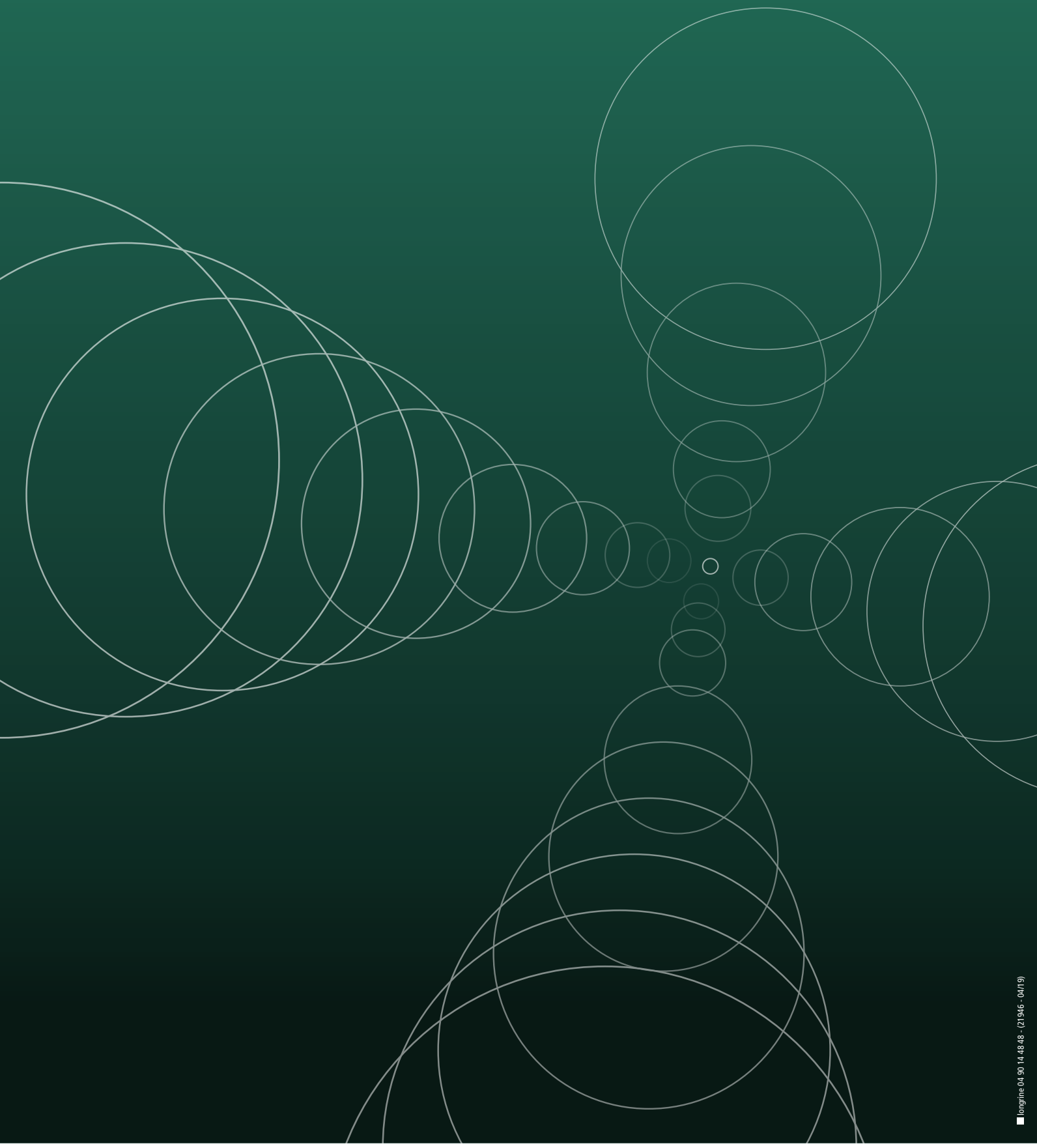

Imprimé par Longrine 04 90 14 48 48 - (21946 - 04/19)

ITA Secretariat - c/o MIE2 – Chemin de Balexert 9 - CH-1219 Châtelaine (GE) - Switzerland
Tel: + 41 22 547 74 41 - Email : secretariat@ita-aites.org - Web : www.ita-aites.org